A compact multi-electrode system to measure in vivo electrical activity in the olivocerebellar system

Measuring sub-threshold oscillations and action potentials spatially and over time

M.E. (Matthijs) Weskin

Delft University of Technology
Section Bioelectronics

Faculty of Electrical Engineering,
Mathematics and Computer Science

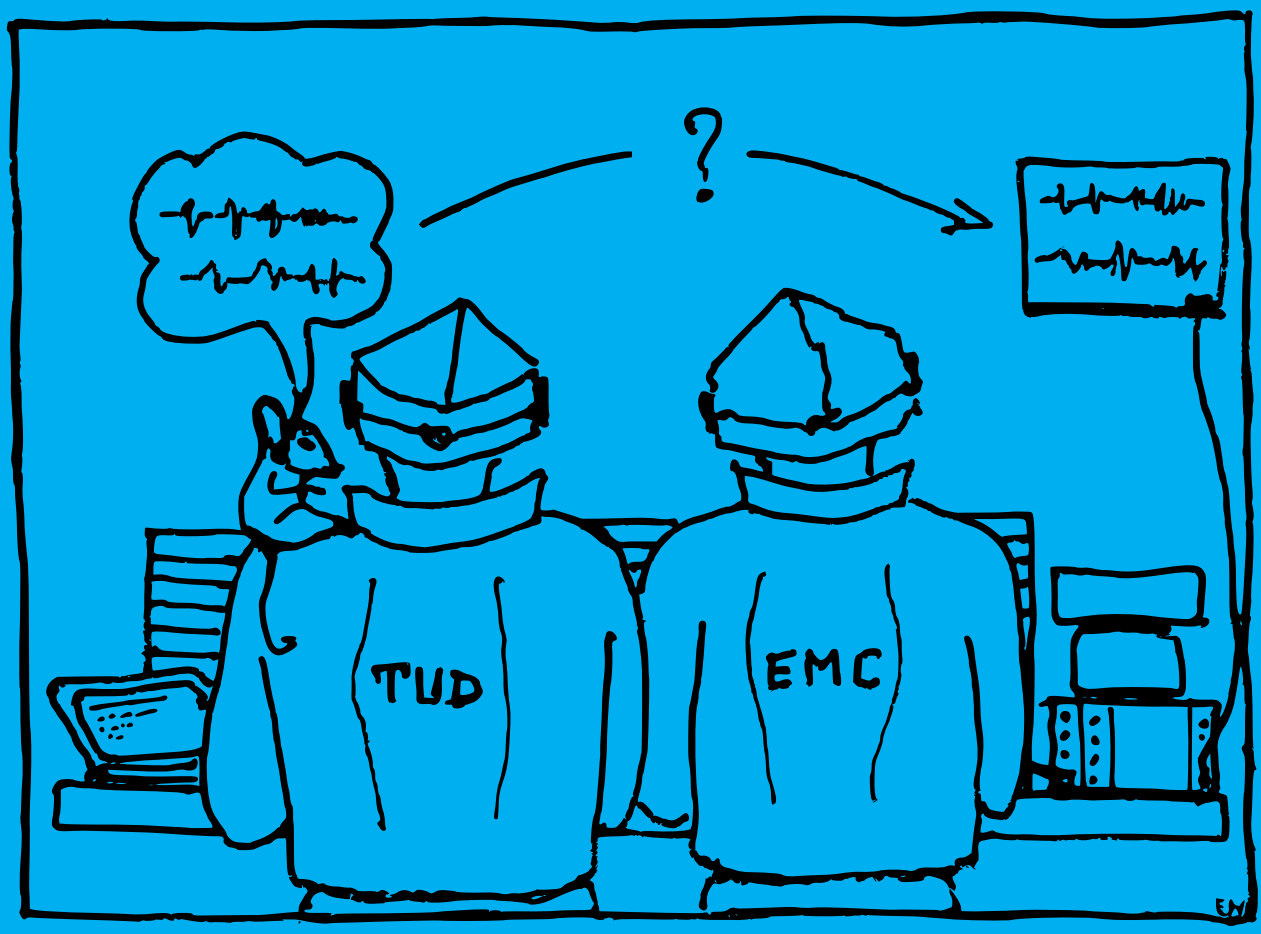

TU Delft

A COMPACT MULTI-ELECTRODE SYSTEM TO MEASURE IN VIVO ELECTRICAL ACTIVITY IN THE OLIVOCEREBELLAR SYSTEM

MEASURING SUB-THRESHOLD OSCILLATIONS AND ACTION POTENTIALS SPATIALLY AND OVER TIME

by

M.E. (Matthijs) Weskin

in partial fulfilment of the requirements for the degree of

Master of Science
in Microelectronics

at the Delft University of Technology,
to be defended publicly on Friday August 26, 2016 at 10:00 AM.

Student number:	1324454	
Thesis committee:	Prof.dr.ir. W.A. Serdijn,	TU Delft, supervisor
	dr.ir. C.J.M. Verhoeven,	TU Delft
	M.J. Negrello, PhD	Erasmus MC

This thesis is confidential and cannot be made public until August 26, 2021.

The cover image is drawn by Eric Weskin.

TU Delft Delft University of Technology

PREFACE

A while ago, neuroscientists from the Department of Neuroscience of the Erasmus Medical Center came to Delft to ask for a new measurements set-up. The demand was a cheap, good, small electrode array to measure 'some signals in the brain'. Despite the 'vague' description we engineers in Delft were interested. After a lot of meetings to determine the demands, the requirements of this project were defined. The project description consisted of roughly three subdesign: electrodes, electronics and the measurement set-up. A lot of work and a lot of unknowns in the project were ahead. Together with Joost Kerpels a division of subdesigns is made and the hard work could start. During the project close collaboration with Joost remained, as well as contact with our friends from Rotterdam. In a later stage in the design process, Ide Swager contributed in the design of the electronics part.

During the project, naming of the different systems became of high importance in understanding each other correctly. The developed electrode array is called the '*Delft Electrode Array (DEA)*' and the designed electronic system is called the '*Delft Analogue Front End (Delft AFE)*'. With this naming, the difference between current set-ups and equipment in the laboratories in Rotterdam and the newly developed equipment is made clear.

The report is written from an engineering point of view, but the neuroscientific relevant information is also discussed in this thesis (Chapter 2). According to the neuroscientific background, requirements are described (Chapter 3). The design is split into three subdesigns (electrodes, electronics, measurement set-up), each described in their own chapter (Chapters 4 to 6). Results of electrical an neuroscientific tests with the Delft AFE are presented in Chapter 7 and the work is concluded with all conclusions and recommendations for future work in Chapter 8.

Thanks to the challenging and multidisciplinary project, I always enjoyed working on the project, both in Rotterdam and in Delft. The results are promising and we would love to see a continuation of the overall project. First of all I want to thank Mario Negrello for all his convincing talks to enthuse us for neuroscience and particularly this project. Also all other colleagues in Rotterdam were always there to help and to perform the measurements. With questions about the inferior olive we always could ask Ruben van der Giessen, our walking encyclopaedia on the inferior olive. My good colleagues, Joost Kerpels and Ide Swager, deserve many thanks for all the sparring during the project and for all the drinks we drunk together. Wouter Serdijn, you are one of the most inspiring people I have ever met. With all your patience and trust, you gave me the opportunity to become a real engineer. Wouter, thank you very much. And last, but certainly not least, I want to thank my parents for all their patience with me, but especially for thinking along and all the support they gave me during the project. Being an electrical engineer and artist, my father is also the perfect person to draw the cover image.

M.E. (Matthijs) Weskin
Delft, August 2016

ABSTRACT

In the Erasmus Medical Center (Erasmus MC) in Rotterdam a lot of research is done to investigate the olivocerebellar system, consisting of the cerebellum (motor behaviour) and the inferior olive (sensory input). The correlation and propagation of signals between both parts are of interest when investigating the influence of sensory input on the motor behaviour. To facilitate this research, *a compact system to measure in vivo electrical neural activity in the olivocerebellar system spatially and over time* is designed and described in this work. The designed system consists of three subdesigns: electrodes, electronics and a measurement set-up. It is small, compact and capable of measuring in vivo neural activity. The Delft Electrode Array proves its concept with four robustly mounted electrode tips, however the number of mounted electrodes should be increased. The Delft Analogue Front End, the electronics system with its custom measurement set-up, can - after only changing software parameters - measure up to 32 channels. Its bandwidth (-3 dB bandwidth from 0.3 Hz to 30 kHz) is wide enough to measure sub-threshold oscillations (1 to 10 Hz) as well as action potentials (up to 10 kHz).

CONTENTS

1

INTRODUCTION

Throughout the years a lot has become known about the human body; except for one part which is barely known: the brain. Bit by bit a little understanding of local brain areas is obtained, but a good understanding of the correlation between different areas is still only a wish of neuroscientists.

The brain constantly produces output to our limbs to regulate our interaction with the environment. To control this interaction, feedback is received. The brain is full of separate control systems, each of those with their own purpose. In the Erasmus Medical Center in Rotterdam (Erasmus MC), at the Department of Neuroscience, much research is done to understand the motor behaviour of the body and therefore the cerebellar cortex is studied extensively. The cerebellar cortex is assumed to be the centre of the motor behaviour and processes sensory input to control motor output. The Inferior Olivary Complex (inferior olive) plays a key role in the sensory input to the cerebellum. Malfunctioning in the control path from input to output can cause serious problems in motor behaviour. To fully understand how the olivocerebellar system accomplishes the integration of sensory information and motor control, electrical measurements with many electrodes in different areas of the olivocerebellar cortex must be performed to measure the interaction and propagation of low frequency sub-threshold oscillations and action potentials from neurons, spatially and over time, in the inferior olive and the cerebellum.

All experiments in the Erasmus MC on the olivocerebellar system are performed on animal models, mostly mice. To measure at many places over a longer period of time multiple electrodes and amplifiers must be used. Electrode arrays and amplifiers are already available, but none of them are small and wearable. The best way to research the behaviour of the brain, especially in the motor cortex, is to measure in vivo on awake and freely moving animals. This requires a small and wearable device that can be implanted in an animal without doing significant damage to any tissue. The above described neuroscientific research question can be translated into a research goal from an engineering point of view:

> *Design a compact measurement system to measure in vivo electrical activity of neurons in the olivocerebellar system, in the range of sub-threshold oscillations to action potentials, spatially and over time.*

As a benchmark, the existing state-of-the-art system available in the Erasmus MC is chosen. This consists of a Faraday cage (to suppress unwanted electromagnetic interference from the outside), an electrode array (to measure the neural signals), a set of pre-amplifiers (to amplify the very small signals from the electrodes), a digitiser (to convert the signals to the digital domain) and a bio-processor (to filter and process the digital signals to a computer). The set-up is large, fixed and the mouse must be anaesthetised and fixated to perform measurements. To reach the design goal a structured approach is followed and the project is split into three subdesigns:

- *Electrode design*
  A characterisation of the measured tissue is made, followed by a design of a small electrode array.
- *Electronics design*
  This part contains the design of pre-amplifiers, digitisers, data processing and data storage.

- *Measurement set-up*
  Integrate the first two parts into a complete set-up.

First the tissue to be measured is investigated and characterised (Chapter 2). With a characterisation of the source, detailed system specifications and requirements are defined (Chapter 3). A single electrode is designed and analysed, followed by a multi-electrode design, concluded with a comparison of this subdesign with the state-of-the-art system (Chapter 4).

The electronics design (Chapter 5) is initially designed to serve measurements in the inferior olive and the cerebellum, but during the research the demand from other neuroscientific projects for a custom designed multi-input amplifier system increased. In the subsequent design process a goal is added: the system must be universal. With a different electrode set and a notification in the software, the system can also be used in other set-ups.

During measurements the existing set-up is analysed, improvements are proposed and a complete measurement set-up with the newly designed electrodes and electronics is described (Chapter 6). Measurement results of the electrodes are presented in the corresponding chapter because they are used as an iteration in the design process, results of the complete system are presented, described, and analysed in Chapter 7. In the final chapter (Chapter 8) conclusions are presented and recommendations are put forward.

All measurements involving mice are performed in the Erasmus MC by certified neuroscientists. Electronic measurements with the subsystems, without animals, are performed in the laboratory of the section Bioelectronics at Delft University of Technology.

2

BACKGROUND: BRAIN ANATOMY AND FUNCTIONALITY

The brain has a very complex structure and is the centre of control of the human body. As this thesis describes measurements in the olivocerebellar system, this chapter will only focus on the Inferior Olivary Complex and the cerebellum. Section 2.1 explains the structure of the olivocerebellar system, Section 2.2 the electrophysiological properties of the inferior olive.

2.1. OLIVOCEREBELLAR SYSTEM

The olivocerebellar system is formed by the cerebellum and the inferior olive. There is extensive interaction between both via several tracts. The inferior olive provides major sensory input to the cerebellum, the cerebellum handles the information and produces output. In the next subsections the anatomical structure of the cerebellum and the inferior olive are made clear, to better understand the connections between parts.

Timing is an essential property for precise motor movement. As the olivocerebellar system plays a key role in motor tasks, there is a lot of information in this brain area [1] [2] [3]. To investigate timing, electrical measurements must be performed over time. To also investigate the relation in timing between different areas inside the olivocerebellar system, multi-electrode measurement are necessary.

2.1.1. CEREBELLUM

In Figure 2.1 schematic sagittal and dorsal views of the brain are shown. In Figure 2.1a the arrow points to the cerebellum (= little brain). The cerebellum is made up of two hemispheres and located under the occipital part of the cerebrum (= large brain), behind the top part of the brain stem. Three peduncles connect the cerebellum to the dorsal part of the brain, as shown in Figure 2.1b. In these peduncles sensory input is received and neural output is transmitted. The cerebellum takes just ten percent of the total volume of the brain, but 70 percent of all neurons are located in the it. This high number of neurons is attributed to the

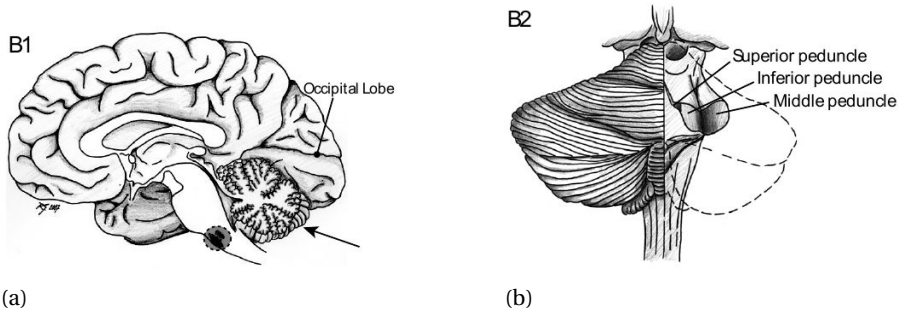

(a) (b)

Figure 2.1: A sagittal and dorsal view of the human brain. (a) A sagittal view of a human brain. The arrow points to the cerebellum, the dashed circle indicates the inferior olive; (b) A dorsal view of the cerebellum. The three cerebellar peduncles are shown. Reprinted with permission from *Role of Electrotonic Coupling in the Olivocerebellar System*, R.S. van der Giessen, 2007.

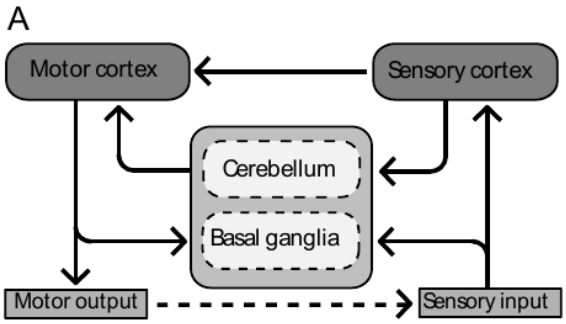

Figure 2.2: A schematic diagram of the motor control system. Reprinted with permission from *Role of Electrotonic Coupling in the Olivocerebellar System*, R.S. van der Giessen, 2007.

many convolutions at the surface of the cerebellum [4] [5].

The cerebellum is part of the control system that regulates motor movement. In Figure 2.2 a schematic diagram of this control system is shown. It receives sensory input (directly and via the sensory cortex), and generates motor output via the motor cortex. The motor output is also fed back to the cerebellum [6].

The cerebellum is involved in four major functions:

- *Maintenance of balance and posture*
  To maintain balance or to obtain a posture, the cerebellum compensates for body movement or muscle load. It receives sensory input and processes it without awareness to motor output.

- *Coordination of voluntary movements*
  Timing and force of muscle groups is coordinated by the cerebellum to obtain regulated voluntary movement.

- *Motor learning*
  Fine-tuning and adapting motor programs to acquire accurate movement for repeated motor tasks. With training and repetition, tasks are fine-tuned.

- *Cognitive functions*
  Several cognitive functions are attributed to the cerebullum, including language, but this function is not yet well understood [7][8].

The first three listed functions are related to the motor system, but the latter one is different. As this thesis focuses on the relation between sensory input, the inferior olive, the processing in the cerebellum and the output, only the first three functions are discussed.

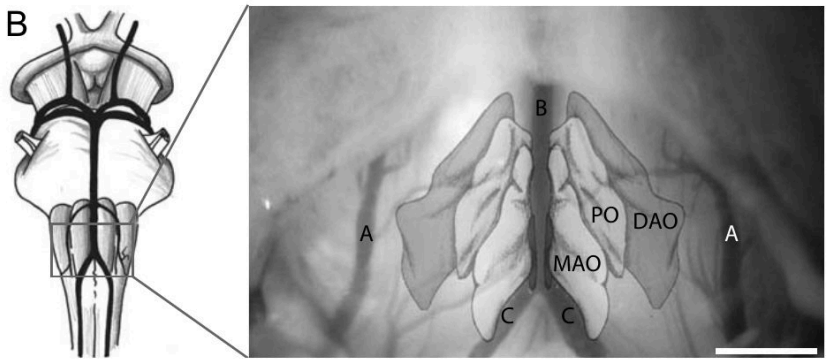

Figure 2.3: Ventral view of the brain stem showing the main artery system, with a zoomed in view. Reprinted with permission from *Role of Electrotonic Coupling in the Olivocerebellar System*, R.S. van der Giessen, 2007.

2.1.2. INFERIOR OLIVARY COMPLEX

The Inferior Olivary Complex (inferior olive) is located in front of the brain stem and consists of three subdivisions: the principle olive (PO), dorsal accessory olive (DAO) and medial accessory olives (MAO), as shown in Figure 2.3. A, B and C indicate the Posterior Inferior Cerebellar Arteries, the Basal artery and Vertebral arteries respectively. It is clear the inferior olive is surrounded by arteries, a possible source of interference.

Olivary neurons have an oval shaped cell body (diameter of 15 to 20 µm). A single axon rises from a neuron, branching out into several climbing fibres. These fibres are long and connect the inferior olive to all parts of the cerebellum. Each olivary neuron rises just a single climbing fibre, innervating about ten Purkinje cells. Purkinje cells receive input from just one climbing fibre, and has many parallel aligned large dendrites. They make up the unique output of all motor tasks in the cerebellar cortex [9] [10].

The density of gap junctions (connections between neighbouring cells; Subsection 2.2.1) in the inferior olive is one of the highest in the brain. This means the direct communication between neurons is high compared to other areas of the brain [11] [12] [13].

In Figure 2.3 the isosceles triangle A-B-C indicates the triangular shape of the inferior olive. The lines A-B and B-C have a length of approximately 3 mm.

2.2. ELECTROPHYSIOLOGY IN INFERIOR OLIVE

To design a well working measurement system, source characterization is necessary. In this section the electrophysiology of the inferior olive is discussed, including the above mentioned source characterization.

2.2.1. GAP JUNCTIONS

Gap junctions are channels connecting electrically active cells to each other. They provide the passage of molecules and ions, which makes the synchronization of electrical activity possible [6]. The more gap junctions are present, the more synchronization takes place. The inferior olive has a relatively high amount of gap junctions compared to other brain areas, suggesting a high synchronization.

2.2.2. CELL MODEL

In Figure 2.4a a schematic view of a neuron cell membrane is shown. The ion channels of Potassium (K^+), Sodium (Na^+), Calcium (Ca^{2+}) and Chloride (Cl^-) are shown. Generally these ions flow through the cell membrane and therefore contribute to the membrane potential, V_m. An equivalent electrical model is shown in Figure 2.4b and based on the above four ion channels. Ionic gradients form an electrical energy storage, represented by the electromotive forces E_K, E_{Na}, E_{Ca} and E_{Cl}. Each source produces an ionic current through the membrane, summing to the total membrane current, I_m. The ionic permeability is represented by the conductances G_K, G_{Na}, G_{Ca} and G_{Cl}. As the cell membrane is a good dielectric and the inner and outer potentials are not equal, the membrane acts as a capacitor, represented by C_m.

In measurements on the olivocerebellar system the extracellular voltage is measured. The model is not used for computations, only for insight in the generation of the neural activity to be measured. With insight in the electrochemical generation of the membrane voltage, it can be concluded that the measured signal can be modelled as an equivalent voltage source with an equivalent source resistance R_{eq} in series and a shunt capacitance C_m. Each type of cell has a different source impedance, so it is not possible to give a general value to the impedance.

2.2.3. ACTION POTENTIALS OF OLIVARY NEURONS

In Figure 2.5 a default shape of an action potential of a neuron is shown. Each type of neuron has its own characteristic values for timing of an action potential. In this subsection the values for olivary neurons are explained.

Number 1 in the figure indicates a stimulus is given and the neuron starts to fire. Firing is done with a sharp depolarization peak (2), followed by a plateau phase with several wavelets on top and a prolonged after-depolarizing potential (ADP; 3 and 4). The membrane voltage recovers to its resting potential after a long-lasting after hyperpolarizing potential (AHP; 5). The ADP typically takes 10 to 15 ms and has multiple small wavelets on top. It is immediately followed by the AHP, which lasts for 150 to 200 ms [14]. A single action potential is usually initiated with a latency of 15 to 30 ms after a sensory stimulation.

During continuous stimulation no ongoing discharge is present. Also olivary neurons fire with an unusual low frequency, between 1 and 2 Hz. To investigate the relation between sensory input, oscillations in the olive and firing output, these action potentials must be observable in the measurements.

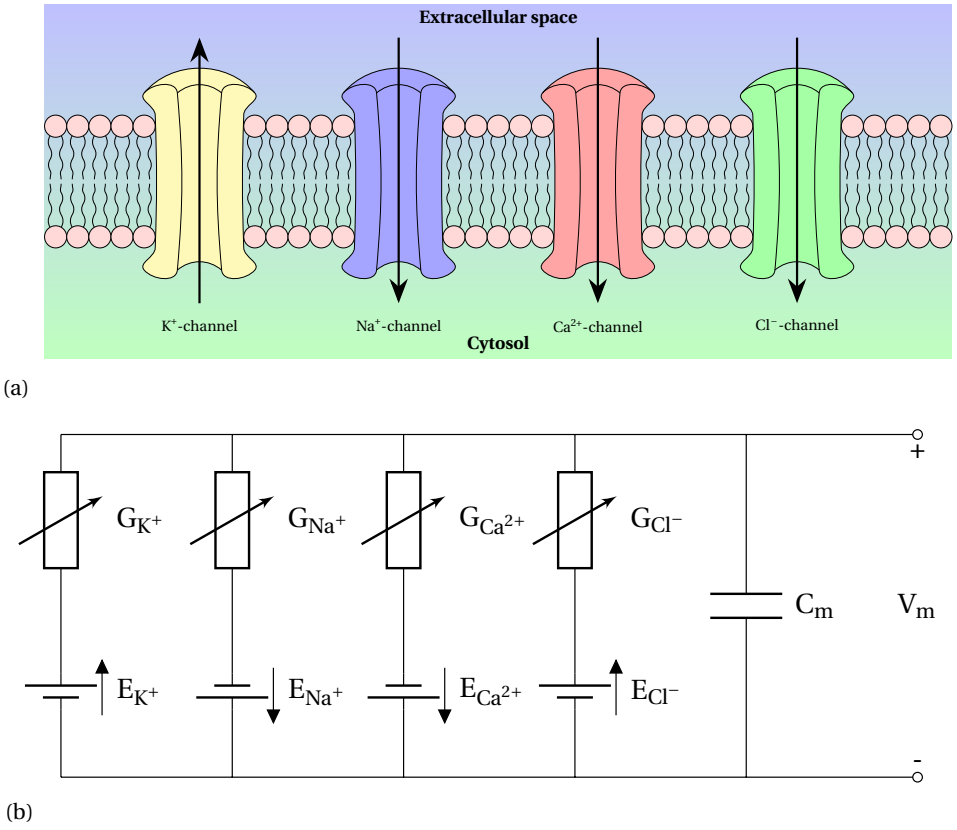

Figure 2.4: (a) A schematic view of a cell membrane and (b) its equivalent electrical model

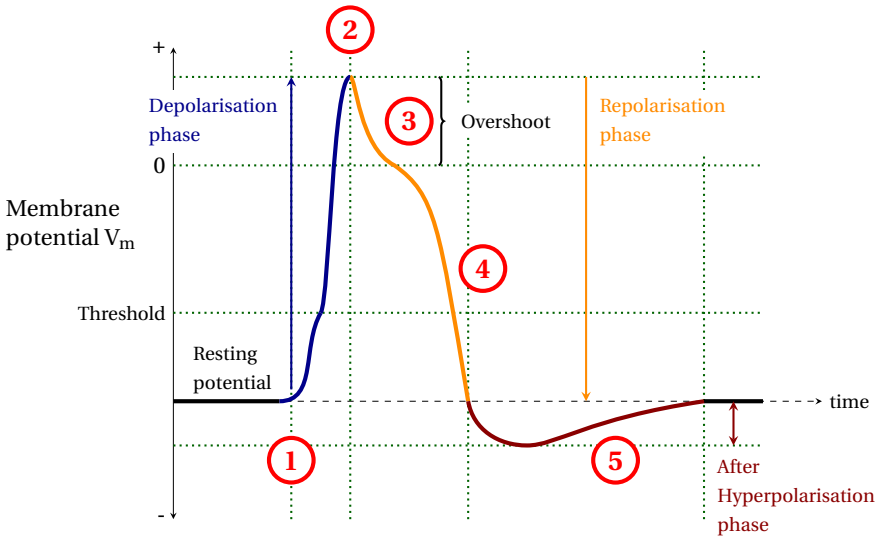

Figure 2.5: A default shape of an action potential

The conduction velocity in the inferior olive is 0.5 to 2.0 $m\,s^{-1}$ for unmyelated axons and 3 to 120 $m\,s^{-1}$ for myelated axons. To measure the propagation of action potentials in the olivocerebellar system, the distance between electrodes (i.e. spatial resolution) and sample frequency (i.e. time resolution) must be based on these velocities [15][16].

2.2.4. SUB-THRESHOLD AND LOW THRESHOLD OSCILLATIONS

The membrane potential of olivary neurons is oscillating. This is called subthreshold oscillations, because the membrane potential is high enough to start firing. These oscillations are in a frequency range of 4 to 10 Hz and have an amplitude that stays below the threshold value. The phase and amplitude of the subthreshold oscillations is assumed to regulate the olivary burst. To investigate this in a multi-electrode measurement set-up, these oscillations must be measurable.

Besides sub-threshold oscillations another type of oscillation is present in the inferior olive: low threshold oscillations. In the range of 1 to 3 Hz, with a slightly smaller amplitude than sub-threshold oscillations, sinusoidal waves are present [17].

Now the nature of electrical activity in the olivocerebellar system is known, requirements following from the desired signals can be set. The next Chapter starts with the description of these requirements and translates them into requirements from an engineering point of view.

3

SYSTEM REQUIREMENTS[1]

In Chapter 2 the waveforms present in the desired signal have been discussed. Based on these waveforms requirements of the measurement system can be obtained. Together with the neuroscientists of the Erasmus MC, Department of Neuroscience, a detailed set of system requirements from a neuroscientific point of view are set. These requirements are presented in the next section. A translation to requirements from an engineering point of view are presented in Section 3.2.

3.1. NEUROSCIENTIFIC REQUIREMENTS

In this section system requirements from a neuroscientific point of view are listed. All requirements are set in collaboration with the neuroscience department of the Erasmus MC. Some requirements are optional in this work, but must be kept in mind for future work. The origin of each requirement is explained shortly.

- **In vivo measurements**
  All measurements are performed *in vivo*. To do so, the used electrodes must be *biocompatible* and the damage to the tissue must be minimized.
- **Measure sub-threshold and low-threshold oscillations**
  Sub-threshold oscillations (STO, see Subsection 2.2.4) are present in the frequency band from *4 to 10 Hz*. Low-threshold oscillations (LTO) in the band from *1 to 3 Hz*.
- **Measure action potentials**
  Action potentials (AP) contain frequencies up to *multiple kHz*, depending on the type of action potential. The repetition frequency of action potentials is *between 1 and 2 Hz*.
- **Measure propagation of oscillations and action potentials**
  To reconstruct all waveforms (STO's, LTO's and AP's) a frequency range of *sub-Hz to multiple kHz* is necessary.
- **Number of electrodes**
  There is *no restriction* on the number of electrodes used in the system. To measure spatially at least two electrodes are required.
- **Tissue and cell size**
  Neural cells in the olivocerebellar system are oval shaped with a *diameter of 15 to 20 μm*. To record single cell potentials, electrode tips in the same order of magnitude must be used.
  The inferior olive is *triangular shaped, 3 by 3 mm* (see Subsection 2.1.2). The inserted electrodes must not exceed these dimensions.
- **Data processing**
  Obtained data must be *displayed in real time* during the measurement to monitor the recording.
  Besides displaying the data, it also must be *saved to a storage device* for extensive processing and

[1] This chapter is partly co-authored by Joost Kerpels

analysing purposes. The data must be importable in Matlab and Spike2 (respectively engineering and neuroscience software).

- **Cheap**
  Without losing signal quality the costs must be reduced. Existing set-ups containing expensive amplifiers, electrodes and accessories will limit the amount of set-ups and can reduce the number of measurements that can be performed, because just several set-ups are available. A new design must be cheaper than the existing measurement set-ups.

- **(Optional) Universal electronics**
  The starting point for measurements is the olivocerebellar system, but with a different configuration of the set-up and perhaps another set of electrodes (depending on the location of the measurement and tissue properties), but without adding or changing electronic hardware, other brain signals also must be measurable.

- **(Optional) Wearable**
  Initially the mice are anaesthetised during measurements, but a future goal is to measure in awake and freely moving mice. To realise these measurements, the used hardware must be wearable.

- **(Optional) Wireless**
  When a set-up with awake mice is realised, a wireless link between the electronics on the mice, and a base station can be implemented. However, this is not in the scope of this thesis.

3.2. ENGINEERING REQUIREMENTS

In the previous section the requirements from a neuroscientific perspective are listed. In this section the translation is made to an engineering point of view. To keep a clear overview, the requirements are split into the following subdesigns: electrodes, electronics and measurement set-up.

3.2.1. ELECTRODE REQUIREMENTS

Specific requirements to the electrodes and the electrode array are listed in this subsection. The chosen values are based on the tissue properties (Chapter 2) and measurements with the existing set-up in the Erasmus MC (Sections 4.1 and 6.1).

- **Material**
  The material for used electrodes or a base material for an electrode array must be biocompatible as it is implanted in an animal.

- **Electrode size**
  Since the neural cells to measure have a diameter of 15 to 20 µm and single cell potentials must be measured, the electrode tip may not exceed the cell diameter: $\varnothing_{\text{tip}} = 20\,\mu\text{m}$.
  The total electrode diameter may not damage the tissue significantly, therefore the maximum electrode diameter is set to five times the cell diameter: $\varnothing_{\text{electrode}} = 100\,\mu\text{m}$.

- **Array size**
  The minimum number of electrodes in the array is not specified by neuroscientists, as long as the spatial and time resolution can be met. The physical size of the array on the other hand is limited to the size of the inferior olive: a triangle of 3 by 3 mm.

- **Connection**
  The system can work *stand-alone*, but to test the electrode array on itself a connection to the existing set-up in the Erasmus MC is required.

- **Impedance**
  The small voltage potential from the source needs a large amplification. The higher the impedance of the electrode, the higher the input impedance of the amplifier has to be. Ideally the impedance of the electrode is zero, but with the small sizes this is fairly impossible. To quantify this measure, the impedance of the existing micro-electrodes is chosen: $Z_{\text{electrode}} \leq 1\,\text{M}\Omega$ at 1 kHz.

3.2.2. ELECTRONICS REQUIREMENTS

The desired signals to measure are studied and translated into requirements for the system, listed in the section. Electronics in the existing set-up are used as a reference. Reference measurements are performed to determine the system requirements.

- **Input impedance**
  The input impedance of the pre-amplifiers must be sufficiently high to prevent loading the source. Due to the expected high impedance of the electrodes, it is even more important to have a high input impedance of the amplifiers.

- **Bandwidth**
  The signal contains the following frequencies:

  - Action potential repetition: 1 to 2 Hz
  - Low-threshold oscillations: 1 to 3 Hz
  - Sub-threshold oscillations: 4 to 10 Hz
  - Action potentials (low frequency components): 5 to 10 Hz
  - Action potentials (high frequency components): up to 10 kHz

  The electronic data acquisition system must have a bandwidth equal to or larger than the signal bandwidth: 1 Hz ≥ BW ≥ 10 kHz. In this bandwidth the transfer function must be within ± 1 dB.

- **Signal-to-noise ratio (SNR)**
  The signal-to-noise ratio (SNR) is derived from the existing measurement set-up. Measured signals have a nominal signal peak-peak voltage of $V_m = 2\,mV_{pp}$, the noise in measured signals is approximately $V_n = 20\,\mu V_{pp}$ over the signal bandwidth (1 Hz to 10 kHz), resulting in the maximum SNR. The SNR of the new designed system must at least equal this value:

$$\text{SNR} = 10 \cdot \log_{10}\left(\frac{V_m}{V_n}\right)^2 \tag{3.1}$$

$$= 20 \cdot \log_{10}\left(\frac{2\,mV}{20\,\mu V}\right) \tag{3.2}$$

$$\text{SNR} \geq 40dB \tag{3.3}$$

  This a quiet low SNR, but the most important measure in behavioural neuroscientific experiments is the overall shape and the timing of the signal, not the detail in the signal.

- **Dynamic range (DR)**
  The desired dynamic range is obtained from reference measurements in the existing set-up in the Erasmus MC. The maximum amplitude to measure is $V_m = 6\,mV_{pp}$. The noise floor, which determines the minimal measurable voltage, is: $V_{m,min} = V_n = 20\,\mu V_{pp}$.

- **Resolution**
  The shape and timing of signals is more important than an extreme high resolution of the system. The resolution requirement is set to 10 µV.

- **Analog-to-digital-converter (ADC)**
  Sampling rate
  To reconstruct all expected waveforms (oscillations and action potentials), a sampling frequency of twice the bandwidth must be used (Nyquist rate). Action potentials can contain frequencies up to kHz, resulting in a sampling rate of: $F_s \geq 20$ kHz.
  Resolution/number of bits
  To achieve a resolution of 10 µV with a maximum input signal of $V_{max} = 6\,mV_{pp}$, the number of bits becomes 10. The effective number of bits of the ADC can be also related to the SNR:

$$\mathrm{SNR}_{\mathrm{ADC}} = 1.76 + 6.02 \cdot \mathrm{ENOB} \tag{3.4}$$

$$\mathrm{ENOB} = \frac{\mathrm{SNR}_{\mathrm{ADC}} - 1.76}{6.02} \tag{3.5}$$

$$= 7 \text{ bits} \tag{3.6}$$

As the highest of the two numbers is the one related to the resolution (10 bits), this will be leading in the choice of an ADC.

- **Data processing**
  Realtime display
  The measured data must be displayed real-time on a display in the measurement room.
  Data storage
  The measured data must be saved to a storage device for later analyses and processing.

- **Size**
  In the future, the electronics are placed on the mouse and data is transferred wirelessly. The electronics therefore must be wearable, and thus small. To not restrict to the proof of concept, no maximum size is defined.

- **(Optional) Universal**
  The electronic data acquisition system must be universal to use in other neural measurement systems. To achieve this, the system must be software controllable.

3.2.3. MEASUREMENT SET-UP REQUIREMENTS

The existing measurement set-up is large and used for different purposes without optimising it to a specific measurement. In this subsection requirements on a new set-up are presented. Besides the design of a new set-up, the existing set-up must be updated and improved.

- **Size**
  Initially the measurement system can be any size, but with an eye on the future, it must be taken into account that the system must become wearable and wireless. No restriction in size is chosen, but the possibility of reducing the size must be investigated.

- **Electromagnetic interference (EMI)**
  Electromagnetic interference (EMI) may not dominate the measured signal. Especially interference inside the bandwidth (e.g. 50Hz-interference from the mains) must be suppressed.

In the next Chapters the design is explained, following the system requirements set in this Chapter. Additional requirements to sub-designs following from the above listed requirements, are discussed in the corresponding chapters. All requirements are evaluated in Chapter 8, Conclusions and Recommendations. Improvements are proposed for requirements that are not met.

4

ELECTRODES

Arrays of electrodes are used to measure multiple signals at the same time. With these arrays signals can be measured on multiple places in a particular brain area. These signals can be analysed and spatial propagation and phase differences of neural signals can be studied. In this chapter single electrodes and their electrical properties will be explained in detail (Section 4.1) to make a characterization of the source used to design matching amplifiers (Chapter 5), state-of-the-art electrode arrays will be discussed (Section 4.2) and finally the design process of a new electrode array is described (Section 4.3).

4.1. SINGLE ELECTRODE

To measure electrical neural activity in the olivocerebellar system neuroscientists at the Erasmus MC use metal micro-electrodes. Most of them are constructed with a tungsten core (diameter of 30 µm), surrounded by a quartz insulation layer (total diameter of 80 µm). To understand electrode arrays, first a close look at single electrodes is taken. In Subsection 4.1.1 an advanced model of an metal micro-electrode will be explained, working towards a simplified model (Subsection 4.1.2) that can be used in further analysis.

4.1.1. ADVANCED MODEL

In the advanced electrical model, every component of the electrode is represented and described by an electrical component. A schematic view of the used micro-electrodes is depicted in Figure 4.1. To fabricate the electrodes and form the tip tungsten wire is pulled under high temperature and in vacuum. The pulled end is polished to remove all imperfections on the surface. Understanding each component will lead to a simplified model, keeping al simplifications in mind. An electrical representation is shown in Figure 4.2. Here V_{neuron} is the ideally recorded voltage of the neuron, R_s the spreading resistance (i.e. the resistance between the electrode tip and the measured tissue), R_{dl} and C_{dl} form the double layer impedance, R_m is the metal resistance of the tungsten wire and C_s is the shunt capacitance to ground from the electrode tip to the amplifier input [18] [19] [20].

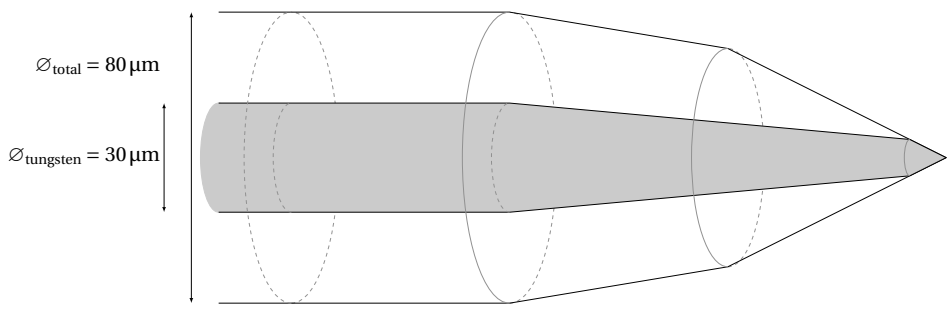

Figure 4.1: A schematic overview of the electrode tip of a Tungsten/Quartz electrode. The core is the Tungsten conductor, surrounded by a quartz insulation layer.

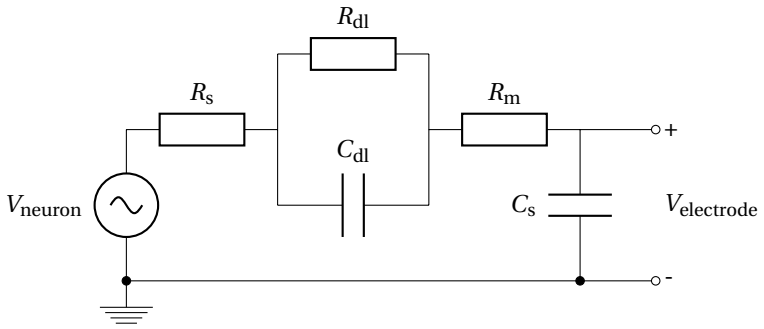

Figure 4.2: Advanced electrical circuit model of a metal micro-electrode used for recordings in the olivocerebellar system.

NEURAL ACTIVITY (V_{NEURON})

V_{neuron} is the ideally measured voltage of the neuron outside the cell. Typically it is in the range of −100 mV to 0 mV for cells in the olivocerebellar system. Measurements with the existing set-up however, show a measured signal amplitude of 6 mV_{pp}.

SPREADING RESISTANCE (R_s)

The spreading resistance R_s is the resistance between the electrode tip and the measured neuron. The resistance represents the current spread into the bulk solution [21]. It depends on the resistivity of the tissue (ρ_{tissue}) and the distance between the neuron and the tip (r_e) as follows:

$$R_s = \int_{r_e}^{\infty} dR_s = \frac{\rho_{tissue}}{4\pi r_e} \tag{4.1}$$

Typically the resistivity of the tissue, ρ_{tissue}, is 75.5 Ω cm [18]. The spherical radius r_e of the tip is estimated to be around 5 µm, which results in a spreading resistance R_s = 12 kΩ. This is relatively small compared to Z_{dl}, the double layer impedance.

DOUBLE LAYER IMPEDANCE (C_{DL} AND R_{DL})

As an interface between electrons in the electrode and ions in the solvent (e.g. the tissue) is present, a charge region is formed at the interface, forming a capacitance (the electrode-tissue interface) [22] [23]. The double layer impedance consists of this capacitance, C_e, in parallel with a resistance R_e which is the leakage resistance of the electrode-tissue interface. The value of the double layer impedance is frequency dependent, but its phase angle is constant. The double layer impedance is mostly determined empirically and varies from hundreds of kΩ to tenths of MΩ.

OHMIC RESISTANCE (R_M)

The Ohmic resistance of the Tungsten wire is found by the equation:

$$R_m = \rho_W \cdot \frac{4L}{\pi d^2} \tag{4.2}$$

where ρ_W is the resistivity of Tungsten, L the length of the electrode and d the diameter of the electrode. The resistivity is dependent of the temperature, but a normalized value of ρ_W = 54 nΩ · m is suitable for a good approximation of the resistance. For use in the existing setup the electrodes have a typical length of 20 cm and a diameter of 30 µm resulting in a resistance of R_m = 15 Ω. This is negligibly small compared to the spreading resistance and the double layer impedance.

SHUNT CAPACITANCE (C_s)

In Figure 4.1 a schematic overview of an Tungsten/Quartz electrode tip is shown. The quartz insulator forms a capacitance together with the tungsten core and the surrounding tissue, called the shunt capacitance. This capacitance, C_s, is inversely proportional to the logarithm of the ratio of the conductor diameter, d = 30 µm, and the total diameter, D = 80 µm of the electrode wire [18]:

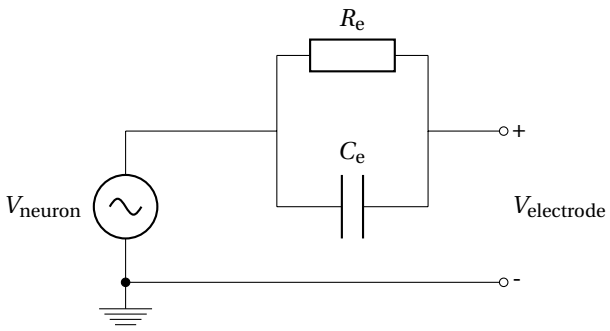

Figure 4.3: Simplified electrical circuit model of a metal micro-electrode.

$$C_s \propto \frac{\epsilon_r}{\log(\frac{D}{d})} \left[\frac{\text{pF}}{\text{cm}}\right] \tag{4.3}$$

The relative permittivity, ϵ_r, of quartz is approximately 5, the ratio D/d is relatively high, for an electrode with a length of 2 mm this results in a capacitance of 1 pF. The effect of this capacitance (low pass filtering) can be neglected, because its cut-off frequency is far above the desired bandwidth, 0 to 25 kHz.

4.1.2. SIMPLIFIED MODEL

In the simplified electrode model, shown in Figure 4.3, the resistance of the Tungsten wire (R_m) and the spreading resistance of the tissue (R_s) will be neglected, because they are negligible compared to the double layer impedance of the electrode. Also the shunt capacitance is omitted, because its effect is negligibly small compared to the double layer impedance. The simplified impedance will be modelled as a resistor (R_e) parallel with a capacitor (C_e). The constant phase angle of the double layer capacitance will not be taken into account in the simple model, so no correction for the constant phase element is implemented [24].

4.1.3. SOURCE CHARACTERIZATION

Taking all simplifications into account, a good estimation of the source can be made. A voltage source in series with a resistance and capacitance in parallel are left over. The values for the components in Figure 4.3 are determined empirically and are listed in Table 4.1. This has to be taken into account when designing the amplifiers in Chapter 5. To determine the parameters of Table 4.1, a micro-electrode is measured with a Hewlett-Packard Impedance Analyser. The impedance is measured from 100 Hz to 2 MHz. The build-in function to determine the component values is used. The test is repeated multiple times, the results were identical and showed the same component values.

Table 4.1: Values of components used in the simplified electrode model, shown in Figure 4.3.

Component	Value
R_e	2 MΩ
C_e	100 pF

4.2. STATE-OF-THE-ART ELECTRODE ARRAYS

In this section the state-of-the-art available metal micro-electrode arrays will be discussed. The main advantages and disadvantages are mentioned. The advantages and disadvantages are taken into account in the next section, where a new design of an electrode array is described.

4.2.1. THOMAS RECORDING 32 ELECTRODES ARRAY

The Thomas Recording 32 electrodes array, shown in Figure 4.4, is currently used as main electrode array in recordings in the olivocerebellar system at the Erasmus MC. It consists of a large frame with 32 individually controllable tungsten/quartz electrodes, as described in Section 4.1 and 32 pre-amplifiers.

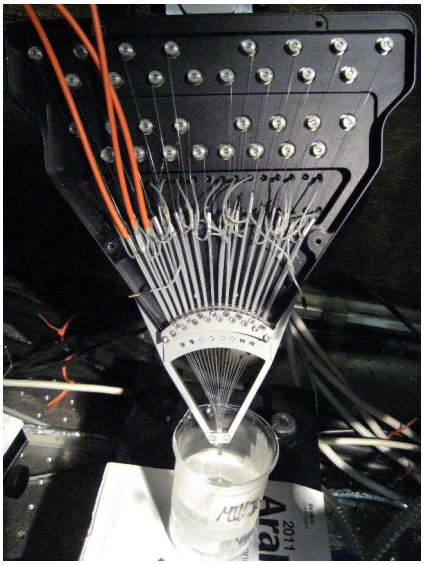

Figure 4.4: Thomas Recording electrode array with 32 tungsten/quartz micro-electrodes.

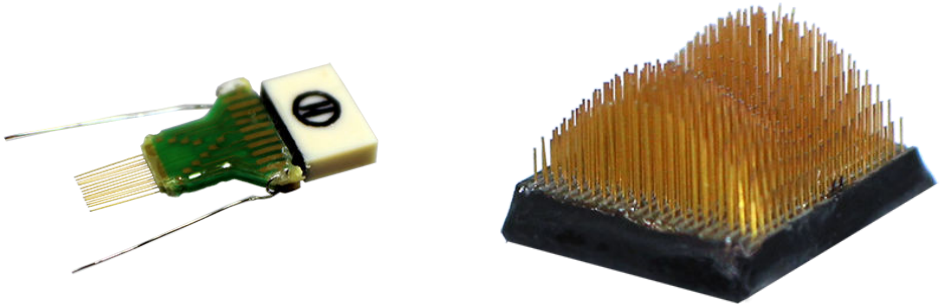

(a) (b)

Figure 4.5: Two highly customisable electrode arrays by Tucker Davis Technologies. The number of electrodes, size, individual electrode length and tip angle can be configured. (a) Omnetics based electrode array, (b) High Density Cortical Array. (Image source: www.tdt.com)

The array is mounted in a large frame around the measured subject. Each electrode is individually controlled by a step motor to control the penetration in depth of each electrode which gives a good variation in measurements. The step motors are controlled by a pulse width modulated signal, causing huge interference on the measurement, so measurement is not possible when the penetration depth is adapted. A huge disadvantage of the array is the length of the electrode wires and the connection to the digitiser. Due to these long wires, the system is susceptible to interference. Individual electrodes can be produced manually and replaced at any moment. This reduces costs and inactivity time in case of broken electrodes [25][26].

4.2.2. TUCKER DAVIS TECHNOLOGIES MULTI-ELECTRODE ARRAYS

Tucker Davis Technologies developed several electrode arrays which are highly customisable in number of electrodes, size, individual electrode length and tip angle. Two are shown in Figure 4.5, the Omnetics Based Electrodes [27] and High Density Cortical Arrays [28]. Although the arrays are customisable, the electrode tip is not polished leading to a rough contact surface instead of a smooth surface. This means the contact surface will be larger, resulting in a higher double layer impedance. The spreading resistance will be reduced, but as this is less significant than the double layer impedance, the total impedance of the electrodes increases. A rough contact surface also does more damage to the tissue.

The electrode array is laser cut, so the reproducibility is very high. But on the other hand the complete array must be replaced when a single electrode breaks down. One of the configurable options is the cut tip angle, but it can only be cut non-symmetrically. This can result in a signal transfer which is non uniform in all directions around the electrode and therefore can cause a loss of signal.

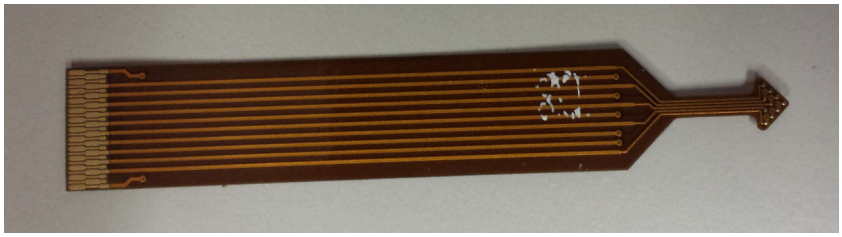

Figure 4.6: Photo of the complete Delft Electrode Array, version 1: a flexible PCB with 10 golden electrode tips. Left: connector to electronics, right: electrode tip triangle

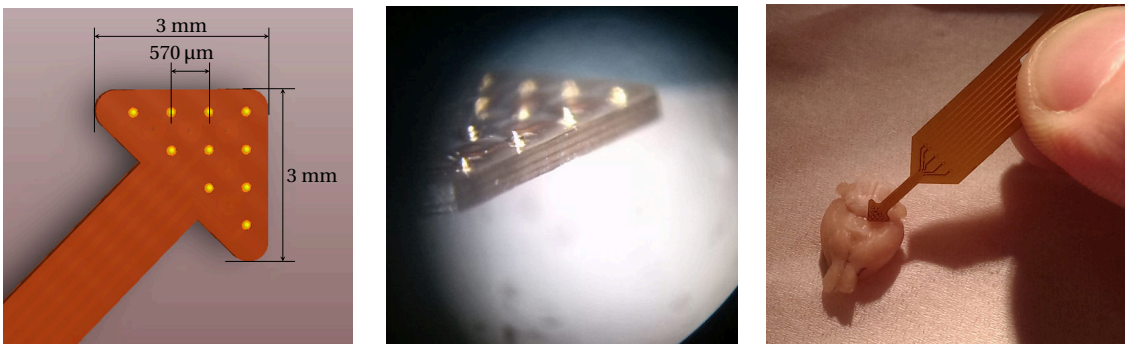

(a) (b) (c)

Figure 4.7: Zoomed in pictures of the Delft Electrode Array, version 1. (a) A schematic overview with sizes of the design, (b) a zoomed in photo of the golden electrode tips and (c) the electrode in proportion to a mouse brain.

4.3. DELFT ELECTRODE ARRAY

To improve the flexibility and to reduce the costs of measurements without loss of signal quality, a new electrode is designed. The subject to measure, in this case the olivocerebellar system in mice, is studied and discussed with neuroscientists to develop an electrode array fitting the needs of their research. A first design (Subsection 4.3.1) is developed and extensively tested. Thereafter improvements are made and a second design is fabricated (Subsection 4.3.2). Also this version is heavily tested and evaluated, followed by a last design (Subsection 4.3.3), with promising results, but still improvements are necessary for higher reproducibility.

4.3.1. DELFT ELECTRODE ARRAY (VERSION 1), 10 ELECTRODES ARRAY

With existing arrays, large, fixed setups and a bunch of large pre-amplifiers are necessary. The measured subject must be fixated and thus cannot freely move. This reduces the flexibility of measurements. There is a huge restriction in behavioural neuroscientific experiments that can be performed due to the fixated and anaesthetised subject.

DESIGN CONSIDERATIONS

Starting point for a new array is a small, robust, cheap, simple to fabricate, wearable design, with the possibility to connect it to a small wearable multichannel amplifier and digitiser placed on the mouse, but also to the existing pre-amplifiers. In the first phase of testing, the existing amplifier setup is used, to compare just the electrode array.

Metal micro-electrodes are very fragile. As robustness is one of the design specifications other constructions are studied. Noble metals won't react with the tissue, are soft and do not damage the tissue. Gold is chosen as electrode tip material for the first design, as this can be applied with the available bonding machine at Delft University of Technology.

The size of the Inferior Olivary Complex in mice is triangle shaped of 3 mm by 3 mm (see Figure 2.3). To fit the shape of the inferior olive a triangle shaped base for the tips is chosen. To fit the rounded shape of the brain, flexible material is chosen. As the individual electrodes have to be connected to pre-amplifiers, a flexible printed circuit board (PCB) is designed to combine flexibility with connectivity.

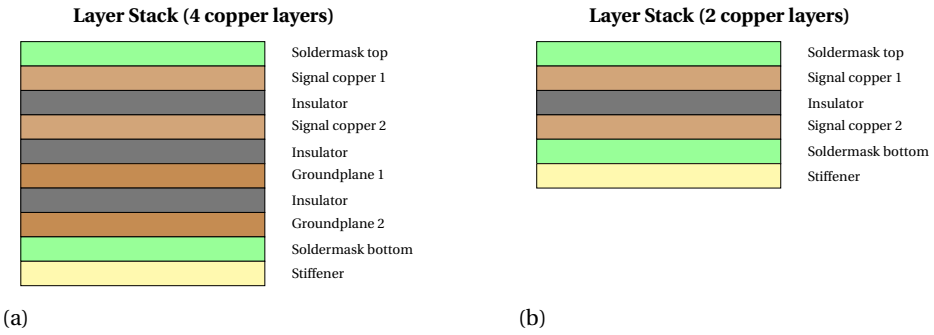

Figure 4.8: Layer stacks of PCB of the Delft Electrode Array, version 1. (a) Four layer version and (b) Two layer version.

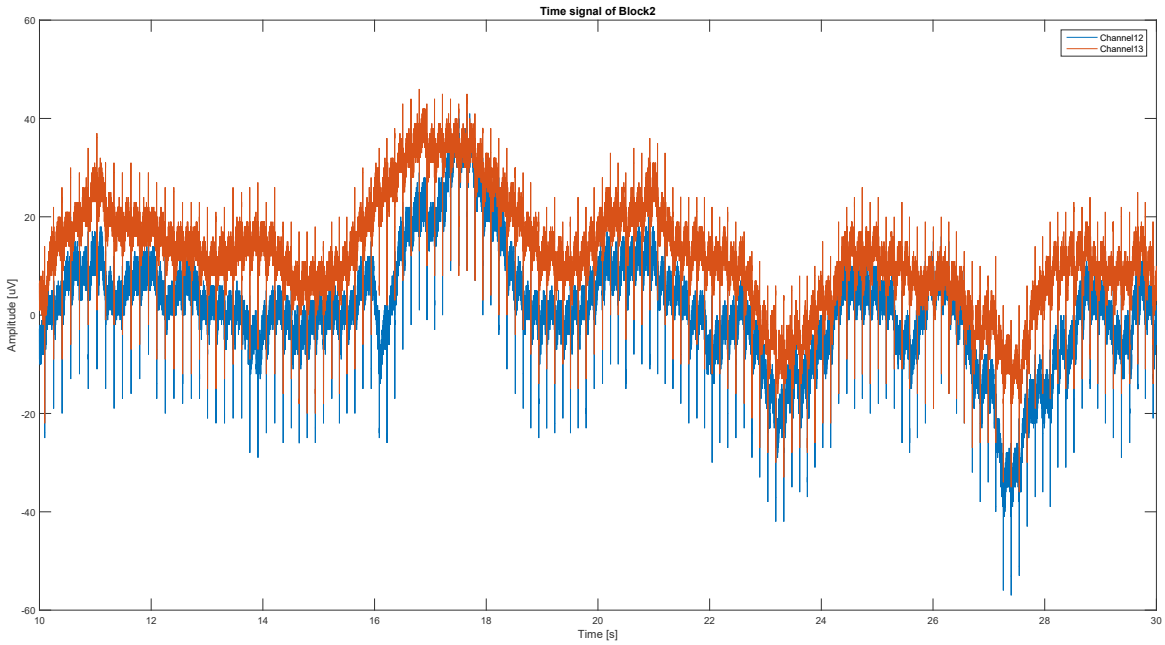

Figure 4.9: DEA version 1: raw signal of two electrode channels (blue, orange).

DESIGN

In Figure 4.6 a photo of the first designed Delft Electrode Array is shown. The connector is fabricated in two versions: with, and without ground layers. Both versions have two signal layers. In one of the versions two additional ground planes are added for extra shielding. Also a version without ground planes is fabricated to measure the difference.

At the left connector pads are visible. This side can be put in the receptor board or custom made electronics. The pads are connected via internal copper traces to the electrode tips. At the right the triangle with the electrode tips is visible. In Figure 4.7a a schematic view of the triangle is shown. The brown material is flexible PCB, the yellow dots are the electrodes. The electrode tips are golden blobs placed on a golden pad and pulled with a gold bonding machine, forming a cone with base diameter of approximately 75 µm and a height of approximately 100 µm. A zoomed in photo of the electrode is shown in Figure 4.7b. In Figure 4.7c the electrode can be compared to the size of a mouse brain. The triangular shaped tip overlaps with the olivocerebellar system.

FINDINGS

After hooking up the electrode array to the existing pre-amplifiers and bio-processor, the base material of the array is placed in a clamp to prevent it from moving during measurement. The tip is folded in a 90° angle to fit better through the opening in the skull of the mouse. The array is positioned in a way it touched the dura above the inferior olive, with the reference on the cerebellum.

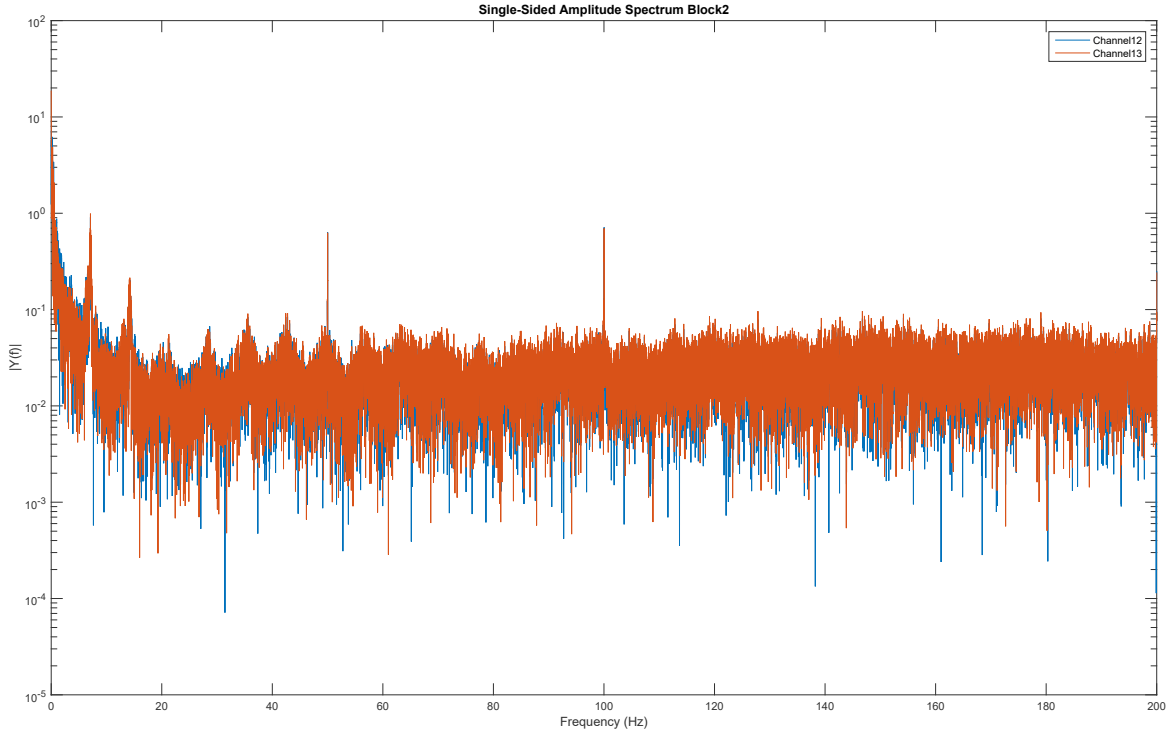

Figure 4.10: DEA version 1: FFT (0 to 200 Hz) of raw signal of two channels (blue, orange).

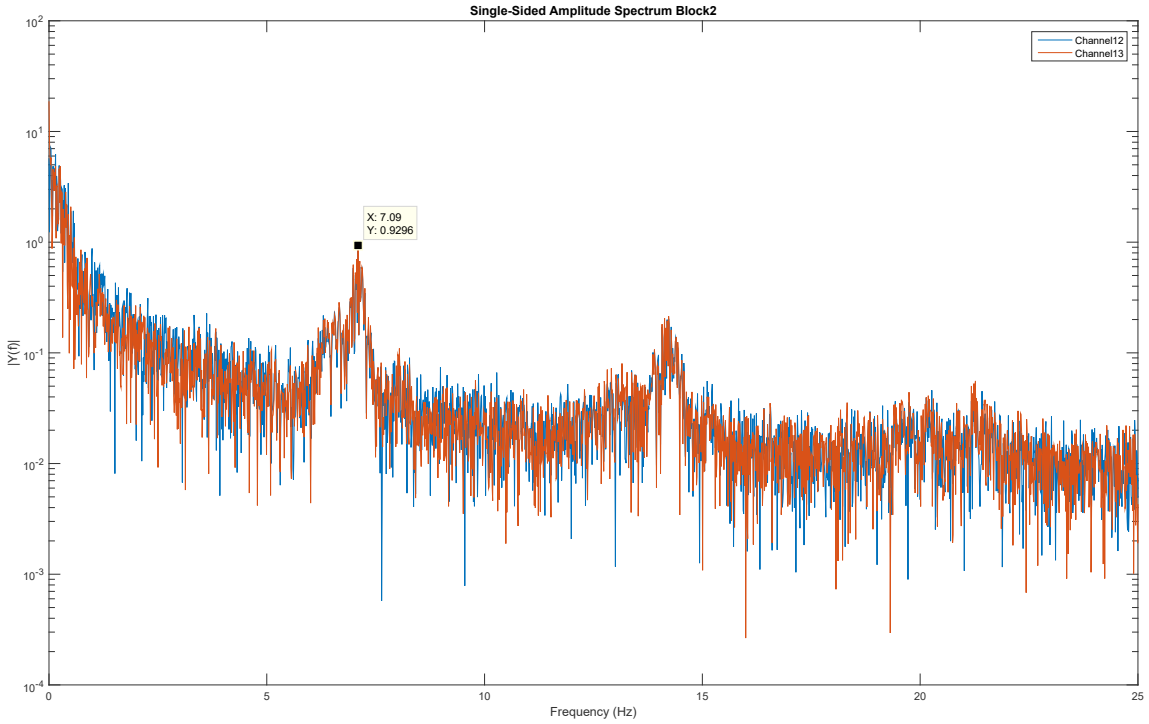

Figure 4.11: DEA version 1: Zoomed in FFT (0 to 20 Hz) of raw signal of two channels (blue, orange).

Several measurement are performed, saved in 'blocks'. The results used in this subsection are from 'Block 2'. In Figure 4.9 a measurement with the Delft Electrode Array version 1 is shown. Two channels are displayed. A lot of artefacts and interference is seen in the graph. An FFT plot of the signal is shown in Figure 4.10 and a zoomed in spectrum is shown in Figure 4.11. A strong 50 Hz signal is visible in the measured signals. It is clear the set-up is not shielded properly to EMI from the mains. Although cables are shielded, ground loops are introduced due to different grounding points in the system.

Besides the 50 Hz interference other signals are visible in the zoomed in spectrum, but all channels show the same: clear oscillations at 7 Hz, corresponding to the mouses heartbeat. After examining the placement of the electrode and the penetration depth, it can be concluded that the electrodes do not penetrate deep enough. For the next measurements the dura is cut open, to place the array underneath the dura. The array lies now directly on the inferior olive.

After placing the array underneath the dura, still all channels measure the same. Still the respiratory rate and heartbeat are clearly traceable in the measurements. As a next improvement the golden tips are insulated, except for a small tip area (approx. 25 µm diameter), so they can't make contact over the complete tip area via the brain fluids.

Although not all channels are the same anymore, there is no correlation between channels, and it must be concluded that the tips are not penetrating into the tissue and the tips are placed too far from eachother to observe phase differences. So a global measurement is performed, instead of local potentials. For behavioural neuroscientific research local potentials are of interest. Examining the shape of the golden tips after the experiment made clear the tips deformed.

IMPROVEMENTS

As the golden tips deform when put inside the tissue, gold turns out to be too soft to serve as electrode tip. Therefore another material must be found. Also the length of the tips is too small. The individual tips are placed too far from each other to observe phase differences.

Taking this into account a next design should contain stronger, longer and better insulated electrodes, placed closer to each other. The tips must penetrate far enough into the tissue. It doesn't matter if the tips are placed underneath or on top of the dura, as long as the tips penetrate into the tissue.

4.3.2. DELFT ELECTRODE ARRAY (VERSION 2), 4 ELECTRODES ARRAY

With the analysis of the results of the first design, solutions for the problems are found. Taking all findings and improvements from the first version into account, a second version is designed. To first introduce a proof of concept, the number of electrodes is reduced from ten to four. It costs a lot of effort to mount more electrodes without improving the meaning of a proof of concept.

DESIGN CONSIDERATIONS

The connection to the pre-amplifiers is good and left unchanged, so the same base material (the flexible PCB) and connector are used. Differences are only made to the tips. The tips must penetrate deeper into the tissue. Therefore metal micro-electrodes (Tungsten/Quartz) are chosen. The tip is much sharper and thinner than of the golden tips, so better penetration is expected. Because these tips are penetrating deeper into the tissue, a better distinction is made between different channels. Care must be taken with the placement of the electrodes. In the longitudinal direction, the metal micro-electrodes are very strong, but in any other direction they are very fragile.

DESIGN

The second design looks the same as the first design (shown in Figure 4.6); only the electrode tips on the triangle are different. In Figure 4.12 a schematic view shows the mounting of the electrode tips to the flexible PCB. In Figure 4.13 a zoomed in photo of the triangle is shown. Two electrode tips are mounted.

To mount the micro-electrode a hole is drilled in the flexible PCB at the place of a via, then the soldermask is partly removed from the PCB. The quartz insulation of the electrode is then removed with tweezers and the tungsten core is soldered to the via. To strengthen the electrode tips and to insulate the soldered connection, a drop of glue is placed on both sides of the PCB. All pads that are still not covered are used as a reference electrode in the brain fluid. The measured signal is thus the voltage at the electrode needle minus the voltage at the base PCB.

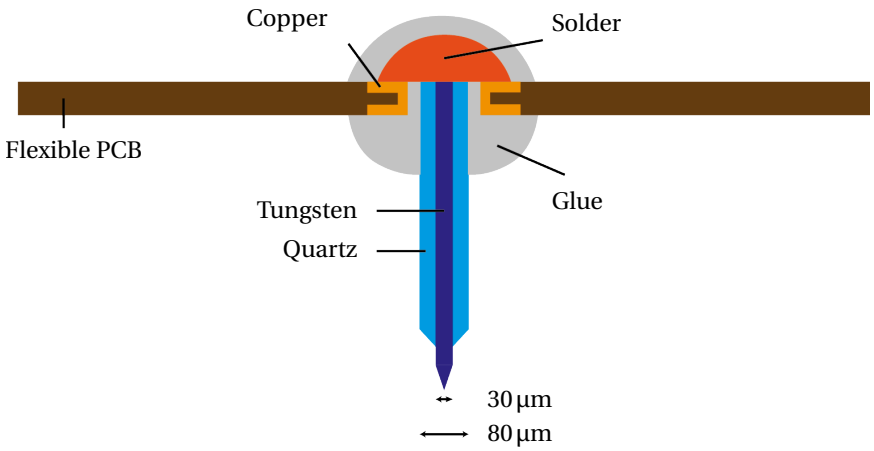

Figure 4.12: Schematic overview of the second design of the Delft Electrode Array. The mounting of a single micro-electrode on the flexible PCB is shown.

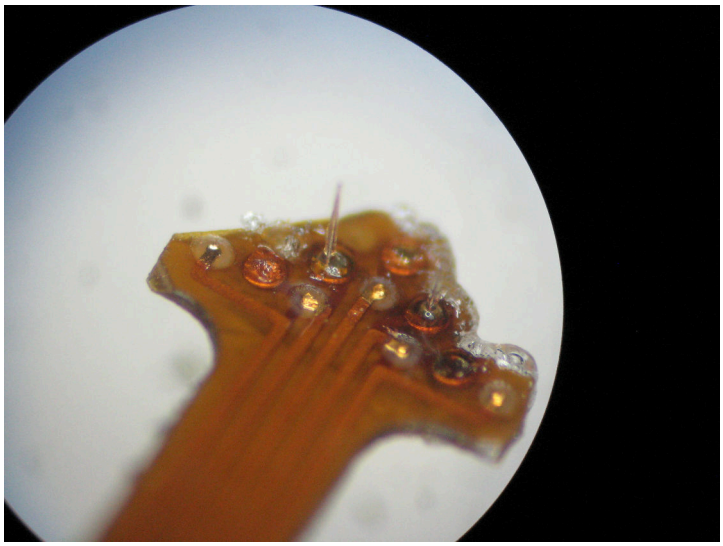

Figure 4.13: Zoomed view of micro-electrode tips. Two micro-electrodes are mounted.

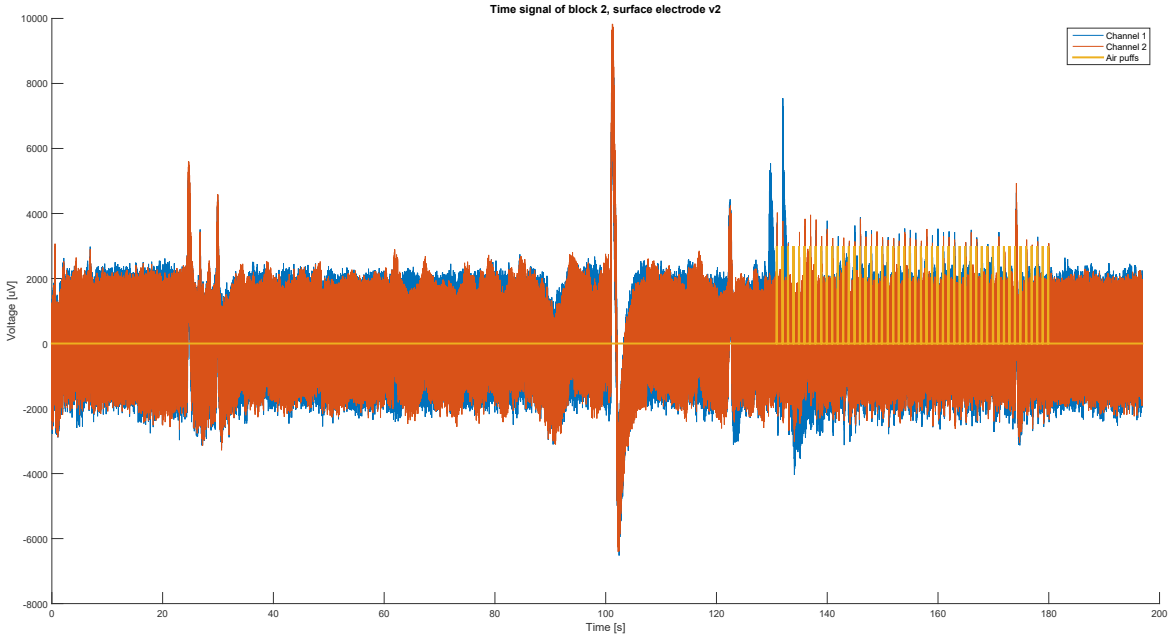

Figure 4.14: DEA Version 2: raw signal of two electrode channels (blue, orange), plotted in the time domain (full range, 0 to 195 s). Stimulation with air puffs (yellow)

FINDINGS

Also with this version, multiple measurements are performed. 'Block 2' contains the most useful data, so this block is used to explain the findings of this version.

As with the first electrode array design, the array is placed in a clamp and the triangle is folded over 90°. To put the electrode tips directly into the tissue, the dura is cut open.

During insertion of the electrode tips in the tissue, it became clear that - despite of the strengthening with glue - the array is still very fragile. It is also very difficult and time consuming to mount the electrodes on the flexible PCB.

Compared to array version 1 there is significantly less presence of the respiratory rate and the heartbeat. Although the grounding of the system and the amplifier is changed, there is still 50 Hz interference (and its harmonics) present in the signal, as can be seen in Figure 4.19, so earthing issues are not solved completely.

In Figure 4.14 the raw data of both electrode channels (Channel 1 in blue, Channel 2 in orange) is plotted from 0 to 195 s. In this recording, the mouse is stimulated with air puffs on its whiskers. it is known that with these air puffs action potentials can be forced in the olivocerebellar system. In this way it is possible to check if action potentials can be recorded with the new design. A series of air puffs (showed in yellow) is used to induce action potentials. The artefact at 100 Hz is from closing the Faraday cage and can be neglected in analysis of the signal. In Figure 4.15 a zoomed in view on the air puffs is plotted. The signal in both figures is clearly very noisy, but evoked action potentials are clearly visible. A Fourier transform is performed on the signal, plotted in Figure 4.16, to analyse the frequency spectrum. A peak is present at 450 Hz, neither a clear interference source has been found nor this frequency is expected to be present in the signal with this amplitude. A zoomed in view between 0 and 200 Hz is shown in Figure 4.17. In this plot 50 Hz and its higher harmonics (100 and 150 Hz) are clearly present in both signals. To get rid of the noise and interference MATLAB is used to apply a digital filter on the signal. As the frequency band of interest is mostly below 200 Hz, the filter is designed to focus on this frequency band. The filter consists of a infinite impulse response (IIR) comb filter and a Butterworth low pass filter (LPF). A comb filter is a filter that blocks integer multiples of its base frequencies. It subtracts a scaled and delayed version of the original signal from the original signal. This causes destructive and constructive interference, used to block and boost particular frequencies. The result is a series of regularly spaced notches. The filter is designed to block multiples of 50 Hz. The notches must be very narrow to filter only the 50 Hz component and its multiples, therefore a high Q-factor is chosen (Q = 256). The filter is applied twice, to create twice the attenuation in the stopbands.

The low pass filter is a sixth order Butterworth filter with a cut-off frequency of 200 Hz. Although the

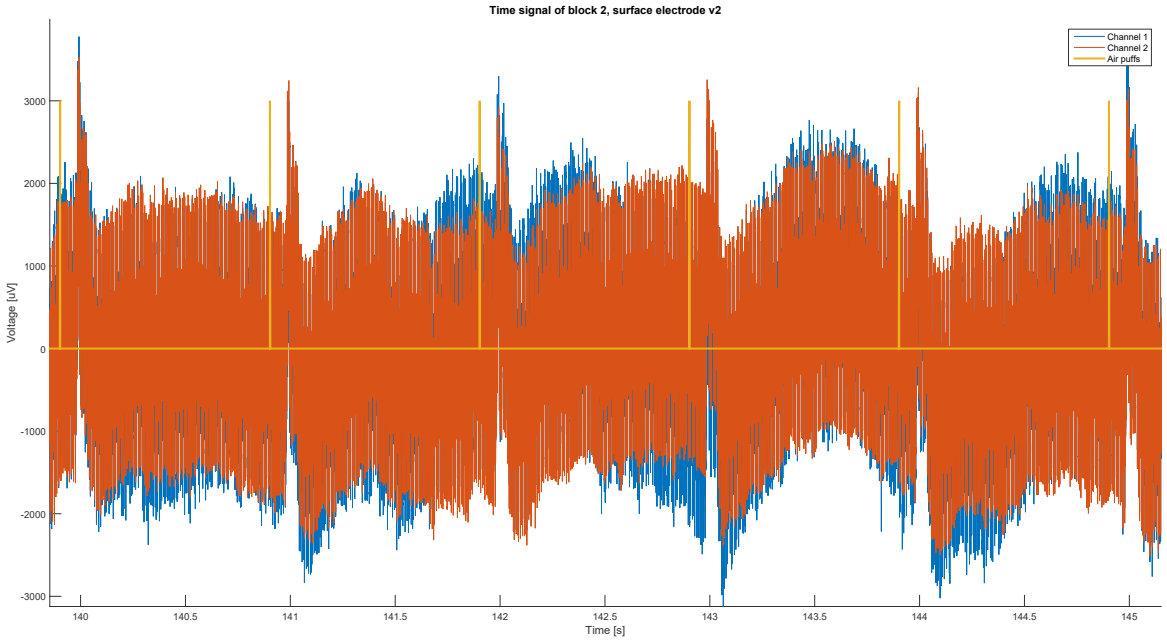

Figure 4.15: DEA Version 2: raw signal of two electrode channels (blue, orange), plotted in the time domain (zoomed in, 140 to 145 s). Stimulation with air puffs (yellow)

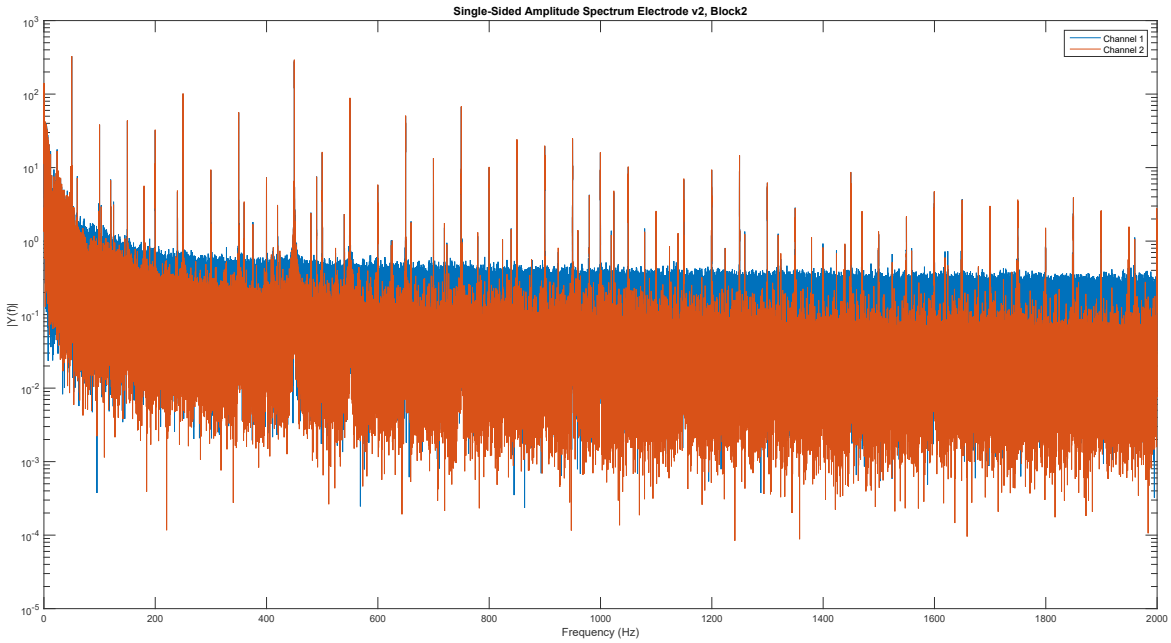

Figure 4.16: DEA Version 2: FFT of raw signal of two electrode channels (blue, orange), 0 to 2000 Hz

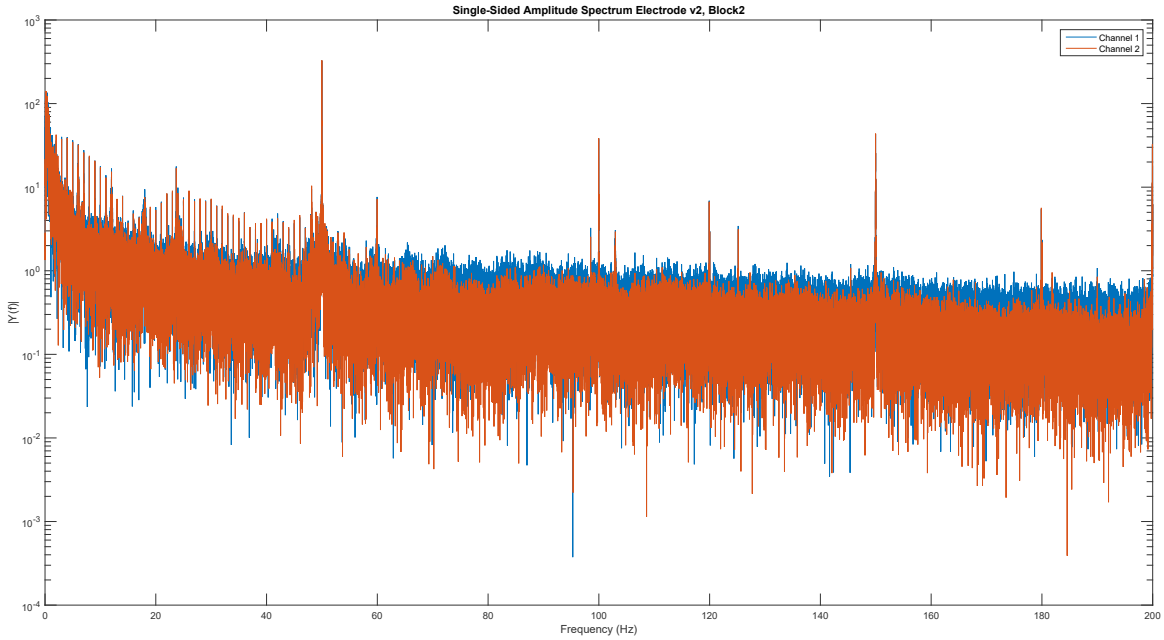

Figure 4.17: DEA Version 2: FFT of raw signal of two electrode channels (blue, orange), 0 to 200 Hz

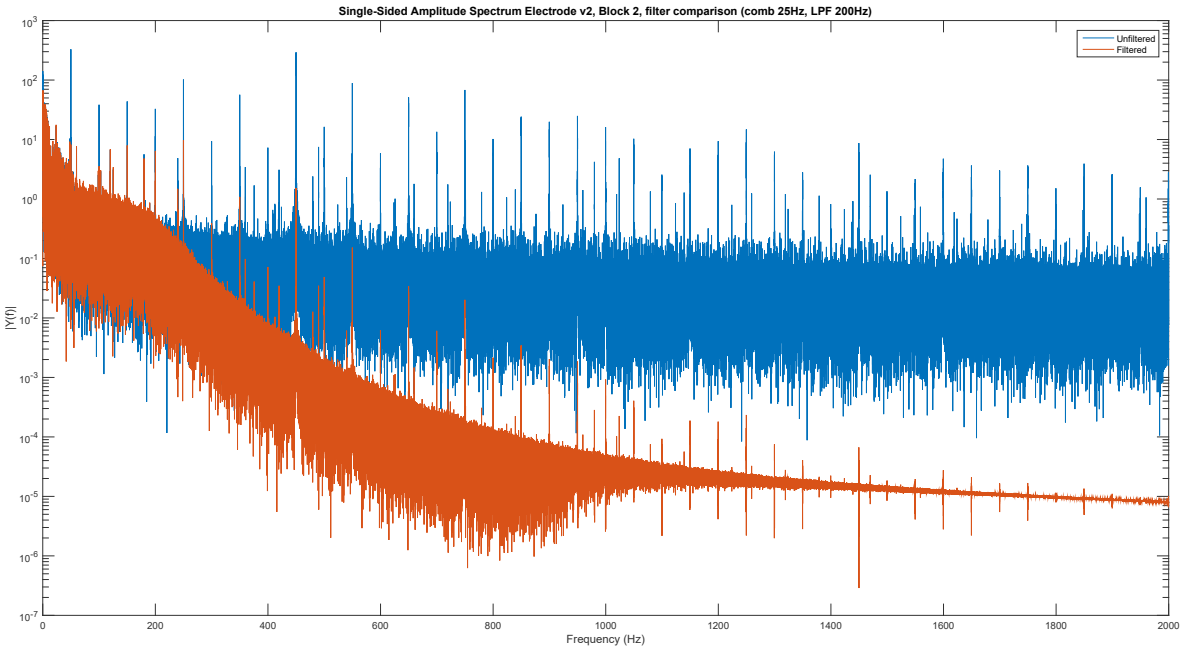

Figure 4.18: DEA Version 2: Comparison of frequency spectrum of unfiltered (blue) and filtered (orange) signal of channel 1, 0 to 2000 Hz

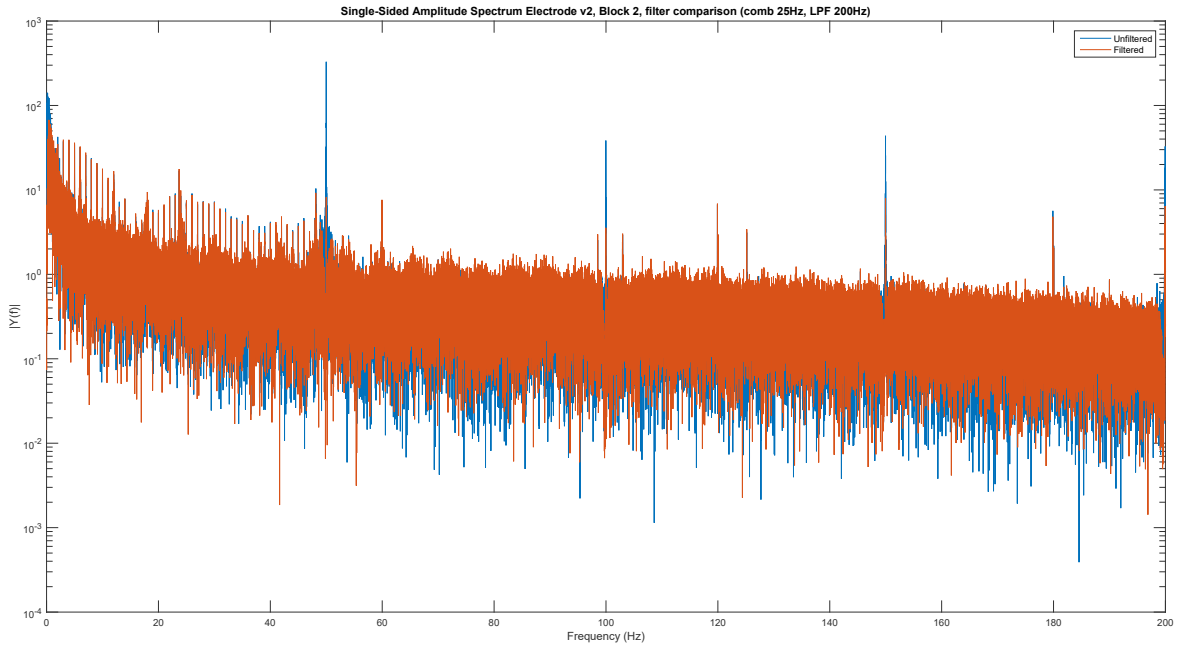

Figure 4.19: DEA Version 2: Comparison of frequency spectrum of unfiltered (blue) and filtered (orange) signal of channel 1, 0 to 200 Hz

Table 4.2: Filter specifications

Comb-filter	
Filter response	Infinite Impulse Response
Filter type	Comb-filter
Base frequency	25 Hz
Q-factor	256

Low pass filter	
Filter response	Infinite Impulse Response
Filter type	Butterworth low-pass filter
Cut-off frequency	200 Hz
Filter order	6

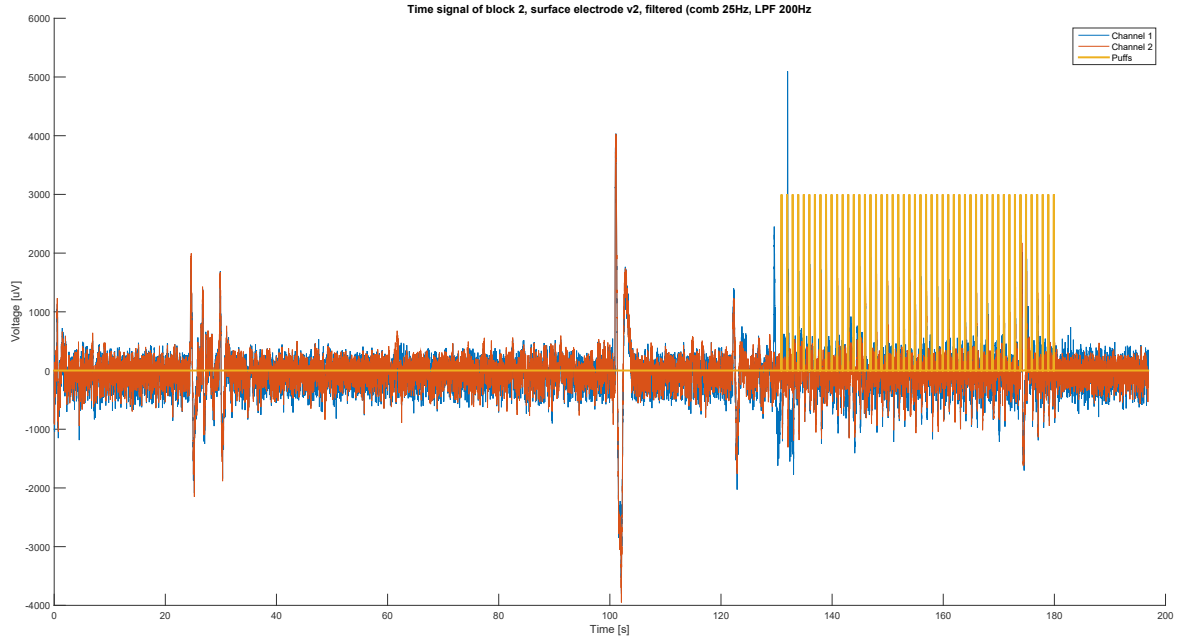

Figure 4.20: DEA Version 2: filtered signal of two electrode channels (blue, orange), plotted in the time domain (full range, 0 to 195 s). Stimulation with air puffs (yellow)

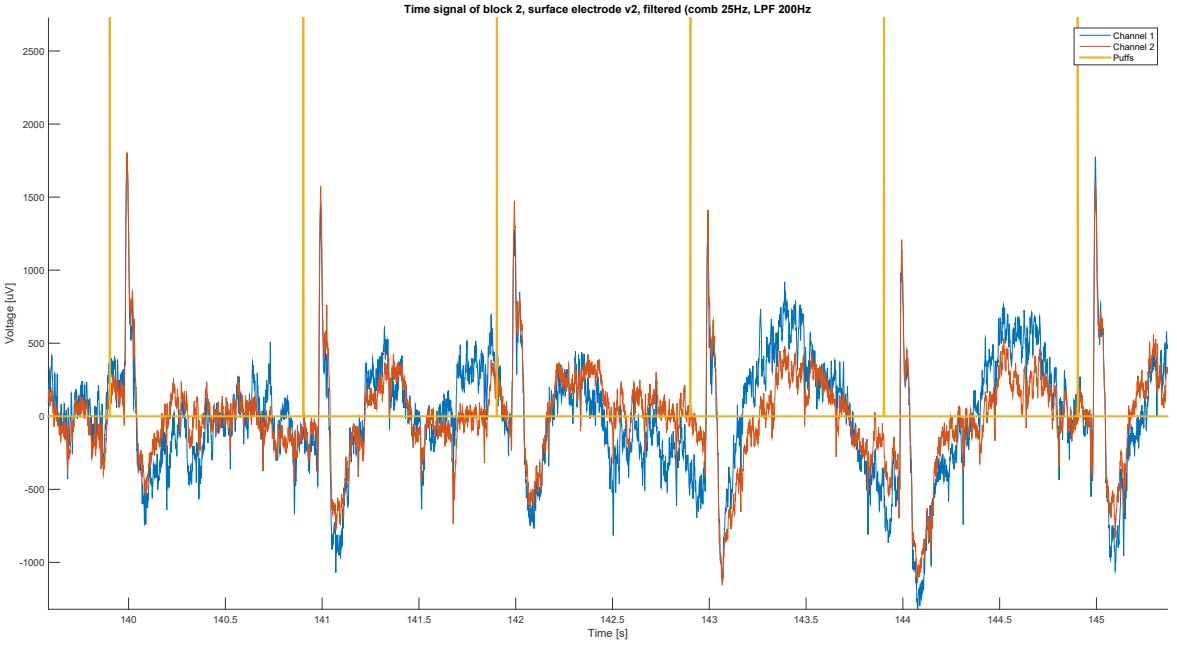

Figure 4.21: DEA Version 2: filtered signal of two electrode channels (blue, orange), plotted in the time domain (zoomed in, 140 to 145 s). Stimulation with air puffs (yellow)

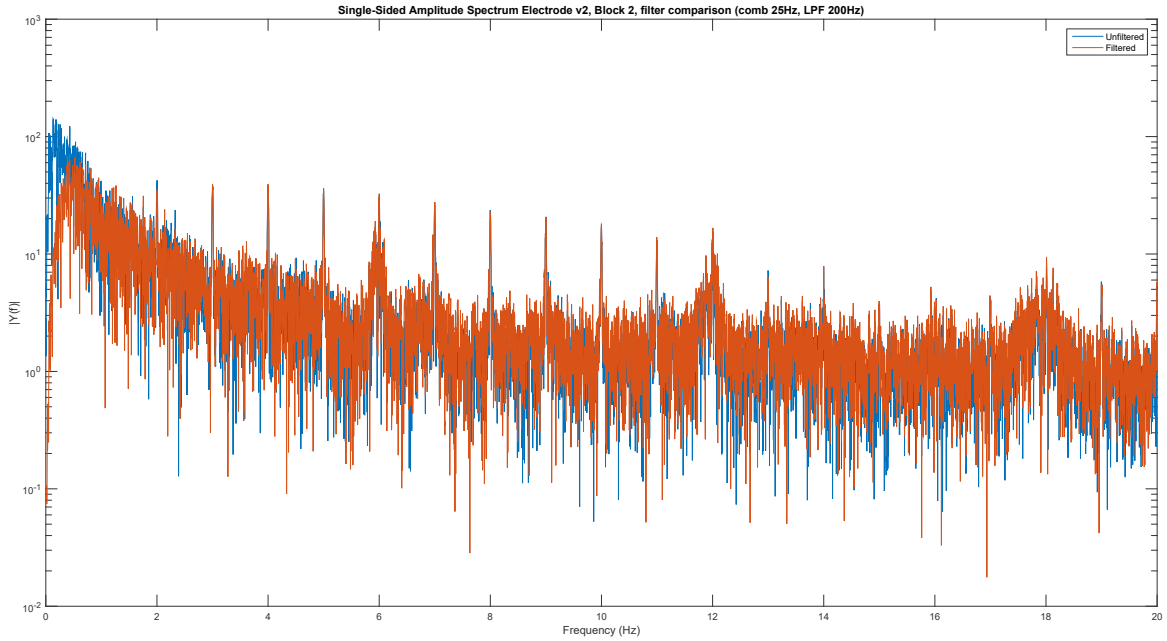

Figure 4.22: DEA Version 2: Comparison of frequency spectrum of unfiltered (blue) and filtered (orange) signal of channel 1, 0 to 20 Hz

450 Hz peak is attenuated, and the filtered signal is much less noisy, it must be noticed the depolarisation phase of action potentials contain frequencies up to multiple kHz. By attenuating all frequencies above 200 Hz, the action potentials are slowed down and slightly deformed. Despite this deformation, the action potentials are still visible, because the repolarisation and hyperpolarisation are slow on themselves. The filter specifications are listed in Table 4.2. A comparison between the frequency spectrum (0 to 2000 Hz) of the raw signal and the filtered signal is shown in Figure 4.18. The roll-off of the low-pass filter at 200 Hz can be clearly seen. After zooming in, the effect of the comb-filter is visible in Figure 4.19. The filtered signals are plotted in Figure 4.20 (full time scale, 0 to 195 s) and Figure 4.21 (zoomed in scale, 140 to 145 s). In the zoomed in plot of the filtered signal (Figure 4.21) action potentials are clearly better visible compared to the raw signal (Figure 4.15). The plotted signals correspond to the described action potentials in Subsection 2.2.3. It can be concluded the electrode array is capable of measuring the desired signals, however extensive filtering is necessary to detect them. This can be due to difficult positioning and insertion of the electrode, the fragile solder connection from electrode tip to PCB, the reference point, and ground loops introducing extra 50 Hz interference. In further designs the measurement set-up and wiring must improve to reduce the need of filters.

In Figure 4.22 a zoomed in view on the low frequencies, 0 to 20 Hz is shown. In this spectrum the most frequencies of interest for neuroscientist are present. These frequencies provide information on the present brain activity, mostly from 1 to 10 Hz. A couple of noticeable trends are visible. A difference at 0 Hz between the unfiltered and filtered spectrum is present. This is due to the comb-filter. It filters with N notches within the normalised frequency (regularly spread between 0 and 2π). As the filter is circular over 2π it also has a notch on 0 Hz.

The peaks at 1 Hz and its harmonics are due to the air puff stimulation. Peaks at 6, 12 and 18 Hz very likely represent the heart rate (and its harmonics) of the mouse. Ideally the heart rate is invisible on all channels, only on a dedicated heart rate channel. It may not be filtered out with a regular notch filter for multiple reason. At first the heart rate is not constant, secondly neural information can be present at the same frequency.

The same holds for the respiratory rate, which can introduce signals around 1.5 Hz. Ideally also an extra channel is added providing the respiratory rate. If the signals of the heartbeat and respiratory rate are presented on a dedicated channel, a combination of these channels with the neural information channels can reconstruct the pure neural information.

(a) (b)

Figure 4.23: 3D-rendered views of the Delft Electrode Array, version 3. (a) Blow-out of electrodes, small tube (electrode holder) and large mounting tube; (b) Zoomed in view on electrodes in the small mounting tube.

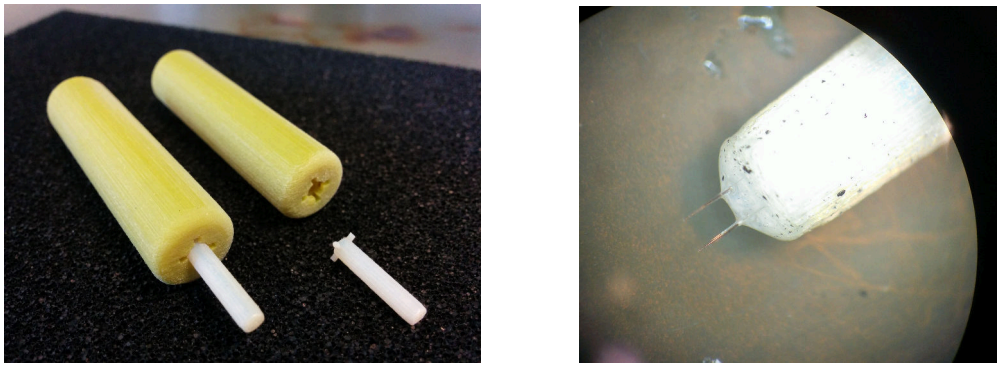

(a) (b)

Figure 4.24: Photographs of the Delft Electrode Array, version 3. (a) Small tube (electrode holder) and large mounting tube; (b) Zoomed in view on electrodes in the small mounting tube.

IMPROVEMENTS

The tungsten/quartz micro-electrode shows to be suitable for use in a small electrode array, but mounting of the tungsten wire is still an issue and certainly must be improved.

The folding of the flexible PCB gives too much uncertainty in placement of the electrodes and must be avoided. In a new design a different shape of the base material must be used.

A difficult to solve issue is the present 50 Hz interference. This can be solved in the connection to the pre-amplifiers and the pre-amplifiers itself and by taking a different reference with the corresponding grounding, but not only in the electrode array design. Therefore this will be discussed further in Chapters 5 and 6, the design of an analogue front end and measurements set-up respectively.

The presence of the respiratory rate and the heartbeat is not avoided on purpose, because these frequencies can contain interesting data for neuroscientific purposes. As long as the electrodes are positioned correctly in the tissue, the presence of these signals are not dominant and can be filtered out afterwards while interpreting the signals. Another method is to record the heartbeat and respiratory separately to subtract them from the channels with neural information.

4.3.3. DELFT ELECTRODE ARRAY (VERSION 3), 4 ELECTRODES ARRAY

Analysing the second version, and to produce a third version, a different approach is taken. Still tungsten/quartz micro-electrodes are used, but the base material and shape is different.

A detailed description of the third design is not the scope of this thesis, but can be found in [29]. In this subsection a brief overview of the design and its findings and improvements is given.

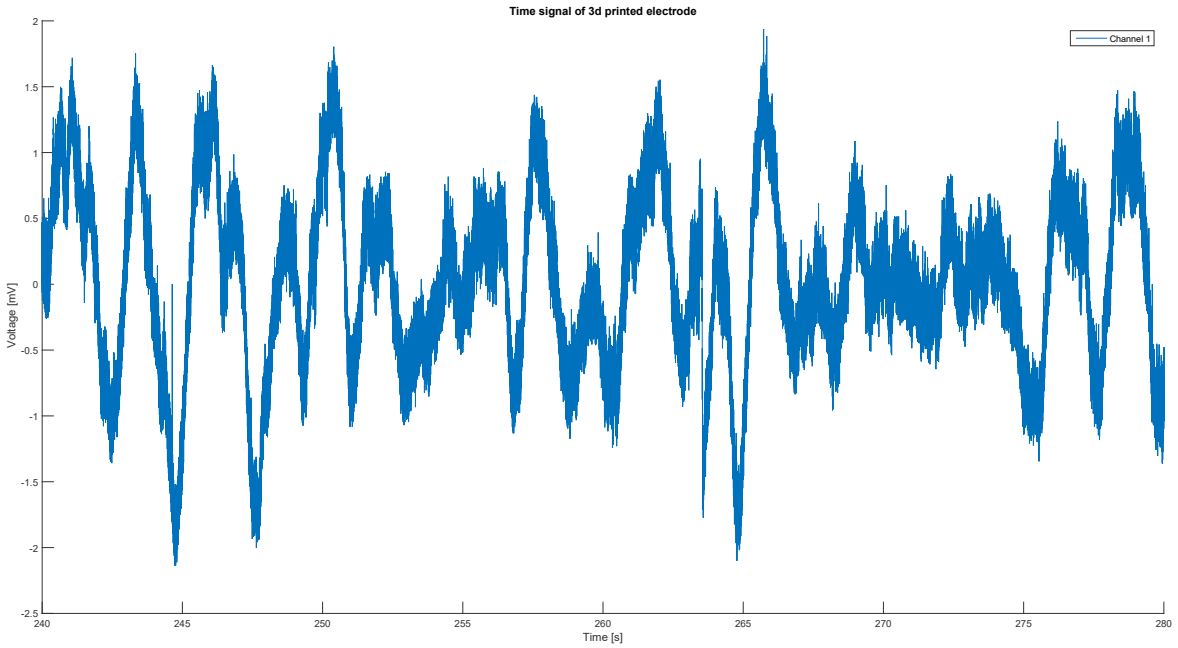

Figure 4.25: DEA Version 3: Raw signal of one electrode tip.

DESIGN

It is concluded from the second version that the electrode tip material with its short length is well suitable for an electrode array. This tip is used as starting point for the new design.

The base material and shape must be changed, so no folding is needed. An initial design requirement is cheap and easy fabrication. With this new approach, 3D-printing is investigated. This technique is cheap, fast and reliable.

In Figure 4.23 3D rendered pictures of the third version are shown. In Figure 4.23a the three different parts of the design are shown: the micro-electrode, a disposable part fabricated for each mouse (the small tube), and a permanent part as connector on to the pre-amplifiers (the large tube). In the disposable part the micro-electrodes are mounted and glued to the connector pads with conductive glue. In the large tube, the pads are made conductive with the same glue. Both parts 'click' in eachother with a bayonet coupling. In Figure 4.24 photographs of the different parts are shown.

Strain relief on the fragile electrode tips is implemented with glue attached to the end of the small tube. The electrodes have much more strength than without fixation on the small tube.

FINDINGS

The third array version seems to be much less fragile in the longitudinal direction as well as other directions, due to the glue on the end of the small tube.

The fabrication of the mounting frames (both tubes) with 3D printing technology is promising and must be investigated further to get yet more benefit from it. The mounting of the electrode tips on the other hand is very time consuming. Very carefully the electrodes are placed and glued piece by piece. When all tips are well positioned, the quartz insulation of each micro-electrode is removed and the tungsten core is glued to the corresponding pad.

A single measurement with this array is done. Due to a lack of time, mice and availability of the neuroscientist performing the surgery, it was not possible to do extensive measurements and compare these to other measurements.

The measurement is done with the amplifiers as described in Chapter 5. In Figure 4.25 the raw data is plotted. Applying the same filter in MATLAB as with the first two versions, gives the signal of Figure 4.26. In Figure 4.27 the spectrum of both signals is plotted. After zooming in (Figure 4.28) again 50 Hz interference is visible. Inspecting the measurement set-up a ground-loop is found. The mouse is lying on a platform. This platform is grounded via the Faraday cage of the existing set-up, which is grounded to the mains. The Delft AFE on the contrary is connected to the oscilloscope which is also grounded to the mains, but on another

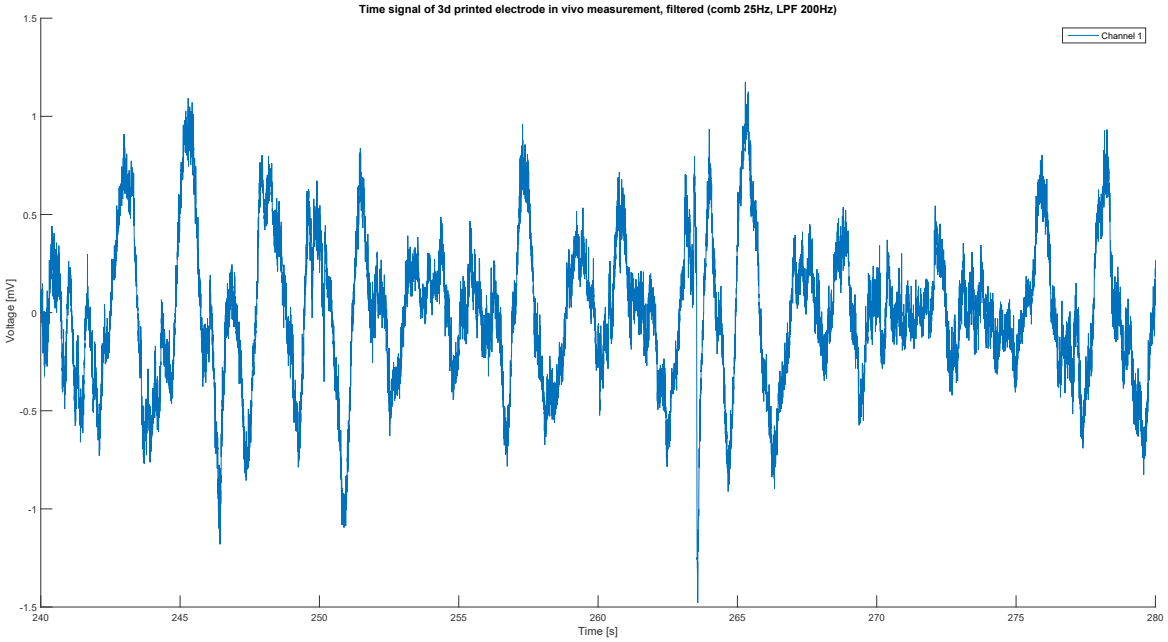

Figure 4.26: DEA Version 3: Filtered signal of one electrode tip.

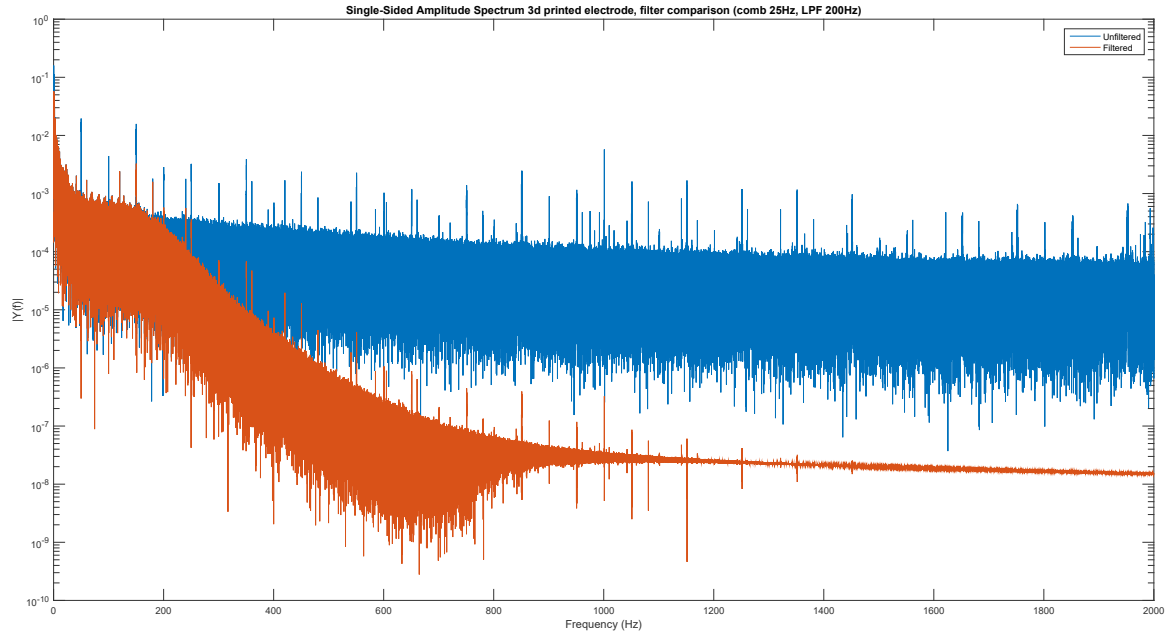

Figure 4.27: DEA Version 3: Comparison of FFT of raw an filtered signal, 0 to 2000 Hz.

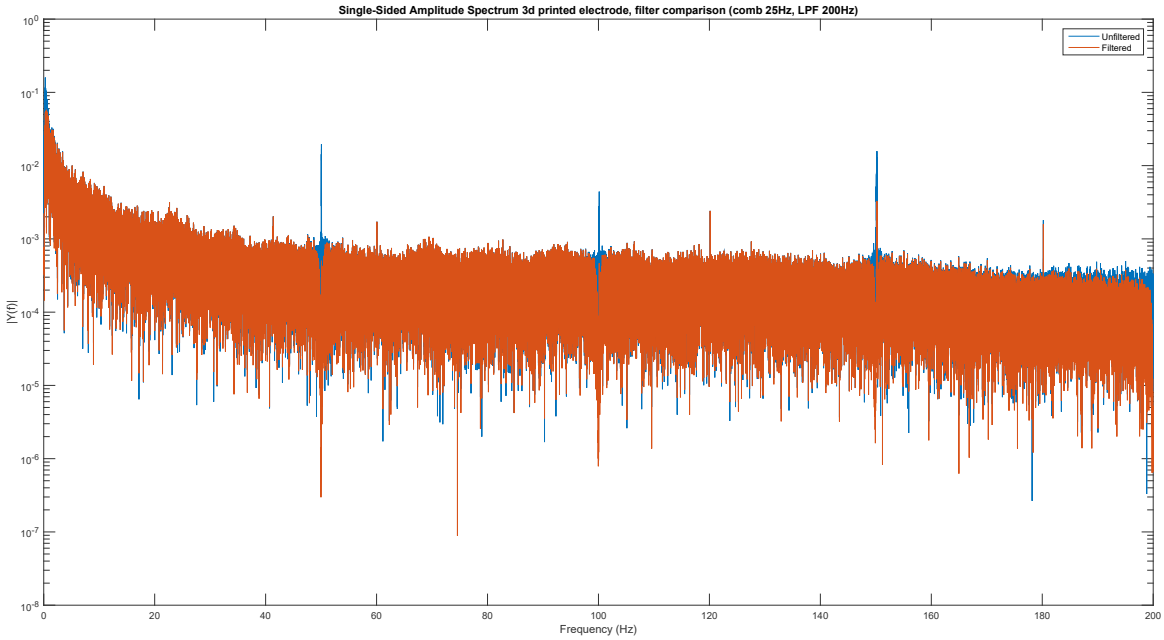

Figure 4.28: DEA Version 3: Comparison of FFT of raw an filtered signal, 0 to 200 Hz.

group. Also the last 10 cm of the wire (where it enters the large tube of the electrode) is not shielded nor twisted, possibly contributing to the interference.

Also this array is mounted in a clamp, but couldn't be moved precisely. In next measurements a micromanipulator must be used to exactly control the arrays position. After the experiment the exact location of penetration couldn't be detected, so it is not possible to say if it was in the olivocerebellar system.

It must be concluded that the measurement performed shows the connections from electrode tip to the amplifiers is right, but no conclusions about the electrical performance can be drawn.

IMPROVEMENTS

The producibility and reproducibility of the array are not as easy and cheap as expected. The 3D-printed frames are cheap and simple to use, but the mounting of the electrode tips is still custom and very time consuming. In the future, this has to be improved. In Chapter 8 this will be discussed further.

Before developing a new version of the Delft Electrode Array, this array must be completely analysed. To analyse the electrical characteristics and findings of the array to improve the array, more measurements must be performed.

4.4. ARRAY COMPARISON

In this section a comparison between the different electrode arrays is made. The chapter is concluded with a check of the design requirements.

With the Delft Electrode Array (DEA) and the Tucker Davis Technologies (TDT) array the depth of the electrodes can only be set for the whole array at once, not for individual electrodes. With the Thomas Recording (TREC) array this can be done, which brings more diversity in the measurements.

The Delft Electrode Array (all versions) is much smaller than the Thomas Recording and Tucker Davis Technologies arrays. So the DEA is much more flexible in applications, it can be used in much smaller measurement set-ups, working towards a wearable design of an array including pre-amplifiers to measure on awake mice. Because the same electrode tips as in the TREC array are used, the signal quality - with proper grounding and a good reference point - is comparable to the state-of-the-art arrays.

The TREC array is connected with relatively long cables to its pre-amplifiers, and with another long cable to a digitiser. When the DEA is used with twisted-pair, shielded cables to the pre-amplifiers described in Chapter 5 (a small box that can be placed near the measured subject), the cables are much shorter than with the state-of-the-art arrays. In this case much less interference will occur on the signals. This only holds if the measurement set-up and cable management are matched to the electrode array.

As with the TREC array, the tips of the DEA are custom made and polished. The TDT array has laser-cut tips, but not polished, resulting in a higher electrode impedance than the DEA and TREC array. Also the TDT electrodes are not symmetrical, providing an unwanted non-uniform transfer around the electrode tip.

It can be concluded that the DEA with tungsten/quartz electrode tips is better in signal quality than the state-of-the-art arrays in terms of interference, but the mounting and fabrication has to be improved. With the third version of the DEA, fabrication is made easier, but not yet simple and reproducible enough. Further research on this must take place. Extensive tests with the last version must show if the robustness and positioning (with a micromanipulator) have improved.

To conclude this chapter the system requirements from Chapter 3 and the subdesign specific requirements introduced in this chapter are recapped. The next two chapters will focus on the electronics and the measurement set-up respectively.

✓ **Material**
The material of the electrode tip used doesn't affect the tissue and it is biocompatible

✓ **Electrode size**
The size of the electrode tip is small enough to record cells and not to damage the tissue

× **Array size**
The array size is not specified in detail, but the number of electrodes used so far is not enough to measure propagation of signal on a larger scale. In next designs the number of electrodes must increase.

✓ **Connection**
It is possible to connect the electrode arrays to the existing set-up and to the newly designed analogue front end, so this requirement is met.

✓ **Impedance**
The same electrode material as with the TREC electrode array is used. The requirement of 'at most the same impedance' is therefore met.

✓ **Cheap**
The construction of the 3D-printed tubes is very cheap. Also the electrode tips are not of high costs. The only part that costs a lot of money is the production time. When this is reduced in newer versions, the costs will reduce even more.

✓ **Robust**
With the implemented strain relief, the last version of the electrode array is much more robust than its predecessor. It is also more robust than the TREC electrode array. The electrode tips still are fragile, but that is mostly due to the small sizes.

~ **Simple to fabricate**
Version 3 is the least difficult to fabricate, but it is still not simple. With a lot of patience and a good fine motor system it is possible to reproduce the electrode array, but it takes a lot of time. Not everyone has the fine motor system needed for the fabrication, let alone the patience. The simplicity of fabrication has to be improved in next versions.

5

ELECTRONICS

Neuroscientists want to investigate electrical neural activity in different areas of the brain. They want to record the signals and have a close look at the recordings afterwards. This means recorded potentials must be stored on a storage device. A lot of data is coming from the brain, especially with many electrodes simultaneous in an array. To keep this data well-organised, to access the data quickly and to apply adjustable filters, digital storage and processing is the most obvious choice.

The positioning of the electrode array and the condition of the mouse are very important during measurements, therefore also displaying the measured signals real-time is desired by neuroscientists. The displayed signals are not necessarily the raw signals, but the expected signals (e.g. sub-threshold oscillations and action potentials) must be clearly distinguishable to determine a correct positioning of the electrodes. If irregularities in the condition of the mouse (e.g. in respiratory rate and heartbeat) appear in the signal, these must be recognisable and actions can be taken to recover the mouse's condition.

To meat the requirement 'cheap' and to speed up the design process and achieve fast improvement of the measurement flexibility, custom designed integrated circuits are not an option. Over the years a huge variety of integrated circuits has become available. This work focusses on an electronic design with components already available.

In this chapter the design of the electronics between the electrode array (as described in Chapter 4) and the neuroscientists are described. First a general overview of the system is given (Section 5.1). Afterwards each block will be discussed in detail (Sections 5.2 to 5.6).

5.1. SYSTEM OVERVIEW

The input from the electrode array is a low-amplitude analogue signal ($V_{in} = \pm 3\,mV$). The recordings must be outputted to a digital storage device and real-time displayed on a screen. It is obvious that a low voltage analogue signal cannot be driven to a digital storage device without any processing. In this section a brief overview of the system is explained. In the next sections it is build up towards the total design, including trade-offs for the implementation of components.

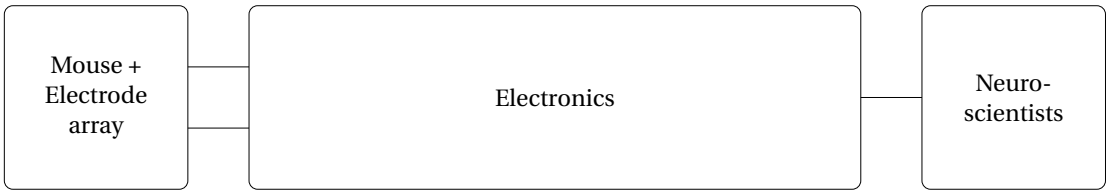

Figure 5.1: A schematic overview of the system.

In Figure 5.1 a diagram of the system overview is shown. The input is coming from the electrode array inserted in the mouse. It has an amplitude of $V_{in} = \pm 3\,mV$ and a bandwidth of $1\,Hz \leq BW \leq 10\,kHz$. The output block contains the desired output by neuroscientists: data storage and a real-time display. To convert the analogue input signal to a digital signal ready for storage and display, without significant signal loss, an analogue-to-digital-converter (ADC) is necessary. To use the full range of an ADC, and thus increase the

resolution of the digital signal, a pre-amplifier is also necessary. To control the ADC a digital controller might be useful. These components are discussed in the next section and are shown in Figure 5.2.

5.2. ANALOGUE FRONT END

To implement the design as shown in Figure 5.2, design choices have to be made. In this section a detailed description of the design choices of the analogue front-end (pre-amplifiers and ADC) is given. Starting with the core of the system, the analogue-to-digital-converter (ADC, Subsection 5.2.1), followed by the pre-amplifiers (Subsection 5.2.2) and both combined in an analogue front end chip (Subsection 5.2.3), concluded with a digital controller to possibly control the AFE (Subsection 5.2.4).

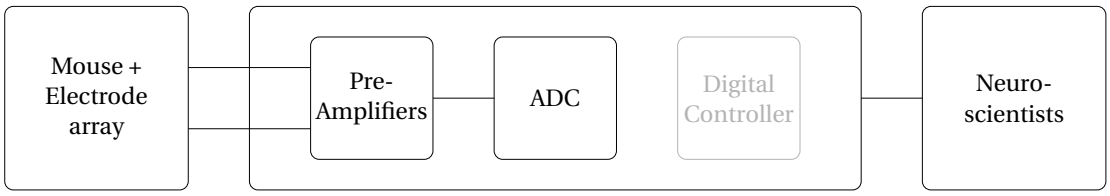

Figure 5.2: A schematic overview of the system. Pre-amplifiers and ADC are added in the electronics block. The digital control block (gray) is optional in this design stage.

5.2.1. ANALOGUE-TO-DIGITAL-CONVERTER

The core of the electronics part is the conversion from the analogue input to the digital output. The input voltage (i.e. the electrode voltage) is very low (order of mV). Multiple options are available to digitise these low voltages: an ADC with a very high resolution to measure µV or amplify the input voltage followed by an ADC. The first method is very costly and many bits are not used, the second method is more straightforward to implement.

From the requirements (Chapter 3) follows an effective number of bits (ENOB) of 7 bits, but to achieve a resolution of 10 µV over a full range of 6 mV_{pp} 10 bits are required. When the input range of the ADC is higher, the number of required bits will increase.

The system must contain many electrodes. Tens of electrodes can be necessary in the final system to measure in the olivocerebellar system. If each channel uses its own ADC, the system costs, power consumption and complexity increase very fast. To limit this increase, it is considered to use a multiplexer before the ADC. In this way multiple electrode channels are sampled by a single ADC. The downside is the sample rate of the ADC which has to be increased by the number of multiplexed inputs. Also an ADC where the next sample is based on the previous one cannot be used, because the value between to samples of one channel is overwritten by one or more other channels that use the same ADC.

5.2.2. PRE-AMPLIFIERS

As described above, to utilise the full range of the ADC, and therefore achieve the best resolution at the output, a pre-amplifier stage must be added. The input signal has a range of V_{in} = 6 mV_{pp}. The input voltage range of an ADC differs from chip to chip, but varies between 1.8 V_{pp} and 5 V_{pp} for the chips considered in this work, implying an amplification factor of 300 to 800. When an input stage with amplification factor 500 is used, the gain-bandwidth product (GBW) must be at least 5 MHz.

The input impedance of the first amplifier stage must be much higher than the impedance of the electrode. If the input impedance is too low, the amplifier can load the electrode too much and it can affect the output voltage of the electrode stage. As the electrode impedance can be as high as 1 MΩ at 1 kHz, the input impedance of the amplifier should be at least 9 MΩ if the voltage may not drop more than 10 percent compared to an infinite input impedance.

As the system is most likely to be scaled up to a lot of electrodes, it is better to have more amplifiers in a single package. The more packages are needed, the larger the design will be. The size of electronics (including the printed circuit board) in the system must be reduced to make the design scalable and wearable (in the future).

Taking both considerations (from the ADC and the pre-amplifiers) into account, a closer look is taken at total packages, containing multiple pre-amplifiers and one or more ADC's. In the next subsection three commercially available off-the-shelf analogue front-end chips are considered and discussed.

5.2.3. ANALOGUE FRONT END

A couple of integrated circuits (IC's) containing both pre-amplifiers and ADC's are available particularly designed for low voltage systems. The ones considered are listed in Table 5.1 and discussed in the subsequent paragraphs.

Table 5.1: Overview of commercially available off-the-shelf (COTS) analog front-ends.

Name	Channels	Power (mW)	Noise	Notes
AD ADUCM360	12	6	-	Microcontroller with AFE
TI ADS1299	8	30	-	Single ADC per channel
Intantech RHD2132	32	2-5	-	Multiplexed ADC

ANALOG DEVICES ADUCM360

This device is - in contrast to the other two mentioned - designed around a microcontroller (MCU). It provides two 24-bit ADC's and a multiplexer which can make combinations of the 12 inputs (single ended or differential). The chip does contain amplifiers after the multiplexer. So far it sounds very suitable for our application, but the sample rate of the ADC's turn out to be 3.9 kSPS, which is not enough to measure signals up to 10 kHz [30].

TEXAS INSTRUMENTS ADS1299

Texas Instruments (TI) has developed a series of front-end chips for dedicated use with electrocardiogram (ECG) and electroencephalogram (EEG) measurements. As ECG is measured at frequencies below 500 Hz, the chips designed for ECG are not suitable for our application. The chip in the series designed for EEG turns out to be suitable for the application. It has 8 channels, each having their own amplifiers and ADC. The resolution of the ADC is 24-bit, a bit of an overkill for this work. Each channel having their own signal path do have their trade-off: power consumption. Multiple ADC's running in parallel will increase the power consumption dramatically. On the other hand, no synchronization problems or delays occur when all ADC's sample at exactly the same time. This can save processing power afterwards. All filters in this chip are delivered 'as is' and are not configurable [31].

INTANTECH RHD2132

Another chip containing amplifiers and an ADC is Intantech's RHD2132. 32 channels, 2x 32 amplifiers (two stages), 1 multiplexer, 1 16-bit ADC and digital control are packaged in one chip. Designed for EEG applications, but also very useful in other biopotential measurements, according to the manufacturer. The chip also contains tunable filters for the amplifier stages, and a digital signal processor (DSP) to remove DC-offset afterwards. The power consumption of this chip is much lower than the ADS1299, because it just uses a single ADC. The RHD2132 is configured and controlled by a digital controller via an SPI-bus (Serial Peripheral Interface) [32].

With the eye on scalability and wearability the RHD2132 is chosen. The number of channels is much more of importance when measuring propagation of signals through the brain than an extreme high resolution. All signals must be recognisable in their shape and timing must be correct, but a higher resolution is not necessary. With the RHD2132 the system is scalable in multiples of 32 electrodes per chip. The size of the electronics will only increase when an extra chip is placed in the system. Per 32 electrodes, the system will be of the same size.

5.2.4. DIGITAL CONTROLLER

To control the ADC and to get the desired output format, a digital controller might be useful. Depending on the other tasks the digital controller must perform, a system must be chosen. The systems considered are a Microcontroller (MCU), a Complex Programmable Logic Device (CPLD) and a Field Programmable Gate Array (FPGA). The main task will be to control the ADC and to process the data to the right output format (i.e. a storage device and a display). The controller can be extended with digital signal processing (DSP; see Section 5.3) to apply for example filtering.

Microcontrollers are often programmed in C or C++, CPLD's and FPGA's must be configured using a hardware description language (HDL). There is a fundamental difference between both: C is a *programming* language, so it provides a program using a fixed set of instructions. The processor follows this program but

cannot execute more parallel processes than the number of cores. HDL is a *description* language where a description is given of the connection of logic gates to each other. With this hardware connection a fixed functionality is given to a sub-block on the CPLD or FPGA. As many sub-blocks can work in parallel as wanted. In this way it is possible to create multiple parallel processes working each having their own functionality.

A MCU has the advantage above an CPLD or FPGA that it is simple and fast programmable and configurable, also by scientists other than engineers. On the other hand CPLD's and FPGA's have the ability to be more precise with an eye towards timing because it can contain many parallel processes.

Keeping simplicity in mind, a microcontroller is chosen for the proof of concept stage. As soon as the system scales up and data processing (see Section 5.3) becomes more extensive, the switch to a CPLD or FPGA can be made. In this stage of the design a microcontroller serves well, and is much faster in development.

A development board with an NXP LPC4357 Cortex M4/M0 was available at the laboratory, so this was used. It is not chosen because of its functionality or optimal performance for this design. It is capable of performing all tasks and it doesn't limit the functionality of the total design, but it costs a lot of power. In further design stages, the digital controller must be optimised, but in that case an CPLD would be recommended. In Figure 5.3 the design so far is shown.

CPLD's and FPGA's look very similar, both are configured using a HDL, both are based on hardware performing a dedicated task and timing and synchronisation is in both very accurate, but they differ fundamentally in architecture. An FPGA is a programmable gate array based on look-up-tables, CPLD's are based on a sea-of-gates. FPGA's are used in larger systems, CLPD's are more suitable for smaller, portable and wireless designs, where it can reach a very low static current. For future designs a closer look must be taken to determine which device is more suitable to use. It is clear an FPGA or CPLD should do the work instead of an MCU.

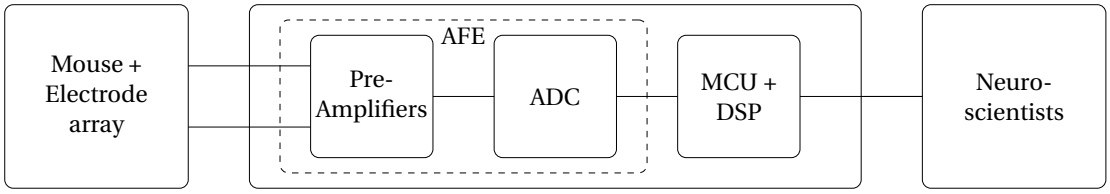

Figure 5.3: A schematic overview of the system. Pre-amplifiers and ADC are merged into AFE. The digital control block is implemented with an MCU and DSP to control the AFE.

5.3. DATA PROCESSING

The low voltage input signal also contains unwanted signals like noise and interference. Unwanted signals outside the signal bandwidth can be removed by applying digital filters to the digitised signal. The system is designed to be universal, so the data processor must be configurable to change the filters according to the measured brain area.

In this design only a digital high pass filter is implemented in the RHD2132 to reduce the DC-offset. A digital configured analog bandpass filter is configured to also limit the noise to the signal bandwidth. In a further stage more advanced filters can be applied to further improve the signal quality.

The digital highpass filter has a cut-off frequency of 0.3 Hz. It is implemented as an infinite impulse response (IIR) filter or order 1. The bandpass filter used in the RHD2132 has a high pass component of order 1 with $f_{c,hpf} = 0.5$ Hz. The low pass component of order 3 has a cut-off frequency of $f_{c,hpf} = 20$ kHz.

5.4. DATA STORAGE

To store data, there are two options possible: a direct storage device or store data via a link to a PC or server. In the next subsections both options will be compared and one is chosen.

5.4.1. DIRECT STORAGE

A direct storage device is attached to the digital controller in the system. Data is directly written to it without the need of an additional device, e.g. a PC. Some examples are Hard Disk Drives (HDD), flash drives, USB storage devices or SD cards. In this design the latter one, SD card, is chosen, because of its write accessibility and file system (FAT).

5.4.2. LINK TO PC

For storage via a PC-link a communication protocol must be used. Nowadays USB is the most commonly used protocol, but because of timing issues, the implementation of it on a microcontroller is very hard. Besides that, USB cannot claim high priority interrupts on a PC and a dedicated driver must be written for use with a PC.

Another option is a RS232 serial port, which can claim a high priority on a PC and is simple to implement in a driver, but it will limit the data rate of the system substantially. The maximum supported speed of RS232 is 115200 baud, which equals a data rate of 14.4 kB/s. With some tweaking a speed of 921600 baud can be reached, which equals 115.2 kB/s. If an ADC with a resolution of 16 bits is used, a maximum sampling rate of one channel at 57.6 kHz can be reached. This will limit the sampling frequency dramatically when multiple channels are measured.

A completely different communication protocol is Ethernet. For example a connection with a server can be made to save data remotely. The communication is platform independent, and data can be accessed everywhere in the network. A huge disadvantage is the driver on the microcontroller. Due to timing issues and the complexity of layers in the ethernet protocol it is very hard and time consuming to implement it on a MCU or FPGA.

With an eye on future work, including a wearable measurement system with a wireless link, the choice has been made to implement the most convenient storage option, a SD card. In a future design this is still a good choice for local data storage if the wireless link is down. All PC links are unsuitable in this situation, and a HDD and USB solution take a lot of space.

5.5. DATA DISPLAY

A real-time display of the measured signal is a requirement set by the neuroscientists. The microcontroller chosen has the option for an audio output. This output is used to provide an analogue output signal with the same bandwidth as the signal bandwidth to an oscilloscope. The choice can be made to let the system work autonomously (only data storage, no display attached) or with a display attached. All components in the block diagram are implemented, as shown in Figure 5.4. In Section 5.8 a detailed diagram (Figure 5.5) is discussed.

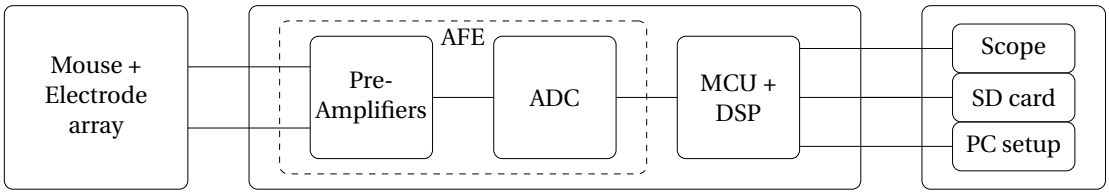

Figure 5.4: A schematic overview of the system. Data displaying and storage is implemented with and oscilloscope (to display data), SD card (to store data) and a PC (to configure the AFE).

5.6. POWER SUPPLY

To supply power to the circuit, three alkaline batteries are used in series (nominal voltage: 4.5 V). To keep a constant voltage of 3.3 V on the circuit a voltage regulator is used. To prevent interference from the voltage regulator no switched mode power supply is used, instead a low drop-out regulator is used (Texas Instruments LP38690).

5.7. ACCESSORIES

To connect the AFE to the electrodes and to make the total system robust, attention is given to all wiring and connections with the AFE.

5.7.1. WIRING

All signal cables from electrodes to the pre-amplifiers used in the set-up are shielded twisted pair cables, causing the least interference. In Subsection 6.2.3 a detailed description on cable management is given. The SPI-bus is connected with shielded cables between the analogue front-end and the microcontroller.

5.7.2. CONNECTORS

The shielded twisted pair cables are connected at the analogue front-end side with three-pin mini-XLR connectors, providing a robust connection. The battery pack is connected with a DC-plug socket. The SPI-bus is connected with default pin header connectors.

5.8. TOTAL SYSTEM DESIGN: THE DELFT AFE

In Figure 5.5 a schematic diagram of the total design is shown. All earlier described sections are combined into the total diagram. The analogue front end chip (RHD2132) is placed inside a Faraday cage. The shielding of the wires is connected to the Faraday cage. All grounding in the circuit is provided by the power supply (battery and voltage regulator). All electrodes are connected via twisted-pair shielded cables. The complete design is called to its roots and function: *Delft Analogue Front End*, shortly Delft AFE. In the next chapter, the measurement set-up is described in detail. In Chapter 7 the Delft AFE is tested electrically and with in vivo measurements. The requirements will be evaluated in that chapter.

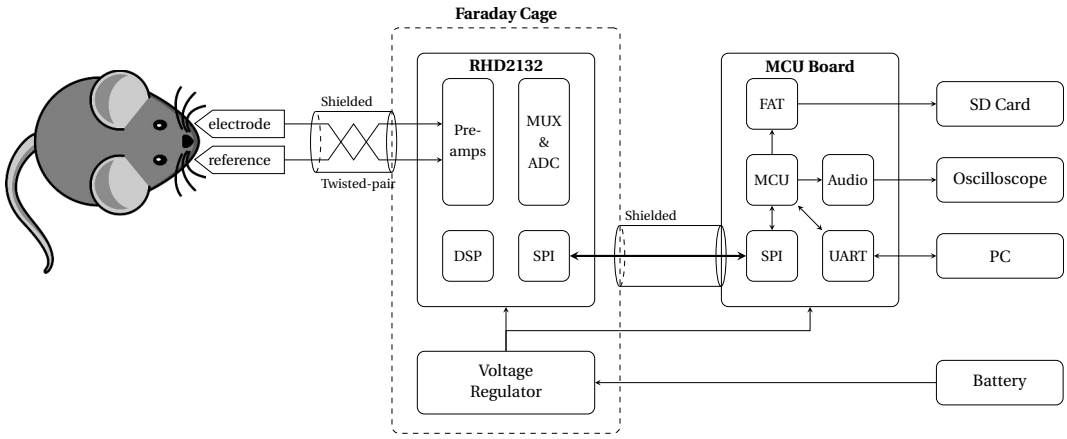

Figure 5.5: A schematic overview of the measurement system. The electrodes are connected via shielded twisted-pair cables to a small box. Inside the box an RHD2132 chip and a voltage regulator are active. An SPI-bus connects the electronics inside the box to an MCU-board. The MCU writes the data to an SD card, is configured via a PC and outputs recordings on its audio output to an oscilloscope.

6

MEASUREMENT SETUP

To record data, without losing useful data and without adding unwanted data, and to be able to analyse signals afterwards, a proper measurement set-up is required. Voltages in the order of µV and mV must be measurable in the brain, so a very small difference or imperfection in a set-up can have a huge effect on the recordings. This chapter first describes the present set-ups (Section 6.1) in two labs at the Department of Neuroscience in the Erasmus Medical Center (EMC), improvements that can be made to these set-ups (Section 6.2) and a new proposed set-up matched to the Delft Analogue Front End (Delft AFE, see Chapter 5) in Section 6.3.

6.1. ORIGINAL SET-UP

This work participates in two projects at the Department of Neuroscience of the Erasmus MC. The first - and original starting point of this work - is an array measurement in the olivocerebellar system. The second is for investigating (and detecting) epileptic seizures. Both have their own measurement set-up, explained in Subsections 6.1.1 and 6.1.2.

6.1.1. MEASUREMENT SET-UP: OLIVOCEREBELLAR SYSTEM

The first set-up described is used to perform extracellular recordings to measure low frequency sub-threshold oscillations and action potentials. A schematic overview is given in Figure 6.1.

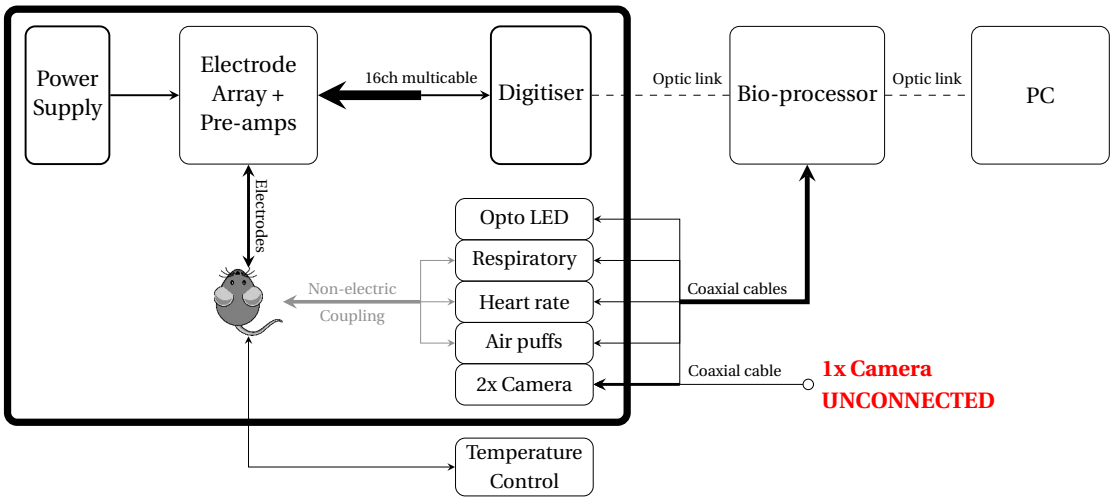

Figure 6.1: Schematic overview of the measurement system to perform extracellular recordings in the Olivocerebellar system. The mouse is placed in a Faraday cage, the signals are pre-amplified and digitised, and sent to the bio-processor via an optic link.

FARADAY CAGE

As can be seen in the schematic overview in Figure 6.1, the mouse, the electrodes, the digitiser and some other equipment to monitor and to control the mouse is placed inside a Faraday cage to reduce the effect of electromagnetic interference (EMI). With a closed conducting surface, the redistribution of charge inside this conductor provides a zero flux inside the closed surface (i.e. inside the Faraday cage).

The cage is constructed shock-free. The front cover can be opened and closed to access everything in the cage. Every side of the cage is connected to each other and to the power ground of the mains. A black cover curtain is placed over the cage to block the mouse to react to light.

MONITORING AND STIMULATING

The mouse is under anaesthesia, and fixated with the pedestal on its head. During surgery and measurements, the temperature is controlled, and its respiratory and heart rate can be monitored.

With air puffs on the mouses whiskers brain activity can be induced. Also LEDs can be lit to let the mouse react on visual light. With these techniques behavioural experiments can be done.

All equipment used to monitor the mouse, is connected to analogue channels of the bio-processor. The stimulation equipment is connected to digital outputs of the bio-processor.

Inside the cage there are two cameras, one portable, one fixed on the roof of the cage, pointing downwards on the mouse. Both are used to link movement to the measured brain signals. When the cameras are not in use, the cables are unconnected.

ELECTRODE ARRAY AND AMPLIFIERS

An electrode array of 32 Tungsten/Quartz micro-electrodes (see Section 4.1 and Subsection 4.2.1) is mounted in a large frame around the mouse. All electrodes in the array can be individually controlled in the longitudinal direction by a motor controller (Thomas Recording 2x EMST-8, 1x CPU ST10).

In the electrode array (Thomas Recording), a set of pre-amplifiers is present, fed by a battery supplied power supply (Thomas Recording Accumulator 2x 6V, 3600mAh). The pre-amplified signal is sent to a multichannel digitiser (Tucker Davis Technologies PZ5). The digitiser is connected via an optic link to the bio-processor (Tucker Davis Technologies RZ2) placed outside the cage. The digitiser can be configured with different filter and amplifier settings per channel.

Also the bio-processor can be configured with extensive DSP filters per channel. The processor is connected to a computer also via an optic link. All configurations (digitiser and bio-processor) are set via the interface on the PC.

CABLE MANAGEMENT

All cables inside the Faraday cage are shielded with aluminium tape, connected to the cage. The connection from the electrode array pre-amplifier to the digitiser is a thick multicable (15mm outer diameter, 16 channels) passed into a very thin multicable (2mm outer diameter, 16 channels).

READOUT

The bio-processor is the core of the measurement set-up, and is controlled via a connected PC. On the PC all channels can be configured and displayed real-time on a screen. The system can be controlled with dedicated software, or via National Instruments Labview.

6.1.2. MEASUREMENT SET-UP: EPILEPTIC SEIZURE DETECTION

The other set-up is used to perform both electrocorticogram (ECoG) recordings (low frequency, low pass cutoff at 500 Hz) and single cell recordings (bandwidth of 20 kHz). With these measurements research on epileptic seizures is done. Optogenetic stimulation is present in the set-up to suppress seizures. Figure 6.2 gives the schematic overview of this set-up.

FARADAY CAGE

Everything in this set-up, except for the amplifier, the analogue-to-digital converter and the PC is placed in a Faraday cage. To monitor the mouse and lab equipment, the front cover is always open, so no closed conducting cage is present, so there is no reduction of EMI. The surface of the conducting enclosure is not closed, so there can be flux - and thus EMI - inside the cage.

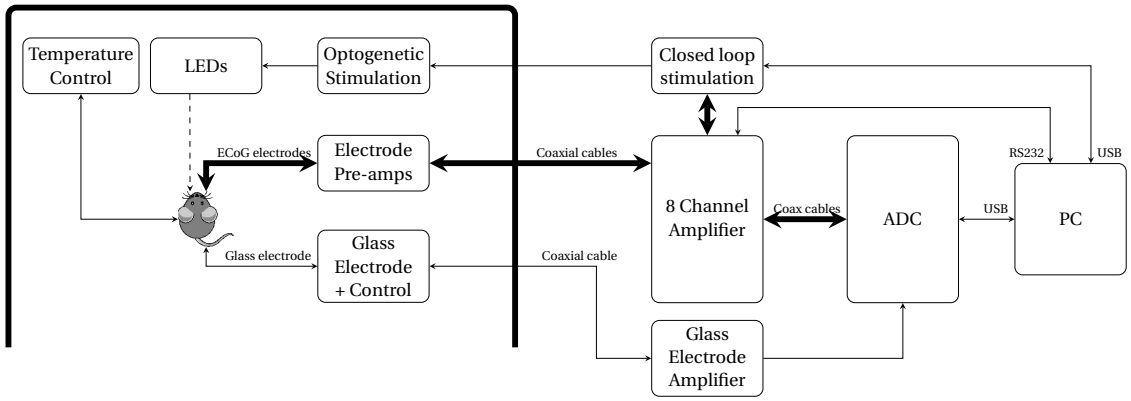

Figure 6.2: Schematic overview of the measurement system to perform seizure detection recordings. The mouse is placed in a Faraday cage, the signals are pre-amplified and digitized.

MONITORING AND STIMULATING

In this set-up, the mouse is awake and fixated in an aluminium tube. When also single cell recordings are performed, the head of the mouse is also fixated with the pedestal on its head. During measurements the body temperature is monitored and controlled.

Optogenetic stimulation is present in the set-up. It consists of a detection circuit and LEDs with optrodes. The optrodes are mounted on the head of the mouse.

ELECTRODES AND AMPLIFIERS

Two types of measurements are performed in this set-up. First ECoG measurements are done, using several electrodes underneath the skull, connected to pre-amplifiers. Second, single cell recordings are done with a glass-electrode connected to its own pre-amplifier.

All pre-amplifiers are connected to the main amplifier outside the cage (CyberAmp 380, Axon Instruments), which is connected to the analogue-to-digital converter (Power 1401, Cambridge Electronic Design). The ADC is connected to the PC, running Spike software to interpret the measured signals.

The settings of the main amplifier and the ADC can be controlled via the PC, including filtering. Also the pre-amplifiers contain filters, but the characteristics of these filters are not fully specified. The filters known are: a notch filter at 50 Hz, a high pass filter at 1 Hz and a low pass filter at 100 Hz.

The glass electrode in the set-up is connected to its own amplifier (Neuro data IR283A, Cygnus Technology), a current-clamp amplifier. This is an amplifier that applies a bias current to the electrode. The differences on the signal are measured.

CABLE MANAGEMENT

The ECoG-electrodes are connected to their pre-amplifiers by simple, thin, unshielded wires. The glass-electrode is connected to its pre-amplifier by the same simple wires, with a silver wire in a sodium-chloride solution on the end to connect to the electrode.

From the pre-amplifiers to the main amplifier the cables are shielded with aluminium tape, connected to cage-ground. From the main amplifier to the ADC coaxial cables are used. The main amplifier and the ADC are both connected via a serial interface to the PC (RS232/USB).

READOUT

A PC running Spike software is used to display the measured signals. Filtering in the software can be configured to make the signals more readable for researchers. The user can configure the post processing filter by himself.

6.2. IMPROVEMENTS

Many measurements are performed with both set-ups. The signals - after extensive filtering - are good enough to interpret them properly, but by filtering a lot of information might be thrown away, even the wanted information. This rejected information can contain useful data, so it is desirable to also have access to this information. Without changing the gear used in both set-ups, a lot of profit can be made by properly using the measurement set-ups. In this section, improvements to both systems will be explained.

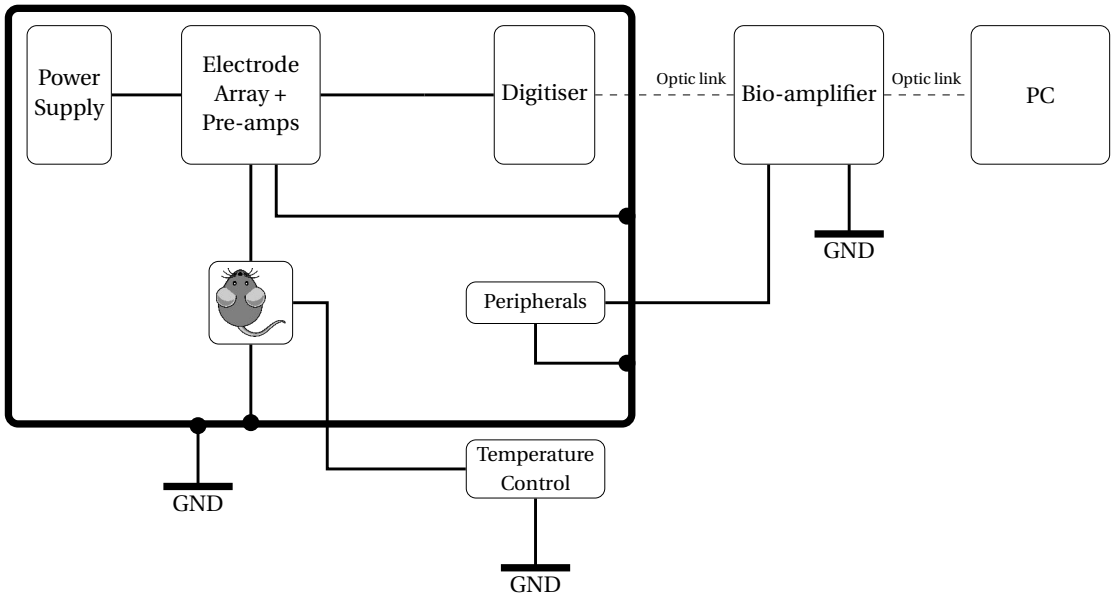

Figure 6.3: Schematic overview of the grounding wires in the inferior olive measurement system. All connections drawn (except for the optic links) are grounding connections. The system is grounded to power ground multiple times, introducing ground loops. The dots indicate the connections to the Faraday cage.

6.2.1. FARADAY CAGE

If a Faraday cage is used, a lot of EMI is kept outside the cage, but care must be taken with the connection of the cage. If the cage is not grounded properly, the cage will introduce other unwanted signals in the system. Also the cage must be completely closed to do its work. So the usage of the cage in Subsection 6.1.2 makes no sense, because one side is completely left open.

6.2.2. REFERENCE POINT / GROUNDING

Grounding the circuits in an organized way is necessary to avoid ground loops. In both original set-ups there are multiple ground points, which must be centralized and connected in a star-shape. In Figure 6.3 the grounding connections in the inferior olive set-up are shown. As can be seen multiple devices inside and outside the Faraday cage, and the cage itself, are connected to the mains ground. As this is on different points in the circuit, ground loops are introduced. These introduce a lot of 50 Hz interference. Multiple ground points must be avoided at all costs, because it can ruin the results obtained by the measurement set-up with very expensive devices. A central grounding point must be chosen. From that point the rest of the system can be grounded.

6.2.3. CABLE MANAGEMENT

Because of the low voltages measured, each small noise and interference source must be minimized or eliminated. Proper cable management can improve performance significantly. Cable size, shielding and twisted pair are described in the next paragraphs.

CABLE SIZE

Reducing cable length, will reduce the resistance of each wire, but more important will reduce the parasitic capacitance of the wire and thus reduces the susceptibility to interference.

Increasing cable thickness, will also reduce the resistance of each wire. Especially the multi-core cable from the pre-amplifier to the digitiser (Subsection 6.1.1) which starts as a thick cable and continues as a thin cable, will increase the signal quality if it remains thick till the input of the digitiser.

SHIELDED TWISTED PAIR

A Faraday cage on it self is not enough to keep all EMI outside the cage. Magnetic interference on wires is not blocked by a Faraday cage. One of the most present magnetic interference sources is the 50 Hz from the mains.

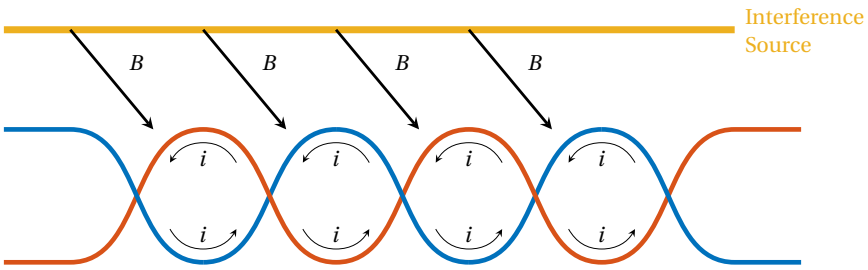

Figure 6.4: Electromagnetic interference reduction with twisted pair cables

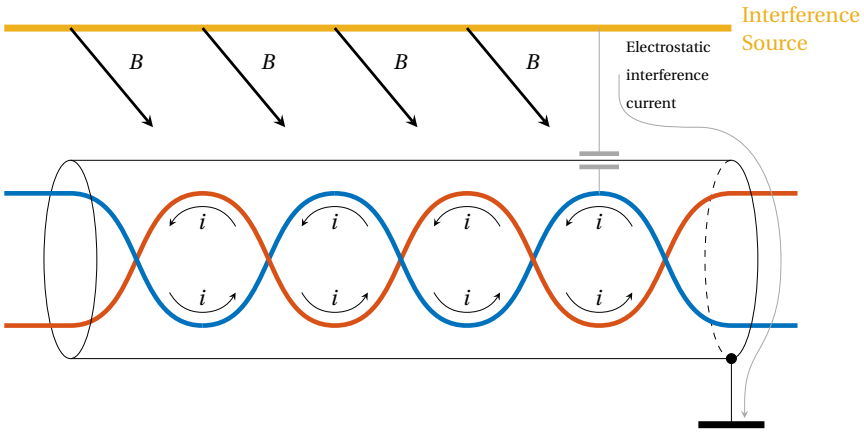

Figure 6.5: Electrostatic and electromagnetic interference reduction and with shielded twisted pair cables

To minimize the influence of this 50 Hz interference, differential signalling must be used. A pair of cables can be twisted around each other, creating local current loops. In Figure 6.4 the magnetic field of an interference source (e.g. the mains) is shown. It induces a current in each loop of the wires. The induced currents cancel each other due to the opposite direction of subsequent loops. In Figure 6.5 shielding is added to the twisted pair wires. The capacitive coupling from the interference source to the wires is blocked by the shield. The current can flow away via the grounded shield, resulting in no capacitive coupling from the interference source to the wires.

If these twisted pairs are also shielded, a combination of twisting wires and shielding is used, resulting in the best possible signal quality. Care must be taken with the connection of the shield. If both sides of the cable are grounded to system ground at another point, a groundloop is introduced, resulting in unwanted behaviour.

6.3. PROPOSED/NEW SET-UP

With the system described in Chapter 5 the big set-ups from the previous sections are not necessary anymore. The system is locally shielded and grounded properly, so EMI is reduced significantly. In this section a detailed description of a proper measurement set-up is given, using the Delft AFE.

In Figure 6.6 an overview of the set-up is shown. The mouse can be placed everywhere, as long as the electrodes are mounted properly, and there are at least two electrodes present in the brain of the mouse. One of these is the reference electrode. Each electrode will measure with respect to this electrode. And one or more measurement electrodes can be placed everywhere in the brain as long as the reference is taken at a good place. The mouse must be electrically isolated from its surrounding (e.g. placed on a plastic platform during measurements), otherwise it can introduce an extra grounding to the system. This can result in a ground loop, introducing additional 50 Hz interference.

The reference electrode is connected to all electrode cables (for clearness, just two are shown in the picture). The electrode pairs (signal plus reference) are connected via shielded, twisted pair cables to the analogue front-end (AFE) box. The negative pole of the battery is defined as system ground. From that point all grounding is provided. The box is connected to a microcontroller (MCU) which controls the AFE and outputs the data to an SD card, display or computer. Power for the MCU is also provided by the battery.

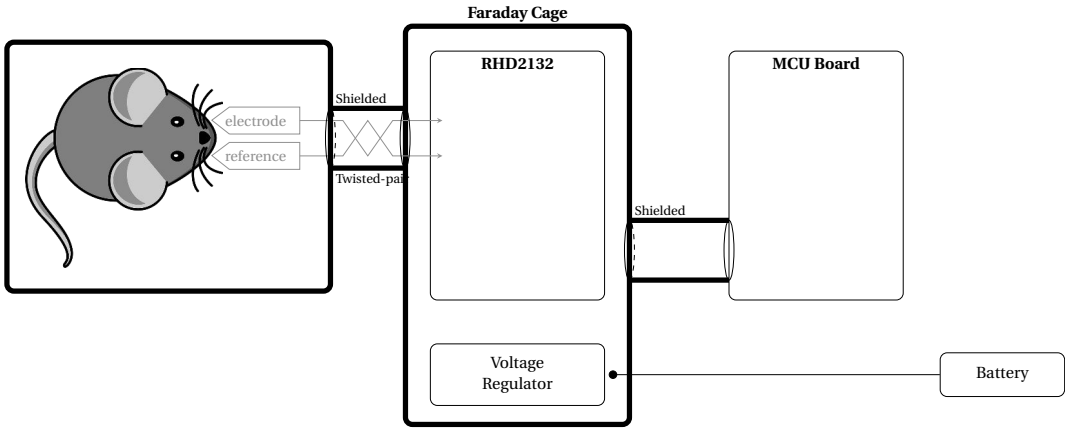

Figure 6.6: A simplified schematic overview of the measurement set-up with the Delft AFE. The thick lines represent the shielding. All ground connections are provided by the negative pole of the battery.

With the improvements listed in section 6.2 the original set-up can perform better without changing the expensive hardware (i.e. amplifiers, electrodes, etc.). In the meantime the proposed set-up with the designed measurement system and set-up described in this thesis can be extended to 32 channels and implemented in laboratories. The results with the measurement set-up based on the Delft AFE are shown and explained in detail in Chapter 7.

7

RESULTS[1]

In this chapter measurement results of the designed system are presented. In Section 7.1 electrical measurement for characterisation of the analog front end are presented. In Section 7.2 three in vivo measurements are presented: an electrocorticogram (ECoG) measurement in mice with absence seizures, a single cell recording in the same mice and measurements in the olivocerebellar system.

7.1. ANALOG FRONT END: ELECTRICAL MEASUREMENTS

To characterise the Delft Analogue Front End (Delft AFE), the set-up of Figure 7.1 is used. The Applicos ATX7006 contains a 20-bits arbitrary waveform generator (AWG20). The waveform generator is connected via a custom made shielded twisted pair cable to the Delft AFE, which saves the data to its SD card. Both the waveform generator and the AFE are configured and controlled by a computer (PC).

Two sets of measurements are performed. First the linearity of the system is characterised with a triangle wave with different amplitudes (f = 30 Hz, V_s = 10 µV, 20 µV, 1 mV, 4 mV and 6 mV). The measured triangle waves are shown in Figures 7.2 and 7.3. At the specified maximum input amplitude of the Delft AFE (V_s = 5.0 mV_{pp}) [32], the signal is still amplified. With a slightly higher input voltage (V_s = 6 mV) the signal is attenuated and clipping. Reaching the lower limits of the AFE in Figure 7.3, a triangle wave is still distinguishable, but it becomes distorted and the noise reaches the same amplitude as the signal (V_n = 15 μV_{pp}).

The second measurement is to determine the frequency behaviour of the AFE. Sine waves with a constant amplitude and varying frequencies are applied (f = 0.5 Hz to 30 kHz, V_s = 1 mV). The frequency behaviour is analysed in MATLAB and plotted in Figure 7.4. The desired bandwidth (1 Hz to 10 kHz) is reached. The signal is slightly attenuated with raising frequency (0.3 dB at 10 kHz, 0.5 dB at 20 kHz), but the passband remains between ± 0.5 dB.

[1] This chapter is partly co-authored by Ide Swager

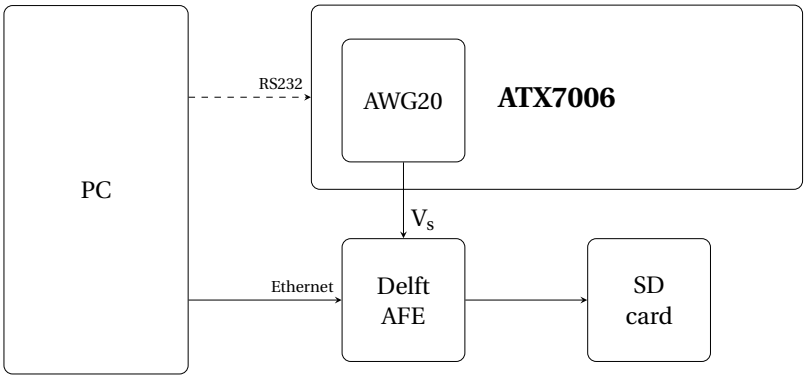

Figure 7.1: Schematic overview of measurement set-up to characterise the Delft AFE. The PC controls the ATX7006 via Ethernet and the Delft AFE via RS232. A waveform generator (AWG20) generates a signal to the Delft AFE, which saves data to its SD card.

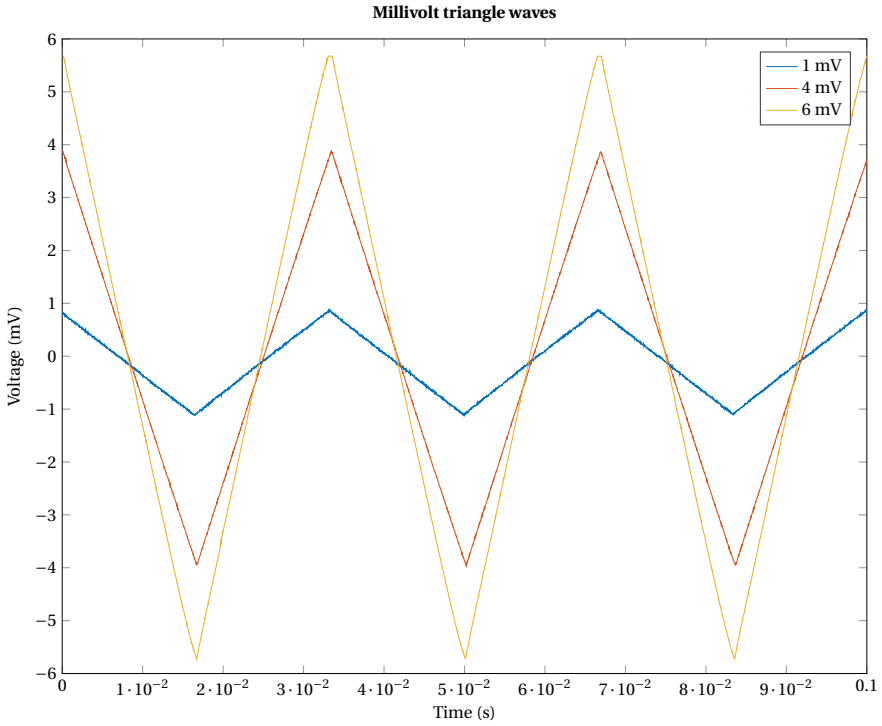

Figure 7.2: Digitised signal measured with Delft AFE for a triangular input signal with frequency f = 30 Hz and amplitudes V_s = 1 mV (blue), 4 mV (red) and 6 mV (orange).

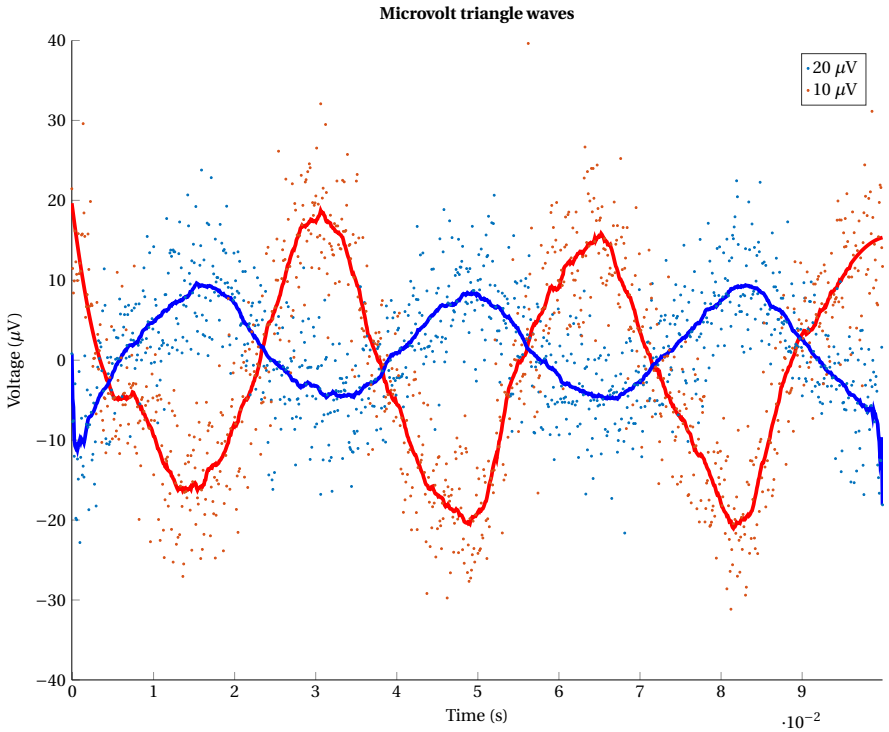

Figure 7.3: Digitised signal measured with Delft AFE for a triangular input signal with frequency f = 30 Hz and amplitudes V_s = 10 µV (blue) and 20 µV (red).

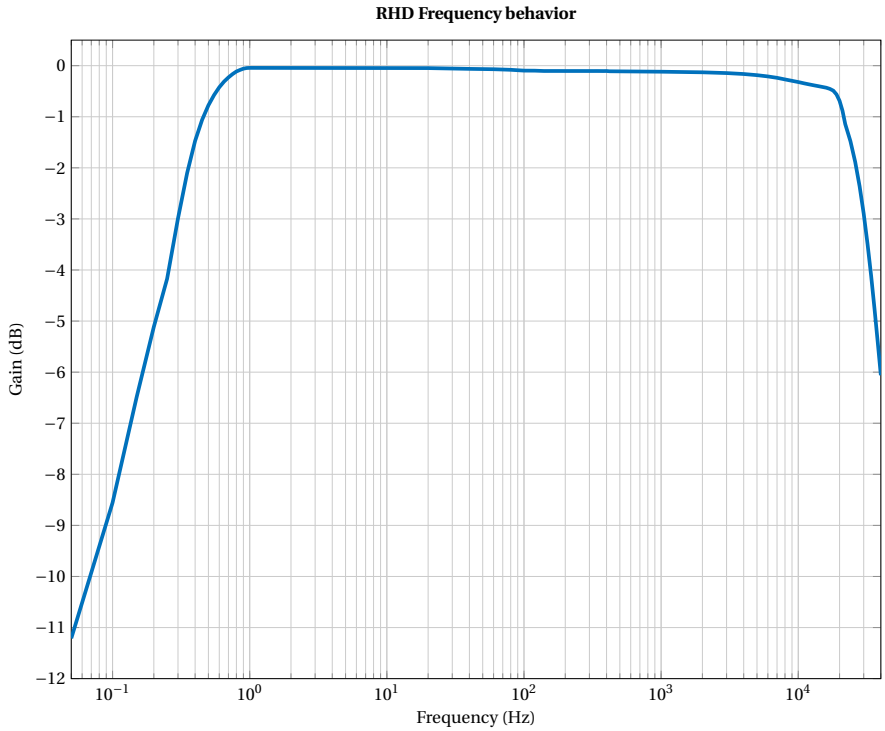

Figure 7.4: Frequency behaviour of the Delft AFE.

In MATLAB the Signal-to-Noise-Ratio (SNR) and the Total Harmonic Distortion (THD) are analysed. The SNR (input signal: sine wave, $f = 140\,\text{Hz}$, $V_s = 1\,\text{mV}$) is 38 dB. This corresponds to a noise level of $8.9\,\mu V_{rms}$ over the bandwidth of the Delft AFE (30 kHz). The waveform generator and the amplifier in the Delft AFE (the amplifiers of the RHD2132) both introduce noise. The datasheets don't specify an equivalent input-referred noise (in $V/\sqrt{Hz}$). All parts of the system (ATX7006 and RHD2132) must be analysed further to draw conclusions on the origin of the noise. If the ATX7006 is the main noise contributor, the Delft AFE has a higher SNR than calculated in MATLAB. Also the bandwidth can be reduced to increase the SNR. The bandwidth is 30 kHz, but can be reduced to 10 kHz. A reduction of the bandwidth with a factor 3, can result in a decrease of a gaussian noise source by a factor $\sqrt{3}$. Also increasing the lower cut-off frequency can reduce the effect of 1/f-noise. The THD (input signal: sine wave, $f = 140\,\text{Hz}$, $V_s = 1\,\text{mV}$) is −46.72 dB.

7.2. ANALOG FRONT END: IN VIVO MEASUREMENTS

In this section three different in vivo measurements with the Delft AFE are presented, each explained and discussed in the corresponding subsections:

1. an electrocorticogram (ECoG) measurement in mice with absence seizures (Subsection 7.2.1)
2. a single cell recording in mice with absence seizures (Subsection 7.2.2)
3. measurements in the olivocerebellar system (Subsection 7.2.3)

In all measurements the Delft AFE samples at 60 kHz and records one channel at a time. To display the data in real time, a Rohde & Schwarz RTO 1044 oscilloscope is connected to the audio output of the AFE. This audio output was duplicating the channel recording. A schematic overview of the measurement set-up is depicted in Figure 7.5. The connection to the Erasmus MC set-up (starred in the Figure) is only present in the first two measurements (ECoG and single cell recording), not in the olivocerebellar system measurement.

7.2.1. ECoG

For the ECoG measurements, custom twisted-pair shielded cables were developed to connect the front-end to the electrodes mounted on the mouse head. In the basic recording, one channel was recorded, while the

Figure 7.5: Overview of the measurement set-up in Erasmus MC with the Delft AFE connected.

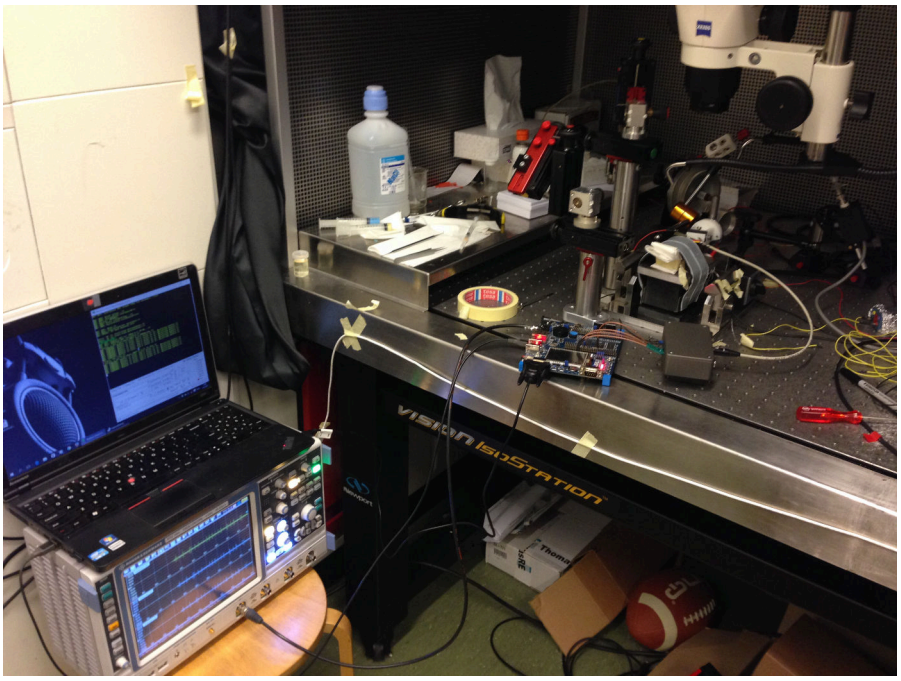

Figure 7.6: Complete ECoG measurement set-up; left: oscilloscope and laptop; centered on the table: MCU and Delft AFE.

other electrodes were left disconnected. In a measurement to compare this work to the current set-up at Erasmus MC, a splitter was made to be able to measure the same channel with two set-ups. A side-effect of this measurement was that there would be more loading of the source, possibly deteriorating the signal quality. A reference measurement was conducted as well, with the set-up in the same place, but with a disconnected electrode. The set-up is displayed in Figure 7.6. All measurements were conducted with a mouse that has absence epilepsy, with frequent seizures.

As a tryout, the audio output of the RHD was fed into the ADC and the amplifier of the EMC set-up. In this way, it was possible to compare the waveforms one-on-one in the Spike2 software. It also ensured that the signals propagated through most of the same path, except for the pre-amplifiers.

To summarize, the following measurements were conducted:

1. Reference (shorted input)
2. 1 channel, no other channels connected
3. 1 channel, other channels connected
4. 1 channel, split between the two set-ups
5. 1 channel, RHD connected to EMC's ADC
6. 1 channel, RHD connected to EMC's ADC and amplifier

Table 7.1: Filter specifications

Band pass filter	
Filter response	Infinite Impulse Response
Filter type	Band-pass filter
Filter order	10
Cut-off frequency (low)	0.5 Hz
Stopband attenuation (low)	50 dB
Cut-off frequency (high)	100 Hz
Stopband attenuation (high)	50 dB
Passband ripple	0.2 dB

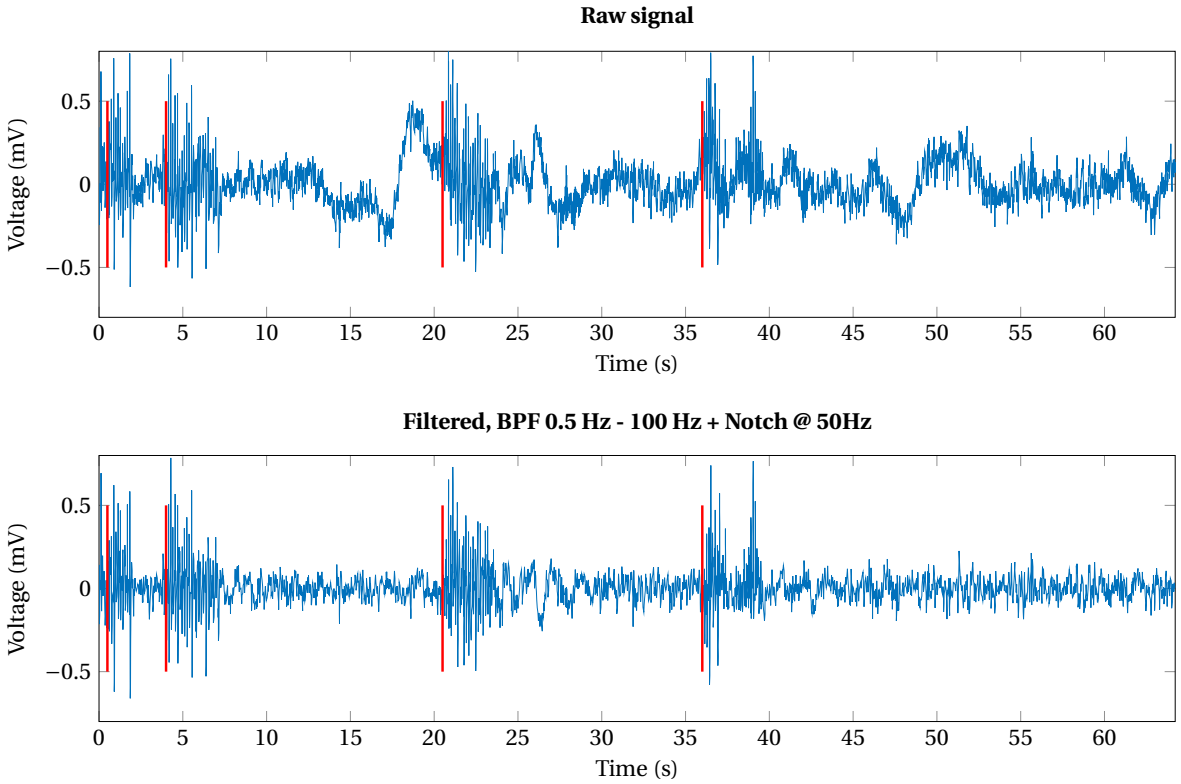

Figure 7.7: Raw and filtered ECoG-signal measured with the Delft AFE. The red lines indicate epileptic seizures.

The first measurement, the reference measurement, was performed to detect possible problems or artefacts in the set-up. No abnormalities were found. The third, fifth and sixth measurements were performed to compare both systems (Delft AFE and existing set-up in EMC). No deviations compared to the second and fourth measurement were noticed, so only measurement 2 and 4 will be discussed in detail.

INDIVIDUAL MEASUREMENT

Figure 7.7 displays the raw, unfiltered, signal and the signal filtered with a band-pass filter (BPF) from 0.5 Hz - 100 Hz and a notch filter at 50 Hz. The filter specifications of the bandpass filter are listed in Table 7.1 In the raw signal, some low frequency information is still present. This can be caused by movement or breathing of the mouse. The filters pre-programmed in the Delft AFE are of low order and can apparently not filter out the strong low frequency content. Clearly, seizure-like activity can be seen at t = 0.5, 4, 20.5 and 36 seconds (marked red in the Figure). A zoom in on the seizure activity around 20 seconds is displayed in Figure 7.8. This Figure contains both a raw and filtered version of the signal. This seizure activity (in the form of generalized spike-and-wave discharges, GSWD's) has a strong frequency component below 10 Hz. In the spectrum displayed in Figure 7.9 a clear peak can be distinguished around 7 Hz (Arrow 2). The high pass component of the filter at 0.5 Hz (Arrow 1) and the notch filter at 50 Hz (Arrow 3) are clearly visible in the filtered spectrum as well. However, as the reader can see, the 50 Hz component in the raw signal is not higher

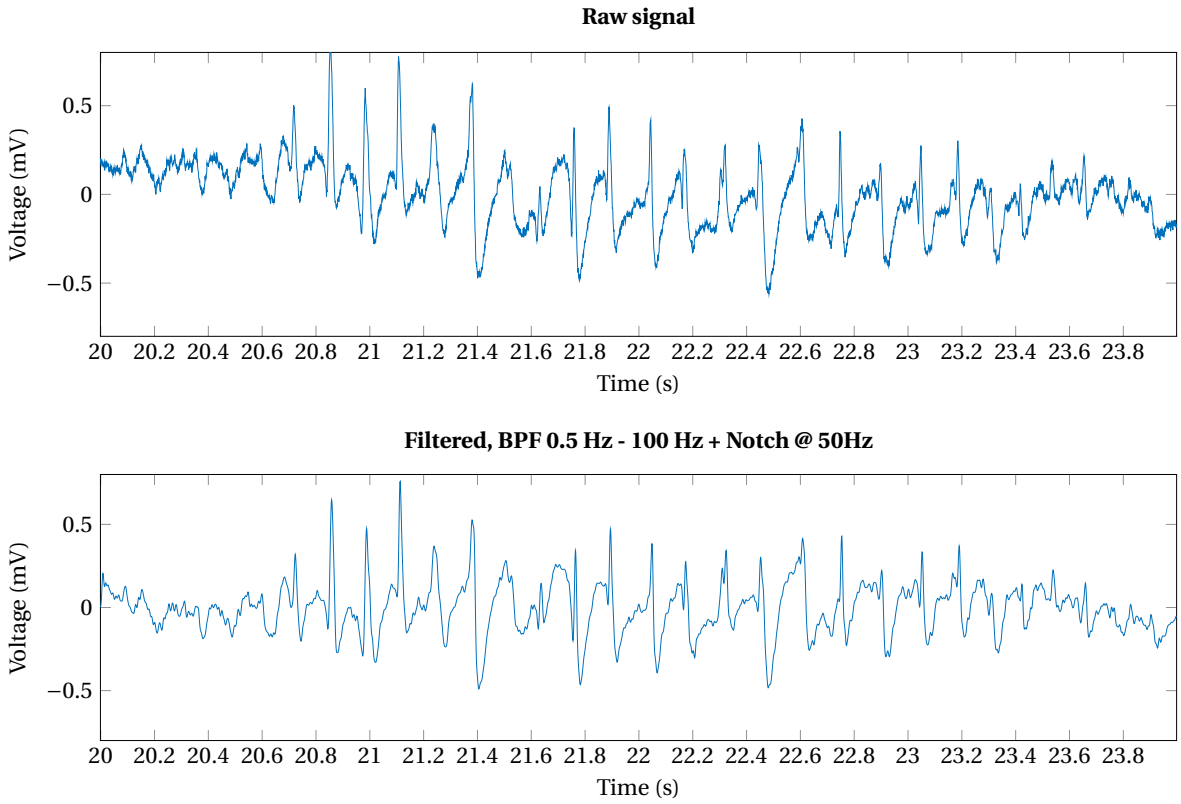

Figure 7.8: Raw and filtered ECoG-signal measured with the Delft AFE, zoomed in on an epileptic seizures.

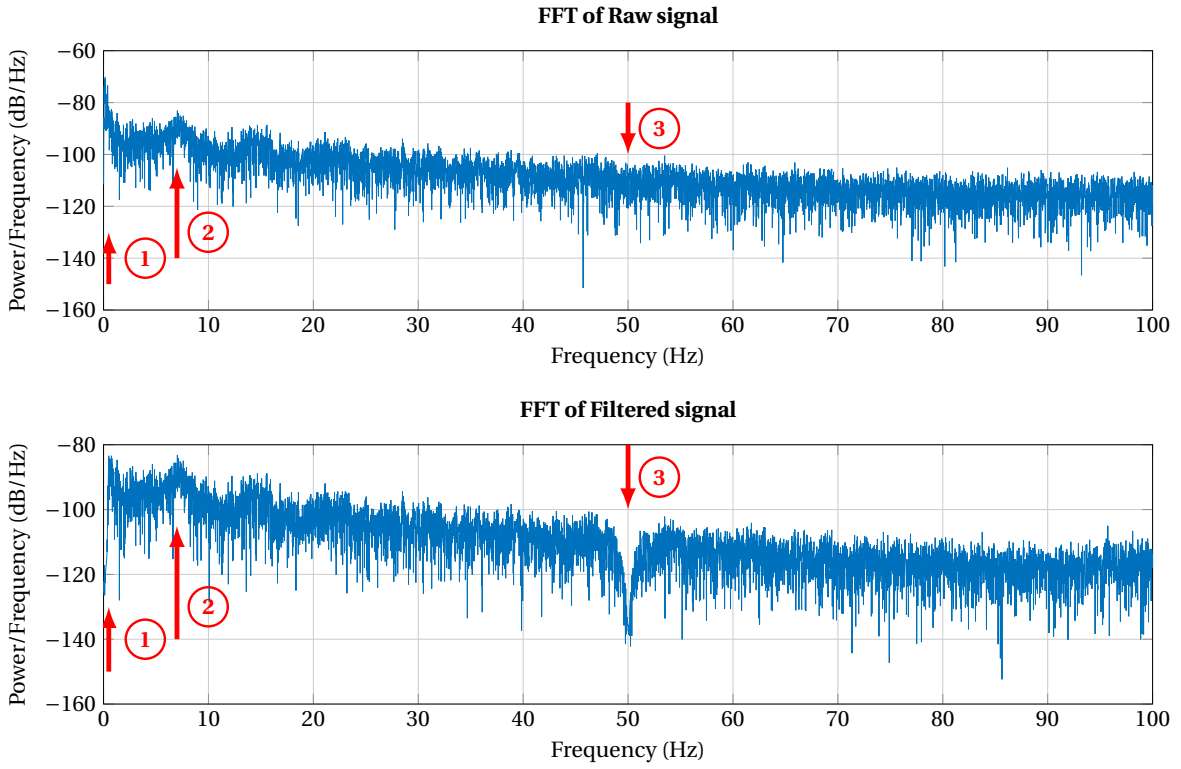

Figure 7.9: FFT of Figure 7.7.

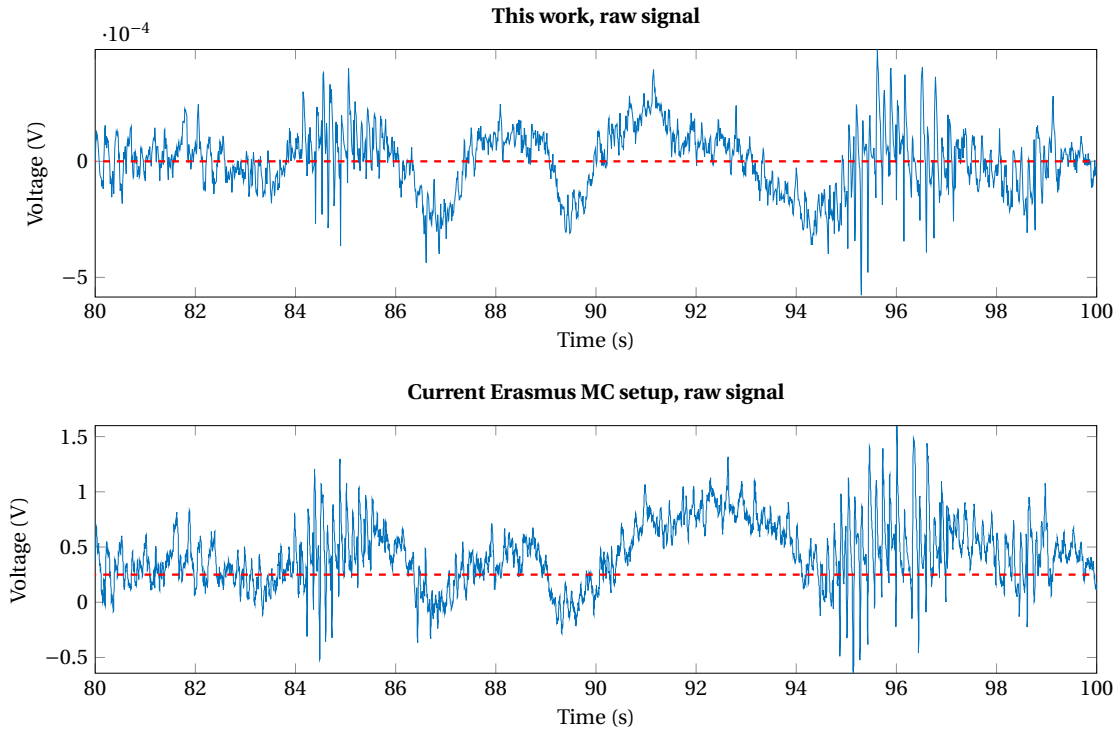

Figure 7.10: Recording made with Delft AFE (top) versus the current set-up at Erasmus MC (bottom).

than other signals around 50 Hz, so it is not a strong interferer. In contrast, when looking at the spectrum of the current EMC set-up in Figure 7.11, a 50 Hz peak can be seen even after the 50 Hz notch filter has been applied. The set-up of this work clearly performs better in terms of 50 Hz interference reduction. This is mainly thanks to the closed Faraday cage surrounding the analogue front-end and the shielded twisted-pair cables connecting the electrodes to the front-end.

SPLIT SET-UP MEASUREMENT

By developing a splitter and measuring the same electrode with two different set-ups, a one-on-one comparison could be made between the set-up of this work and the current EMC set-up. The graphs are displayed in Figure 7.10 (raw signal) and Figure 7.12 (after digital filtering). In Figure 7.10 a DC-offset in the EMC measurement is visible (horizontal dashed red line), after filtering (Figure 7.12) the offset is gone. When optically comparing the results of both set-ups (both raw and filtered signals), it seems that the peaks of the Delft AFE are a little bit more pronounced, possibly improving seizure detection. Furthermore, in Figure 7.11 (an FFT of the raw signals) it can be seen there is a wide notch-filter around 50 Hz present in the current EMC set-up. The Delft AFE doesn't have a notch filter and looking at the spectrum it doesn't require one (Arrow 1). In the spectrum a slight peak at 200 Hz is present (Arrow 2). The origin of this frequency is not known. The FFT of the EMC measurement stops at 250 Hz because the signal is sampled at 500 Hz (Arrow 3). In Figure 7.13 an FFT of the filtered signal is shown. The 200 Hz peak is gone, DC-offset is removed (Arrow 1), the 50 Hz notch is still present in the EMC set-up (Arrow 2) and the low pass component of the filter at 100 Hz is clearly visible (Arrow 3). It can be seen that a notch filter is not required in the new set-up, potentially conserving information around 50 Hz. A zoom in on a seizure is depicted in Figure 7.14. As an electrical engineer, it is hard to qualitatively assess the quality of these signals.

When inspecting the Y-axis of the comparison graphs, it can be seen that the scale differs almost 4 orders of magnitude between the two set-ups. Using the Delft AFE, the signal strength is calculated back to the input. This can be done with the EMC set-up as well, but the problem is that the amplification factor of the pre-amplifiers is unknown. The company that manufactured those devices is not manufacturing those amplifiers anymore, and datasheets are not obtainable. In the authors opinion, these set-ups should always work with input referred voltage levels, because the neuroscientists that work with them sometimes start to interpret those voltage levels. But for the current research with seizure detection these voltage levels don't matter yet.

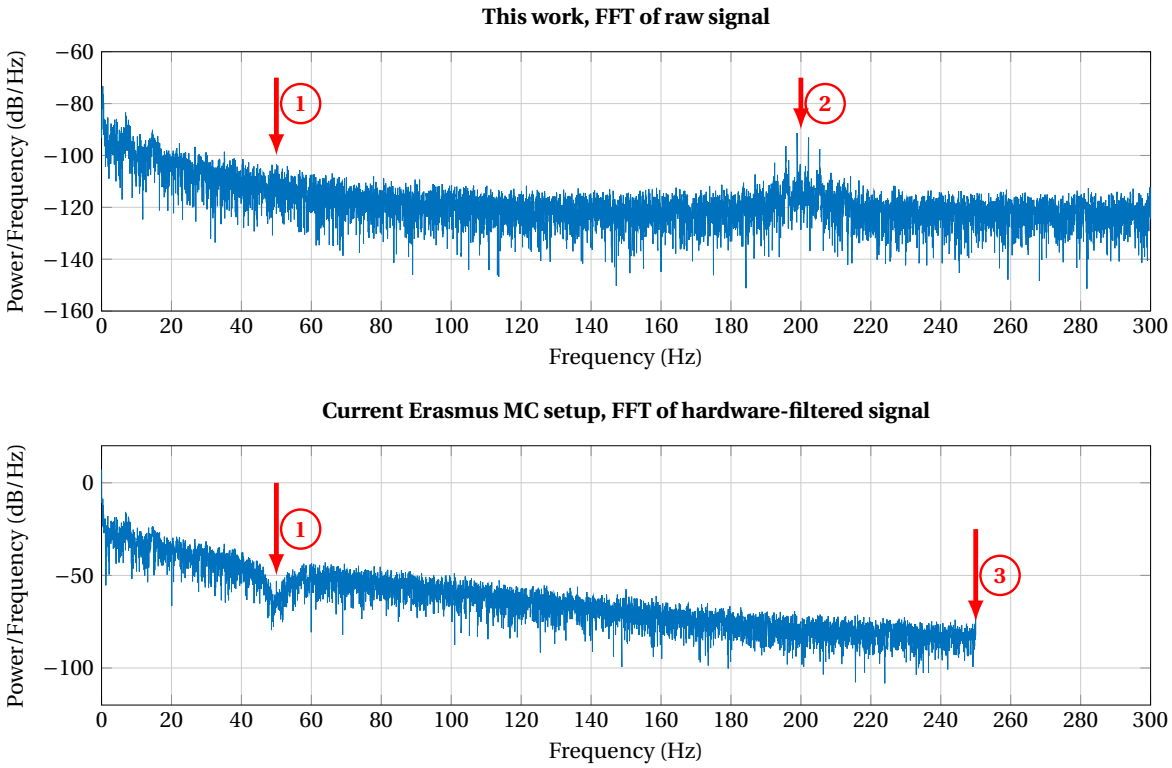

Figure 7.11: FFT of Figure 7.10.

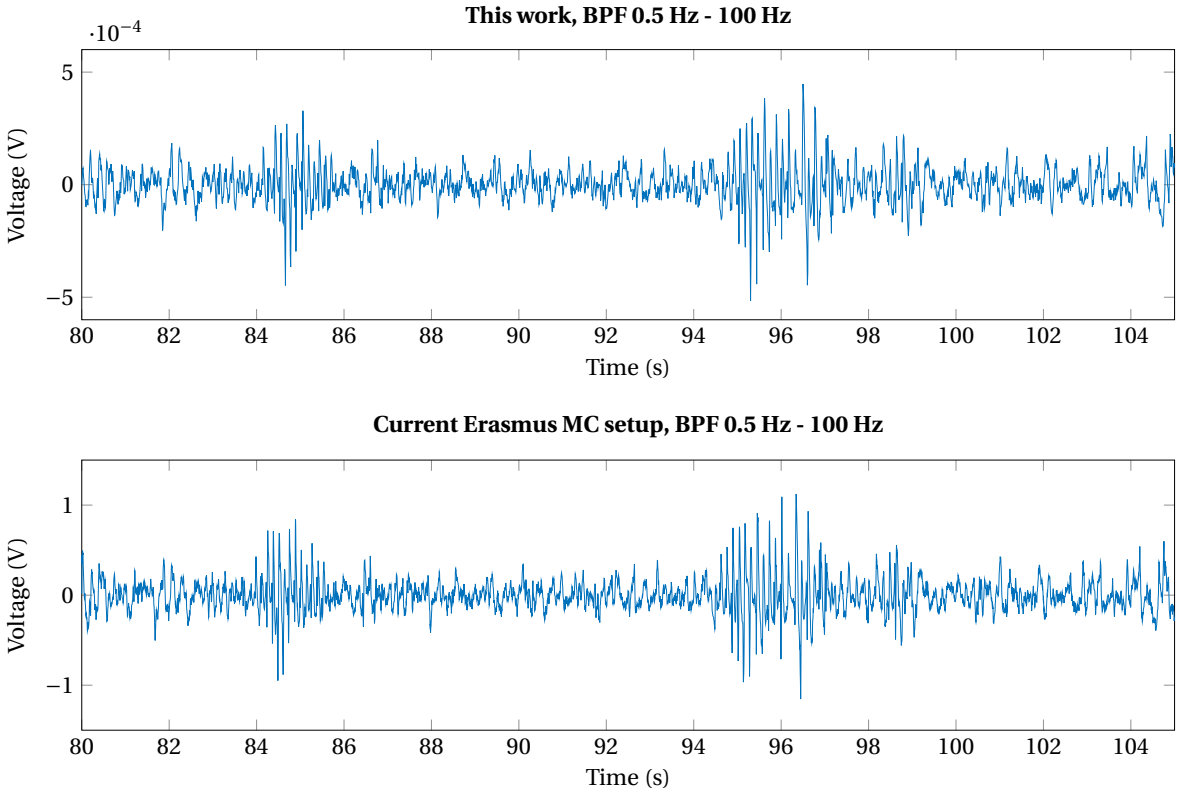

Figure 7.12: Filtered recording made by the Delft AFE (top) versus the current set-up at Erasmus MC (bottom); band-pass filtered from 0.5 - 100 Hz.

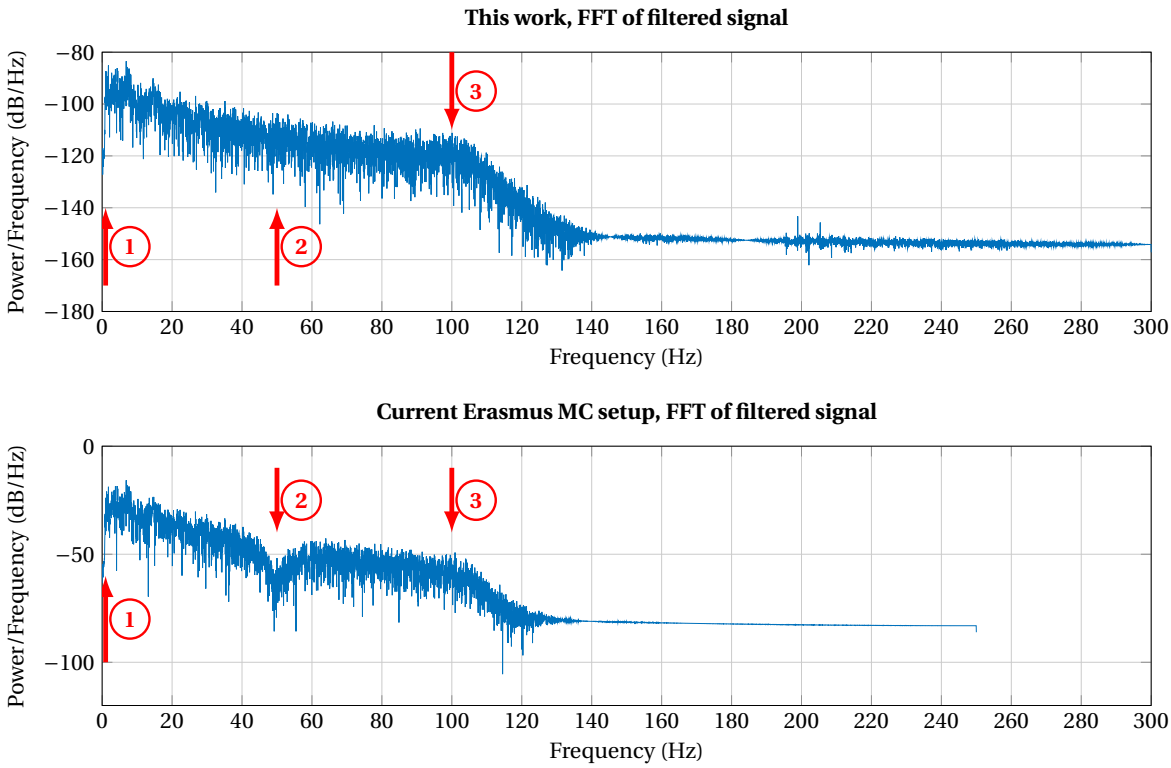

Figure 7.13: FFT of Figure 7.12.

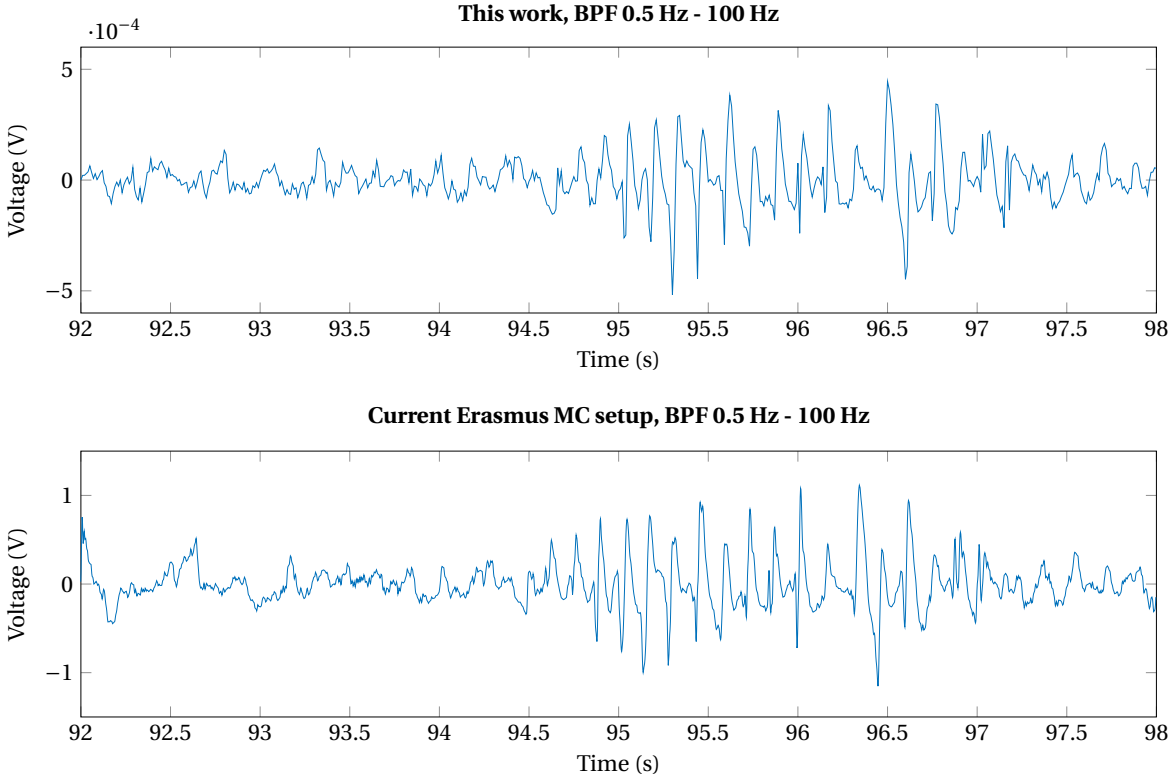

Figure 7.14: A zoomed in view of Figure 7.12.

7.2.2. SINGLE-CELL RECORDINGS

In the same set-up as the ECoG-measurements (see Figures 7.5 and 7.6), a single cell recording was made. Single cell recordings are performed with a glass electrode. The connection to this electrode is of a nature that is completely different from the ECoG electrodes, it is connected via a silver wire in a tube containing a Sodium-Chloride solution. This tube connects the pre-amplifier with the glass electrode. The glass electrode is mounted on a frame of which the position can be controlled very precisely. A specific pre-amplifier for glass-electrodes is used (different from the ones of the ECoG set-up, same manufacturer, also unknown specifications).

In the single-cell recordings the real-time display signal helps the neuroscientist to detect if a useful area is measured. When the electrode was positioned well, the Delft AFE was also attached to the electrode. The glass electrode is now attached to both amplifiers via two silver wires in the NaCl-tube. The first interesting result was a drop of the signal amplitude on the EMC amplifiers and a significant increase in the noise floor. The most obvious reason for this can be a drop in impedance due to two parallel pre-amplifiers. Another reason can be the nature of glass electrodes. Glass electrodes have a high source impedance and is used with a current clamp amplifier, having a huge input impedance. When the Delft AFE is connected in parallel to the current clamp amplifier, the input impedance drops dramatically, resulting in a signal drop at the amplifiers input. Also the current clamp is loaded by the Delft AFE, so it doesn't provide the correct current to the electrode anymore. This will also result in a signal change.

In Figure 7.15 10 seconds of recording with both systems in parallel are shown. In Figure 7.16 the frequency spectrum is shown. Neuroscientist can analyse these data better than us engineers, but during the measurements it was clear to the author the measurements with glass electrodes cannot yet be performed with the Delft AFE due to the relatively high electrode impedance compared to the input impedance of the Delft AFE. Also the Delft AFE cannot be configured yet to function as a current clamp amplifier.

7.2.3. OLIVOCEREBELLAR SYSTEM

The Delft AFE is also used with the most recent version of the Delft Electrode Array (Version 3). The results are presented in Chapter 4. The measurement set-up seems not to be correct, introducing 50 Hz-interference. In further measurements with the Delft AFE and the Delft Electrode Array a different should be used. After a

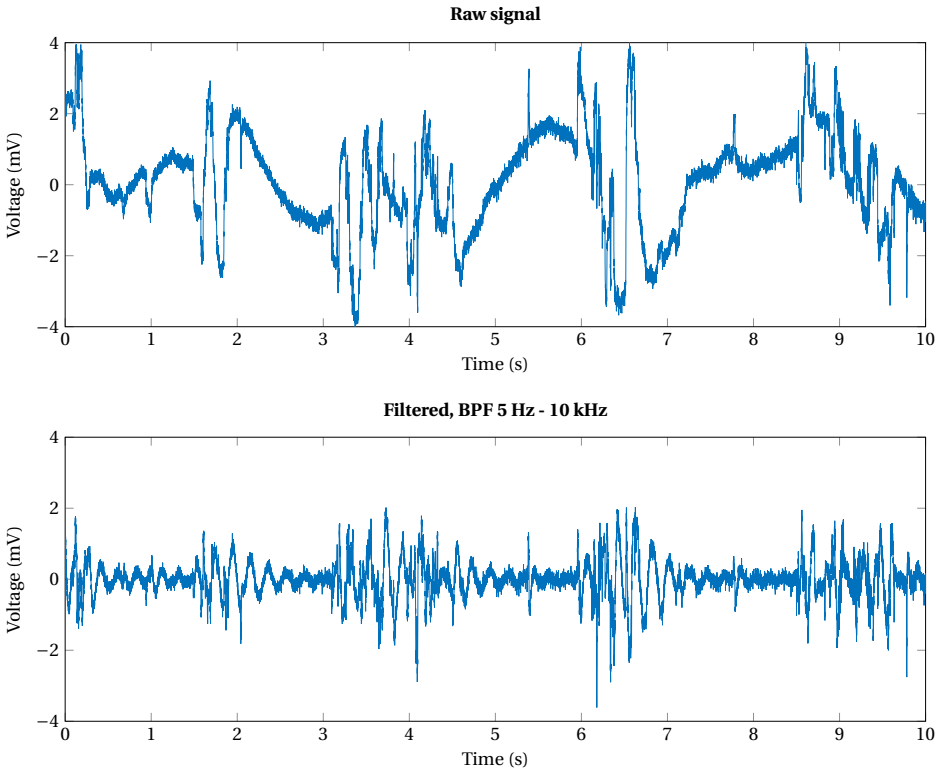

Figure 7.15: Single cell recording with a glass electrode.

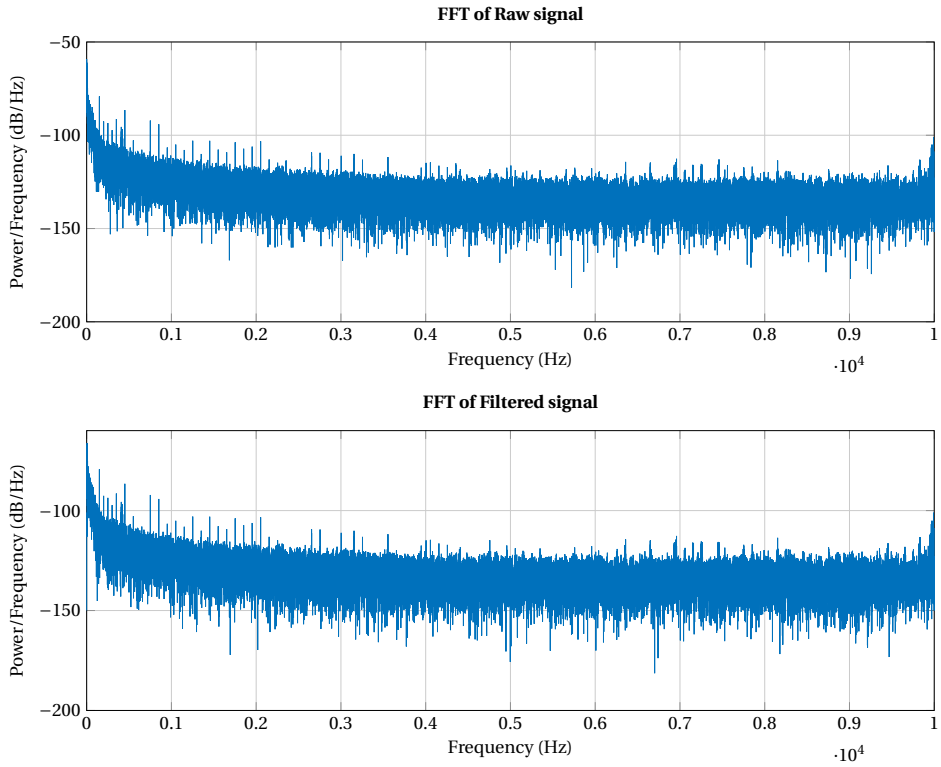

Figure 7.16: FFT of Figure 7.15.

new set of measurements conclusions can be drawn about the functioning of this set-up.

The Delft AFE is evaluated according to the requirements together with the measurement set-up. The system requirements of the electronics and the measurement set-up are listed below together with the evaluation. In the last chapter (Chapter 8) this complete work will be concluded and recommendations will be put forward. The recommendations are based on findings of the different subsystems and on requirements that are postponed on purpose.

~ **Input impedance**
No quantity is given to this requirement. It is clear the input impedance of the system is sufficient to measure signals in ECoG-recordings, but for glass-electrodes the input impedance is too low. No good (checked with a reference signal) measurements with the last version Delft Electrode Array could be performed, so it cannot be concluded if the input impedance is sufficiently high to not have a signal loss at the output of the electrodes. This requirement will be postponed until measurements results are available.

✓ **Bandwidth**
The defined bandwidth is 1 Hz to 10 kHz. The -3dB-bandwidth bandwidth of the Delft AFE is from 0.3 Hz to 30 kHz.

× **Signal-to-noise ratio (SNR)**
The required signal-to-noise ratio is 40 dB. An SNR of 38 dB is reached by the Delft AFE. The measurement is not fully optimised yet.

✓ **Dynamic range**
The amplitude of the smallest measurable signal not disappearing in the noise floor is less than 10 µV. The largest measurable amplitude is 5.5 mV. The dynamic range is set from 20 μV_{pp} to 6 mV_{pp}, so this requirement is met.

✓ **Resolution**
The measured resolution of the system is less than 10 µV, so the requirement is met.

- ✓ **Analogue-to-digital converter (ADC)**
  - ✓ *Sampling rate*
    The sampling rate is 60 kHz, three times higher than the minimum required rate.
  - ✓ *Number of bits*
    The number of bits of the analogue-to-digital converter is 16. The minimum of 10 bits is met.
- ✓ **Data processing**
  - ✓ *Real-time display*
    One electrode channel of the Delft AFE is copied to the audio output of the system. With this output connected to an oscilloscope a real-time display is provided. In next designs a dedicated display output must be considered.
  - ✓ *Data storage*
    An SD-card is used to store the data.
- ✓ **Size (electronics & measurement set-up)**
  The Delft AFE is much smaller than the existing set-ups in the laboratories. The system can be even smaller when the digital controller is moved to the same PCB as the analogue front end chip. Care must be taken with the placement of digital switching elements near the AFE-chip, interference can occur.
- ✓ **(Optional) Universal**
  As long as the signals provided by the connected electrodes are of the same nature as the ones the AFE is designed for (voltage source with an impedance of at most 1 MΩ), the system is universal. When other electrodes (e.g. glass electrodes) are connected, unexpected behaviour can occur.
- ✓ **Electromagnetic interference (EMI)**
  The system is not susceptible to interference as long as the measurement set-up is connected properly. The measured subject must be electrically isolated from its surrounding or also shielded by the system. If a grounding of the subject is present without connecting it to the system grounding, interference can be introduced.

8

Conclusions and Recommendations

The design goal from an engineering point of view of this work is to *design a compact measurement system to measure in vivo electrical activity of neurons in the olivocerebellar system, in the range of sub-threshold oscillations to action potentials, spatially and over time.* The designed system, consisting of three parts: electrodes, electronics and a measurement set-up, is compact and capable of measuring in vivo electrical neural activity in the brain. In this stage of the design only one channel is measured, but the hardware is designed to measure multiple channels with a maximum of 32 channels. The electronic system can - after only changing software parameters - measure up to 32 signals. The number of the electrodes in the array should be increased to acquire this amount of signals from the brain. For now the electrode array is not suitable to measure spatially in the brain. The bandwidth (-3 dB bandwidth from 0.3 Hz to 30 kHz) of the analogue front end is wide enough to measure sub-threshold oscillations (1 to 10 Hz) as well as action potentials (up to 10 kHz).

The design of the Delft Electrode Array has passed three stages. The first version was not suitable to measure in the olivocerebellar system. It was not strong enough, the placement was too imprecise, though it was cheap and simple to fabricate. With the second version only the electrode tips were changed to improve the penetration depth and strength without losing simplicity. This was a good choice, because the electrode tips are penetrating well into the tissue, the tip diameter is small enough to not damage the tissue, it is still cheap, but more difficult and time consuming to fabricate. Like with the first version the placement of the electrodes is still imprecise, due to the mounting on the base material. In the last version of the Delft Electrode Array the electrode tips are kept the same and the base material is changed. The fabrication of the system is simpler but even more time consuming than the second version, but the result is stunning: a very robust mounting of the electrode tips. Although it couldn't be tested in a measurement, the author's expectation about mounting is that it can be placed more precise than the other two versions, thanks to the rigid base material. The material costs of the last version are decreased dramatically with respect to the other two versions, because of 3D-printing techniques.

With the Delft Analogue Front End a big step forward is taken in the reduction of the size of measurement set-ups. Without losing signal quality compared to the existing set-ups, neural activity can be measured. The bandwidth of the system (-3 dB bandwidth from 0.3 Hz to 30 kHz) is wide enough to measure neural activity. The dynamic range (amplitude < 10 µV to 5.5 mV) and resolution (< 10 µV) meet the requirements. The analogue-to-digital converter used in the AFE is configured with a sampling rate of 60 kHz and has a resolution of 16 bits. At the audio output of the microcontroller an oscilloscope can be connected to function as real-time display to monitor the signals during measurements. An SD-card is used to store the data. The size of the system is extremely reduced with respect to the existing set-ups, but still not small enough to make it wearable. The Delft AFE can be used in different neuroscientific projects, as long as the signals provided by the connected electrodes are of the same nature as the ones the AFE is designed for.

Besides a new designed measurement set-up, the existing set-ups were evaluated. Recommendations on these set-ups, without adding or removing devices, are put forward. The grounding of the set-ups must be reorganised. The system is grounded to the mains at multiple points in the system. To avoid ground loops (and thus interference) the grounding for a set-up only can be provided from a single point in the system. When the grounding issues are solved, cable management can improve the system significantly. By reducing cable lengths and by shielding an twisting cables, interference can be reduced even more.

The Delft Electrode Array is designed in collaboration with Joost Kerpels. This work contributes to the hardware design of the first two versions, the fabrication process of all three versions and the mounting of the arrays on the mouse. The work of Joost Kerpels cover the data processing and analysis. Ide Swager was involved with the design of the Delft Analogue Front End. As his work focusses on wireless data communication, this work contributed the most in hardware and software design. A high level design overview is made in close collaboration, the implementation is mostly done in this work.

All parts of the designed system have proven their concept, but the development is not yet far enough to use them in neuroscientific research. To improve their functionality and to scale them to be usable, recommendations are put forward. The second and third version of the Delft Electrode Array prove the principle of a compact electrode array used in neural recordings. To become useful in neuroscientific research, the number of electrodes should be increased and the fabrication process must be made simpler. Although the tube with the electrodes mounted on it are very robust, the coupling with the large tube with wiring is not robust at all. This should be improved in a next version. As soon as the electrode array has more electrodes and the mounting issues are solved, the used 3D-printing material should be replaced by a biocompatible material. It is available, but not used yet.

The Delft Analogue Front End is well suited to measure electrical neural activity. The proof of concept is presented in this work, but to replace the existing set-ups in neuroscientific research, it must be further developed. In the next list the recommendations are described.

- First of all the Delft Analogue Front End must be extensively tested with the Delft Electrode Array (Version 3) to determine if the input impedance is sufficient. If not, the input impedance should be increased.
- Action potentials contain frequencies up to 10 kHz, so the bandwidth can be reduced from 30 kHz to 10 kHz. This will reduce the accumulated noise and the susceptibility to interference above 10 kHz.
- The digital controller used in this work, a microcontroller, is not the best solution. An FPGA (Field Programmable Gate Array) or CPLD (Complex Programmable Logic Device) could do the job much better in terms of timing and power consumption. Additionally digital processing can be implemented on the digital controller. The digital controller must be configurable by the user via an interface to change the application of the set-up and the connected electrode array.
- When the system is equipped with an FPGA or CPLD, the number of parallel measured channels of the AFE must be increased in the software. The hardware is capable of measuring 32 electrodes at the same time.
- The digital controller and the AFE-chip can be placed on the same PCB to save space and reduce the size even more. Care must be taken when this is implemented. Placing digital switching components near the AFE can increase the interference when it is not done properly.
- A dedicated display can be used and connected to the digital controller. In this case no audio output (and therefore an extra digital-to-analog-to-digital conversion) is needed any more.
- The signal-to-noise ratio (SNR) must be improved to match the system requirements. All components in the Delft AFE must be evaluated on their own to determine the individual noise contributions. Also a reduction of the bandwidth will increase the SNR.
- More improvements on the susceptibility to interference can be made by reducing wire lengths and by extending the shielding over the electrode array. The Delft Electrode Array (Version 3) doesn't have shielding around its mounting parts. Extending the shield in these mounting parts can reduce unwanted signals.
- An user interface would be recommended. The user can select the connected electrode array, load the correct filter configurations and can be warned when errors occur.

To improve the existing set-ups, grounding of these set-ups must be reorganised. Implementing these improvements will reduce the interference present, so no extensive filtering inside the signal bandwidth is needed anymore.

It can be concluded that this work is a big step forward in the reduction of the size of neuroscientific measurement set-ups, without a loss of signal quality. The proof of concept of measuring neural activity in an array is delivered. Further research should build on this proof of concept. If the number of electrode tips in the array is increased, and the digital controller in the AFE is upgraded, the system will be very well suited for neuroscientific research. It provides a low cost, high quality multi-electrode measurement system which opens the way to extended behavioural experiments. Because its relatively low costs much more set-ups can be afforded, which can speed up research.

BIBLIOGRAPHY

[1] D. Xu, *Role of the Olivo-Cerebellar System in Timing,* Journal of Neuroscience **26**, 5990 (2006).

[2] X. Wu, J. Ashe, and K. O. Bushara, *Role of olivocerebellar system in timing without awareness,* Proceedings of the National Academy of Sciences **108**, 13818 (2011).

[3] T. Liu, D. Xu, J. Ashe, and K. Bushara, *Specificity of inferior olive response to stimulus timing.* Journal of neurophysiology **100**, 1557 (2008).

[4] S. Herculano-Houzel, *Isotropic Fractionator: A Simple, Rapid Method for the Quantification of Total Cell and Neuron Numbers in the Brain,* Journal of Neuroscience **25**, 2518 (2005).

[5] E. Le Strange, N. Saeed, F. M. Cowan, A. D. Edwards, and M. A. Rutherford, *MR Imaging Quantification of Cerebellar Growth Following Hypoxic-Ischemic Injury to the Neonatal Brain,* American Journal of Neuroradiology **25**, 463 (2004).

[6] R. S. van der Giessen, *Role of Electrotonic Coupling in the Olivocerebellar System*, Ph.D. thesis, Erasmus Universiteit Rotterdam (2007).

[7] S. W. Ranson, *The anatomy of the nervous system; its development and function*, 10th ed. (Saunders, Philadelphia, 1959).

[8] W. F. Boron and E. L. Boulpaep, *Medical Physiology, 2e Updated Edition: with STUDENT CONSULT Online Access* (Elsevier Health Sciences, 2012).

[9] I. Sugihara, *Microzonal projection and climbing fiber remodeling in single olivocerebellar axons of newborn rats at postnatal days 4-7,* Journal of Comparative Neurology **487**, 93 (2005).

[10] R. E. Foster and B. E. Peterson, *The inferior olivary complex of guinea pig: Cytoarchitecture and cellular morphology,* Brain Research Bulletin **17**, 785 (1986).

[11] D. F. Condorelli, N. Belluardo, A. Trovato-Salinaro, and G. Mudò, *Expression of Cx36 in mammalian neurons,* Brain Research Reviews **32**, 72 (2000).

[12] C. I. De Zeeuw, E. Chorev, A. Devor, Y. Manor, R. S. Van Der Giessen, M. T. De Jeu, C. C. Hoogenraad, J. Bijman, T. J. H. Ruigrok, P. French, D. Jaarsma, W. M. Kistler, C. Meier, E. Petrasch-parwez, R. Dermietzel, G. Sohl, M. Gueldenagel, K. Willecke, and Y. Yarom, *Deformation of network connectivity in the inferior olive of connexin 36-deficient mice is compensated by morphological and electrophysiological changes at the single,* The Journal of neuroscience : the official journal of the Society for Neuroscience **23**, 4700 (2003).

[13] C. I. De Zeeuw, E. L. Hertzberg, and E. Mugnaini, *The dendritic lamellar body: a new neuronal organelle putatively associated with dendrodendritic gap junctions.* The Journal of neuroscience : the official journal of the Society for Neuroscience **15**, 1587 (1995).

[14] R. Llinás and Y. Yarom, *Electrophysiology of mammalian inferior olivary neurones in vitro. Different types of voltage-dependent ionic conductances.* The Journal of physiology **315**, 549 (1981).

[15] C. J. Forehand, *The action potential, synaptic tranmission, and maintenance of nerve function,* Cellular Physiology , 37 (2011).

[16] M. R. Baker and S. A. Edgley, *Non-uniform olivocerebellar conduction time in the vermis of the rat cerebellum,* J Physiol **5703**, 501 (2006).

[17] S. Khosrovani, R. S. Van Der Giessen, C. I. De Zeeuw, and M. T. G. De Jeu, *In vivo mouse inferior olive neurons exhibit heterogeneous subthreshold oscillations and spiking patterns.* Proceedings of the National Academy of Sciences of the United States of America **104**, 15911 (2007).

[18] D. Robinson, *The electrical properties of metal microelectrodes,* Proceedings of the IEEE **56**, 1065 (1968).

[19] R. Gesteland, B. Howland, J. Lettvin, and W. Pitts, *Comments on Microelectrodes,* Proceedings of the Ire (1959).

[20] N. Joye, A. Schmid, and Y. Leblebici, *An electrical model of the cell-electrode interface for high-density microelectrode arrays.* Conference proceedings : ... Annual International Conference of the IEEE Engineering in Medicine and Biology Society. IEEE Engineering in Medicine and Biology Society. Conference **2008**, 559 (2008).

[21] N. Joye, A. Schmid, and Y. Leblebici, *Electrical modeling of the cell–electrode interface for recording neural activity from high-density microelectrode arrays,* Neurocomputing **73**, 250 (2009).

[22] D. a. Borkholder, *PhD thesis*, Ph.D. thesis, Stanford University (1998).

[23] W. Franks, I. Schenker, P. Schmutz, and A. Hierlemann, *Impedance characterization and modeling of electrodes for biomedical applications,* IEEE Transactions on Biomedical Engineering **52**, 1295 (2005).

[24] A. Yúfera, D. Cañete, and P. Daza, *Modeling microelectrode sensors for cell-culture monitoring,* Proceedings of IEEE Sensors , 936 (2011).

[25] *Thomas Electrode Data Sheet*, Thomas RECORDING GmbH (2014), rev. 1.0.

[26] *Eckhorn Matrix System*, Thomas RECORDING GmbH (2013), rev. 2.0.

[27] Tucker Davis Technologies, *Omnetics Based Electrodes,* (2016).

[28] Tucker Davis Technologies, *High Density Cortical Arrays,* (2016).

[29] J. Kerpels, *In vivo multicell inferior olivary recordings: alternative design methods for creating cheap and flexible electrode structures*, Master's thesis, Delft University of Technology (2016).

[30] *Low Power, Precision Analog Microcontroller with Dual Sigma-Delta ADCs, ARM Cortex-M3*, Analog Devices (2016), rev. D.

[31] *Low-Noise, 8-Channel, 24-Bit Analog Front-End for Biopotential Measurements*, Texas Instruments (2012), rev. August 2012.

[32] *RHD2000 Series Digital Electrophysiology Interface Chips*, Intan Technologies (2012), rev. September 2013.